



NTNU – Trondheim
Norwegian University of
Science and Technology

Evaluation of CO₂-precooled Nitrogen Expander Systems for Natural Gas Liquefaction

Siv Avdal Hasle

Master of Science in Mechanical Engineering

Submission date: June 2013

Supervisor: Jostein Pettersen, EPT

Norwegian University of Science and Technology
Department of Energy and Process Engineering

EPT-M-2013-48

MASTER THESIS

for

student Siv Avdal Hasle

Spring 2013

Evaluation of CO₂-precooled nitrogen expander systems for natural gas liquefaction*Evaluering av naturgasskondenseringsprosesser med ekspansjon av nitrogen,
og CO₂ forkjøling***Background and objective**

Liquefaction process solutions based on non-flammable refrigerants such as nitrogen and carbon dioxide are advantageous for safety on floating LNG (FLNG) installations. The number of hydrocarbon leakage sources and inventory of hydrocarbon fluids are greatly reduced compared to mixed refrigerant (MR) processes, e.g. of the Dual Mixed Refrigerant (DMR) type. A significant disadvantage is the higher power needs, with resulting increase in fuel gas needs and CO₂ emissions.

In the 2012 Specialization Report an initial comparison was made between a CO₂-precooled nitrogen expander process and a DMR liquefaction process, both with given configurations. Even though published data indicated an efficiency difference of only 15%, the initial calculations gave almost 40% difference between the two systems. Also, preliminary plot size and weigh data indicate quite some disadvantage for the CO₂/N₂ system.

These preliminary results need to be further developed and refined through process optimization and modified configurations, including optimized temperature differences, temperature split levels, pressure levels, staging, and driver optimization. Alternative CO₂/N₂ processes may also be considered when there is potential for higher process efficiency, and/or simplified process and equipment configurations.

A main objective of the Master Thesis is to compare the energy efficiency, capacity, plot areas, weight and availability of CO₂-precooled nitrogen expander processes with baseline DMR process technology. The comparison need to consider varying feed gas and environmental parameters, as well as driver options.

The following tasks are to be considered:

1. Summary of background information and basis of study, including basis for comparison and analysis in terms of feed gas parameters, production capacity and environmental parameters.

2. Further development of process models and optimization of process and system design, including alternative configurations of the CO₂-precooled nitrogen expander process
3. Systematic analyses of process and system performance parameters to establish a data for comparison between the main solutions
4. Discussion and analysis of results
5. Conclusions from study and recommendations for further work

-- ” --

Within 14 days of receiving the written text on the master thesis, the candidate shall submit a research plan for his project to the department.

When the thesis is evaluated, emphasis is put on processing of the results, and that they are presented in tabular and/or graphic form in a clear manner, and that they are analyzed carefully.

The thesis should be formulated as a research report with summary both in English and Norwegian, conclusion, literature references, table of contents etc. During the preparation of the text, the candidate should make an effort to produce a well-structured and easily readable report. In order to ease the evaluation of the thesis, it is important that the cross-references are correct. In the making of the report, strong emphasis should be placed on both a thorough discussion of the results and an orderly presentation.

The candidate is requested to initiate and keep close contact with his/her academic supervisor(s) throughout the working period. The candidate must follow the rules and regulations of NTNU as well as passive directions given by the Department of Energy and Process Engineering.

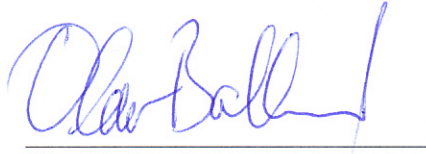
Risk assessment of the candidate's work shall be carried out according to the department's procedures. The risk assessment must be documented and included as part of the final report. Events related to the candidate's work adversely affecting the health, safety or security, must be documented and included as part of the final report. If the documentation on risk assessment represents a large number of pages, the full version is to be submitted electronically to the supervisor and an excerpt is included in the report.

Pursuant to “Regulations concerning the supplementary provisions to the technology study program/Master of Science” at NTNU §20, the Department reserves the permission to utilize all the results and data for teaching and research purposes as well as in future publications.

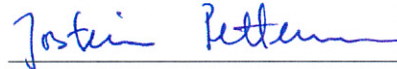
The final report is to be submitted digitally in DAIM. An executive summary of the thesis including title, student's name, supervisor's name, year, department name, and NTNU's logo and name, shall be submitted to the department as a separate pdf file. Based on an agreement with the supervisor, the final report and other material and documents may be given to the supervisor in digital format.

- Work to be done in lab (Water power lab, Fluids engineering lab, Thermal engineering lab)
 Field work

Department of Energy and Process Engineering, 16. January 2012



Olav Bolland
Department Head



Jostein Pettersen
Academic Supervisor

Research Advisor: Knut Arild Maråk, Statoil

PREFACE

This thesis is submitted for the degree Master of Science, Mechanical Engineering with specializations in Energy and Process Engineering. The work was performed under the supervision of Professor Jostein Pettersen at Faculty of Engineering, Science and Technology at The Norwegian University of Science and Technology.

This dissertation is the result of my work, and it is to the best of my knowledge original, except where references are made to previous work. The material included here has not been submitted for a degree at any other university.

I am grateful to my supervisor Professor Jostein Pettersen for his patience and support.

Siv Avdal Hasle

June 2013

Summary

This Master thesis is a continuation of a project thesis written fall 2012 "*Evaluation of Liquefaction systems for Floating LNG*". Two processes for liquefaction of natural gas for a floating unit were compared and evaluated. The main basis for comparison came from simulations conducted in the simulation program Aspen HYSYS. These two processes were a dual mixed refrigerant process, DMR, from Air Products and Chemicals and a turbo-expander process from TOTAL. The specific power consumptions for the processes were 284 kWh/ton LNG for the DMR process and 395.8 kWh/ton LNG for TOTAL's turbo-expander process.

Two additional liquefaction processes were simulated and studied in this Master thesis; a turbo-expander process from APCI and a turbo-expander from US patent 5,768,912. The simulations gave a specific power consumption of 405.7 kWh/ton LNG for APCI's turbo-expander process and 422.5 kWh/ton LNG for the US patent model. These models were compared with the mixed refrigerant process from APCI and TOTAL's turbo-expander process in terms of power consumption, volume flow rates of refrigerant and heat exchanger properties. The expander processes from TOTAL and APCI were dual expanders while the process from US patent 5,768,912 had three turbo-expanders. All expander processes were simulated with a CO₂ precooling system.

The liquefaction units had a production capacity of 3.5 Mtpa of LNG. The equipment in the DMR process was assumed large enough to handle the production capacity while the turbo-expander processes had to be divided in several production trains. The limitations for the expander process were a maximum compressor capacity of 15 MW. TOTAL's and APCI's turbo-expander had expander powers of respectively 49 and 55 MW for the largest expander in the processes and were divided into four trains. The turbo-expander from US patent was suggested with two production trains with a released power of 29 MW for the largest expander. A common CO₂ system served the parallel trains for the turbo-expander processes.

Process parameters of feed gas composition and pressure, water cooling temperature and split temperatures in the processes were some of the parameters included in a sensitivity analysis of the processes. A richer feed composition and a higher feed gas pressure gave reductions in power consumptions due to higher condensing temperature of the natural gas. Alternative systems for the precooling units with several evaporation stages of the CO₂ were also studied and compared with the initial precooling system of one evaporation stage. A CO₂ system with three evaporation stages gave reductions in specific power consumption of 0.6%, 2.1% and 4.7% for the expander processes from TOTAL, APCI and US patent respectively.

The liquefaction processes were suggested with electric drive of the compressors. LM 6000 gas turbines were used for drivers of the processes.

Sammen drag

Denne masteroppgaven er en fortsettelse av en prosjektoppgave skrevet høsten 2012 på NTNU; "Evaluering av kuldeprosesser for flytende LNG". I denne oppgaven ble to kondenseringsprosesser for naturgass sammenlignet og vurdert opp mot hverandre. Hovedgrunnlaget for sammenligningen mellom de to prosessene var simuleringer i simuleringsprogrammet Aspen HYSYS. De to prosessene som ble evaluert var en blandet kuldemedium-prosess, også kalt DMR, fra Air Products and Chemicals (APCI) og en turbo-ekspander prosess fra TOTAL. Den spesifikke effekten for prosessene var 284 kWh/tonn LNG for DMR prosessen og 395.8 kWh/tonn LNG for TOTALs turbo-ekspander prosess.

To nye kondenseringsprosesser for LNG ble simulert og studert i denne masteroppgaven; en turbo-ekspander prosess fra APCI og en turbo-ekspander prosess fra US patent 5,768,912. Simuleringene ga spesifikke effekter på 405.7 kWh/tonn LNG for APCI's turbo-ekspander prosess og 422.5 kWh/tonn LNG for modellen fra US patent. Disse modellene ble sammenlignet med den blandede kuldemediums-prosessen fra APCI og turbo-ekspander prosessen fra TOTAL. Prosessene ble sammenlignet med tanke på blant annet energiforbruk, volumstrømninger av kuldemedium og varmeveksleregenskaper. Prosessene fra TOTAL og APCI var doble ekspansjonsprosesser mens turbo-ekspander prosessen fra US patent hadde tre ekspansjonstrinn av kjølemiddelet. Alle de tre turbo-ekspander prosessene ble simulert med et CO₂ forkjølingsystem.

Kondenseringsprosessene hadde en produksjonskapasitet på 3.5 megatonn per år av LNG. Utstyrsenhetene i DMR prosessen ble antatt å være stort nok til å håndtere hele produksjonsmengden av LNG mens turbo-ekspander prosessene måtte deles inn i flere produksjonstog. Begrensningene for disse prosessene var en kompannderkapasitet på 15 MW. TOTAL og APCI hadde kraftproduksjon på henholdsvis 49 og 55 MW for de største turboekspanderene i prosessene og ble delt inn i fire kondenseringstog. Turbo-ekspander prosessen fra US patent var foreslått med to produsjonstog basert på en kraftproduksjon på 29 MW for den største turboekspanderen. Et felles CO₂ system ga forkjøling for de parallelle produksjonstogene for ekspander prosessene.

Prosessparametere av fødegass komposisjon og trykk, vannkjølingstemperatur og splitttemperaturer i prosessene var noen av parameterne inkludert i en sensitivetsanalyse av prosessene. En fødegass bestående av tyngre hydrokarboner og et høyere trykk av naturgassen ga reduksjoner i kraftforbruk grunnet høyere kondenseringstemperatur av gassen. Alternative konfigurasjoner for CO₂-anlegget med flere fordampningstrinn av CO₂ ble også studert og sammenlignet med det opprinnelige forkjølingsystemet med ett fordampningstrinn. Et CO₂ system med tre fordampningstrinn av CO₂ ga redusert i spesifikk kraftforbruk med henholdsvis 0.6%, 2.1% og 4.7% for ekspander prosessene fra TOTAL, APCI og US patent.

Kraftgenerering med elektrisk drift ble foreslått for kompressorene i prosessene. LM 6000 gas turbiner ble brukt som drivere i prosessene.

Table of contents

1. Introduction.....	14
2. Summary of previous work	15
3. Assumptions & basis for comparison.....	20
3.1 Assumptions	20
3.2 Natural gas composition entering liquefaction	20
3.3 Conditions of natural gas entering liquefaction	21
4. Alternative configurations of the turbo-expander process	22
4.1 Turbo-expander process from APCI.....	22
4.2 Turbo-expander process from U.S. patent.....	23
5. Simulations and results of the turbo-expanders from APCI and US Patent 5,768,912	26
5.1. Simulation of APCI turbo-expander process.....	26
5.2 Results from the simulation of APCIs turbo-expander	29
5.3 Simulation of turbo-expander process from US patent 5,768,912	32
5.4 Results from the simulations of turbo-expander from US patent 5,768,912	37
5.4.1 Evaluation of the integrated end flash system of U.S patent 5,768,912	41
6. Evaluation of different process parameters	43
6.1 Richer feed gas composition.....	43
6.2 Increased feed gas pressure.....	46
6.3 Decrease in cooling temperature.....	49
6.4 Additional stages for the main compressor in the turbo-expander process	52
6.5 High pressure of nitrogen	53
6.6 Split temperatures in heat exchangers.....	55
6.6.1 TOTALs turbo-expander	55
6.6.2 APCIs turbo-expander.....	56
6.6.3 Turbo-expander from US patent	56
6.7 Isentropic to polytropic efficiency in rotating equipment.....	57
7. Evaluation of CO2 precooling system for turbo-expander processes.....	61
7.1 General	61
7.2 Results from simulations of alternative CO2 system for the turbo-expander process.....	65
7.2.1 TOTALs turbo-expander process	65
7.2.2 APCIs turbo-expander process.....	67

7.2.3 Turbo-expander from patent number 5,768,912	68
8. Discussion and analysis of liquefaction processes for FLNG.....	70
8.1 Compression in liquefaction processes.....	71
8.1.1 Improvements of nitrogen compression	72
8.2 LMTD, UA values and minimum approach temperature in heat exchangers	73
8.2.1 Improvements of LMTD, UA values and minimum approach temperature in heat exchangers.....	75
8.3 Heat transfer properties	75
8.3.1 Improvements of heat transfer properties	76
8.4 Production capacities and liquefaction trains.....	77
8.5 Volume flow of refrigerant	78
8.5.1 Improvement in volume flows for the process	82
8.6 Split temperatures of feed gas and refrigerant.....	83
8.6.1 Improvements in split temperatures of feed gas and refrigerant	84
8.7 Precooling systems	85
8.8 Equipment	87
8.9 Refrigerant flow rate & storage of refrigerant.....	89
8.10 Availability of rotating equipment	91
8.11 Power generation & driver configurations.....	92
9. Conclusions.....	94

List of Figures

Figure 1: Model of TOTALs turbo-expander process with equipment labels.....	18
Figure 2: Model of APCIs DMR process with equipment labels.....	19
Figure 3: APCI turbo-expander (Bukowski, 2011).....	23
Figure 4: Three versions of the liquefaction process from U.S patent 5,768,912 showing versions A, B and C (Dubar,1998)	24
Figure 5: Model of APCI turbo-expander process with equipment lables	26
Figure 6: Simulation of APCIs turbo-expander process in HYSYS	28
Figure 7: Model of expander process from US patent 5,768,912	33
Figure 8: HYSYS model of US patent 5,768,912	36
Figure 9: Heat flow curves for Versions A, B and C	38
Figure 10: TS-diagram showing liquefaction of the gas at 60 bar (Pettersen, 2012)	47
Figure 11: Mollier diagram with isentropic and polytropic compression	58
Figure 12: CO2 Precooling system used in the initial modeling of the turbo- expander processes.....	61
Figure 13: Heat flow curves for CO2 system several evaporation stages	62
Figure 14: Alternative CO2 system with two evaporation stages of CO2.....	63
Figure 15: Alternative CO2 system with kettle heat exchangers and three evaporation stages of the refrigerant.....	64
Figure 16: Availability of direct driver configurations (Pettersen, 2012)	91
Figure 17: Schematic of a LM 6000 multispool gas turbine (Hundseid, 2012)	92

List of tables

Table 1: Power for TOTALs turbo-expander process	15
Table 2: Power consumption for APCIs DMR process	16
Table 3: Assumptions for the simulations of liquefaction processes	20
Table 4 Gas composition entering liquefaction unit.....	21
Table 5: Feed gas conditions entering the liquefaction unit	21
Table 6 Results APCI turbo-expander with an LNG production of 3.5 Mtpa.....	29
Table 7: Heat exchanger values for APCIs turbo-expander	29
Table 8: Volume flow rates of expanders in APCIs turbo-expander process.....	30
Table 9: Suction volume of compressors in APCIs turbo-expander process	30
Table 10: Compressor and expander work for APCIs turbo-expander	31
Table 11: Results from simulations of Versions A, B and C	37
Table 12: Heat exchanger values for Version C	39
Table 13: Volume flows of the expander outlets of Version C.....	39
Table 14: Volume flows of the compressor suction of Version C.....	39
Table 15: Compressor and expander work for Version C	40
Table 16: Results from simulations with integrated flash gas	41
Table 17 Gas composition from TOTALs article (Chrétien, 2011)	44
Table 18: Comparison of the turbo-expander processes with a richer feed gas..	45
Table 19: Results for DMR process with a richer feed composition.....	46
Table 20: Increased pressure of the feed gas for the expander processes	48
Table 21: Results for APCIs DMR processes with a higher feed pressure.....	49
Table 22: Comparison of the expander processes with lower cooling temperature	51
Table 23: Results for the DMR processes with lower cooler temperature	52
Table 24: Several compressor stages of the main compressor for expander processes.....	53
Table 25: High-pressure of nitrogen for the expander processes	54
Table 26: Split temperatures in TOTALs process	55
Table 27: Split temperatures in APCIs expander process	56
Table 28: Split temperature in the US patent process	57
Table 29: Adiabatic to polytropic efficiency for the expander processes	59
Table 30: DMR process with adiabatic vs polytropic efficiency	60
Table 31: Compressor power for CO2 systems, TOTAL.....	65
Table 32: Heat exchanger properties for CO2 systems, TOTAL.....	66
Table 33: Volume flow rates of compression suction for CO2 systems, TOTAL...	66
Table 34: Compressor power for CO2 systems, APCI.....	67
Table 35: Heat exchanger properties for CO2 systems, APCI	67
Table 36: Volume flow rates of compressors for CO2 systems, APCI.....	68
Table 37: Compressor power for CO2 systems, US patent.....	68
Table 38: Heat exchanger properties for CO2 systems, US patent.....	69
Table 39: Volume flow rates of compressor for CO2 systems, US patent.....	69
Table 40: Specific power consumption for all four liquefaction processes.....	70
Table 41: Main compressor for turbo-expander process.....	71
Table 42: Heat exchanger properties for the four liquefaction processes.....	73
Table 43: Power production of turbo-expanders	77
Table 44: Suction volume of compressors	80
Table 45: Volume flow from expansion of the gas for all processes.....	81

Table 46: Split temperatures of feed gas and refrigerant for all liquefaction processes.....	83
Table 47: Description of precooling systems for turbo-expander processes	85
Table 48: Results for CO2 systems with one and two evaporating stage of CO2 .	86
Table 49: Equipment count for the liquefaction processes	87
Table 50: Refrigerant flow rate and make-up refrigerant for all four liquefaction processes.....	90

1. Introduction

Small and remote gas fields can be exploited more economically with floating LNG technology. The gas can be liquefied and transported to markets all over the world and the floating unit can be set into production at other gas fields when required. The two types of processes considered most suitable for floating LNG are turbo-expander processes and mixed refrigerant processes. These liquefaction processes give a balance between efficiency, safety and the strict size and weight requirements on the floating unit.

In a project thesis written fall 2012, one turbo-expander process and one dual mixed refrigerant process were studied (Hasle, 2012). The turbo-expander process was from TOTAL and had CO₂ precooling of the nitrogen (Chrétien, 2011). The dual mixed refrigerant process was a liquefaction process from Air Products and Chemicals (APCI) (Bukowski, 2011). The two liquefaction processes were simulated in the simulation program Aspen HYSYS V7.3. These simulations will also be used in this master thesis to investigate the models further. Two additional versions of the turbo-expander processes will be simulated in HYSYS and compared to the previous models.

The findings from the preliminary work also showed that the DMR process had superior numbers in terms of efficiency over the turbo expander process. A number close to 400 kWh/ton LNG was found for TOTALs process while a specific power consumption of below 300 kWh/ton LNG was the result for APCIs mixed refrigerant process. The DMR process would also require less space and weight according to the numbers found in the project thesis. The turbo-expander process is however assumed to have a less complex operation with a shorter start-up time and higher availability.

A disadvantage with using nitrogen as refrigerant is the difficulties of matching the warming curve of the nitrogen to the cooling curve of the natural gas. Large spacing between the two curves represents inefficiencies in the process with excessive power used to liquefy the natural gas. The gap between the temperature curves should be decreased to make the turbo-expander processes more efficient. Splitting the nitrogen streams in portions, with different temperature and pressure, use of several expanders, and precooling of the refrigerant are approaches to reduction of the gap in the heat flow curves.

Volume flow rates of the refrigerant entering and exiting equipment in the process and UA values of the heat exchangers will give an indication of the size of pipes and equipment needed in the process.

Two additional turbo-expanders will be studied for comparison with the two models from APCI and TOTAL. One is a dual-expander process from APCI (Bukowski, 2011) and the other is a three-expander process from US patent 5,768,912 (Dubar, 1998).

2. Summary of previous work

This section gives a short summary over the main results found in the project thesis “*Evaluation of Liquefaction systems for Floating LNG*” written at NTNU fall 2012. (Hasle, 2012) Two liquefaction processes were simulated and evaluated for production of LNG on a floating unit. The turbo-expander process from was simulated based on a model from an article by TOTAL (Chrétien, 2011). Statoil ASA provided a simulation of the DMR process from APCI. Modifications in terms of heat exchanger properties and efficiency of rotating equipment were conducted for the liquefaction process. The liquefaction processes were modeled with a production capacity of about 3.5 Mtpa.

Table 1: Power for TOTALs turbo-expander process

TOTALs turbo-expander process	
Specific power consumption (kWh/ton LNG)	395.8
Total refrigerant flow rate (ton/hr)	5013
<i>Power consumption</i>	
Power consumption main compressor (MW)	159.7
Power consumption CO2 compressors (MW)	15.7
Total power consumption (MW)	175.4
<i>Expander power</i>	
Warm expander (MW)	48.5
Cold expander (MW)	12.6
LNG liquid expander (MW)	1.3
Total expander power (MW)	62.4

The total power consumption from the main nitrogen compressor and the CO2 compressors are listed in Table 1. The CO2 system accounts for a specific power consumption of 35.7 kWh/ton LNG in the process and 9% of the total power consumption. The total power production in the process determined the number of LM 6000 gas turbines required for the process. The process required 6 LM 6000 each to run the liquefaction process with a power output of 32 MW. Five liquefaction trains were chosen based on assumptions of direct drive of the process; one LM 6000 to power the common CO2 system and five LM 6000 gas turbines to power each of the liquefaction trains. Another approach to determine the number of trains is the power output from the largest expander. A maximum capacity of 15 MW (Pettersen, 2013) for the compander systems equals a number of four liquefaction trains. The last approach with four liquefaction trains will be used in this Master thesis. The LNG production rate will then be lower than 3.5 Mtpa for mechanical drive, decided by the driver output. Electrical drive of the compressors is assumed for the compressors to maintain a production capacity of 3.5 Mtpa.

Table 2: Power consumption for APCIs DMR process

APCIs DMR process	
Specific power consumption (kWh/ton LNG)	284.0
Total refrigerant flow rate (ton/hr)	2412.6
<i>Power consumption</i>	
1 st MR circuit	
LP Warm (MW)	20.1
HP Warm (MW)	30.1
P WMR Pump (MW)	0.4
2 nd MR circuit	
LP Cold (MW)	39.0
MP Cold (MW)	25.0
HP Cold (MW)	5.2
HHP Cold (MW)	5.2
Total power consumption (MW)	125.0

Table 2 lists the total power consumption for the DMR process by the compressors and liquid pump in the two MR circuits. The process required four LM 6000 gas turbines to power the liquefaction process by direct mechanical drive. One DMR train was assumed sufficient to handle the production capacity of LNG. Two additional gas turbines were required for electric power generation covering, pumps, HVAC, thrusters, lighting etc. for the two liquefaction processes.

The turbo-expander processes use nitrogen refrigerant for liquefaction of the natural gas. CO₂ is used for precooling of a portion of the nitrogen stream to -40°C. Nitrogen and CO₂ are not considered flammable and will be relatively safe to store and operate on an FLNG. Release of large amounts of CO₂ can however cause suffocation. The DMR process uses a mixed refrigerant and the fire and explosion risks associated with storage of these hydrocarbons are considered much higher than for nitrogen and CO₂. Safety zones are necessary on the FLNG if a DMR process is selected. The nitrogen is in single-phase throughout the liquefaction process and has an advantage over the DMR process where liquid motions of the mixed refrigerant must be considered. The complexity of the system increases with two-phase operation and possible liquid maldistribution in the heat exchangers. A complex operation of the DMR process results in a longer start-up time after stop in production than for the turbo-expander process.

An equipment count for the processes gave a number of 25 components for each train in the turbo-expander process and 28 for the DMR process. The total equipment count for the turbo-expander with five liquefaction trains was however substantially higher with 73 units. The turbo-expander process will have a higher amount of rotating equipment, which is closely linked to the availability of the system. Five trains in parallel will however have advantage with production of LNG from functional cells if one train is out of operation. An approximate size and weight analysis for the two processes gave numbers of

1260 m² and 4810 tons for the turbo-expander process and 455 m² and 1740 tons for the DMR process.

TOTALs article stated that the power consumption for the turbo-expander was 262 kWh/ton LNG (Chrétien, 2011). This is a power consumption of 51% less than the simulation of the same process in the project thesis with a power consumption of 396 kWh/ton LNG. The low power consumption in the article was explained by a high feed gas pressure and low cooling temperature. Process parameters were different in the study, but cannot explain a difference in 51%. The turbo-expander process should be investigated further to determine thermodynamic losses in the process. Change in process parameters should also be studied to see the influence in efficiency of the process. Comparison with other turbo-expander processes can give an indication if the numbers for TOTALs process are reasonable. The CO₂ system should be optimized. A DMR process similar to the one studied in the project thesis was also described in TOTALs article (Chrétien, 2011). This model had power consumption of 227 kWh/ton LNG, which is 25% less than for the DMR process in the project thesis with a power consumption of 284 kWh/ton LNG. Process parameters should be studied for the DMR process to identify losses in this process. Change in process parameters should also be studied.

Heat exchanger properties and volume flows of the processes were not discussed in the project thesis. The LMTD and UA values in the heat exchangers and the volume flows in rotating equipment for the two processes are included in the study of process parameters in Chapter 5 and in the discussion in Chapter 8. Models with equipment labels for TOTALs turbo-expander process and APCIs DMR process are included in Figures 1 and 2 respectively.

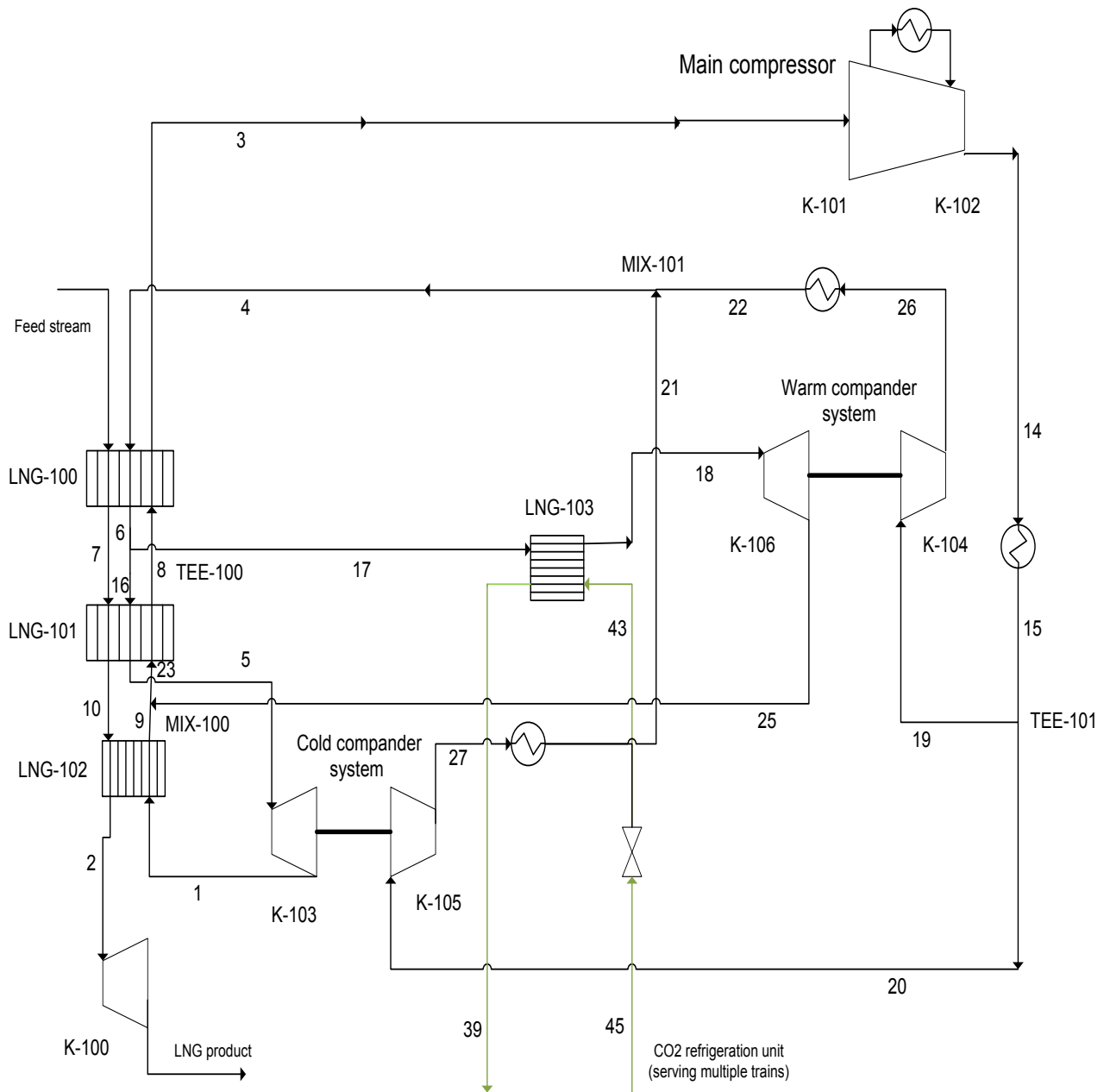


Figure 1: Model of TOTALs turbo-expander process with equipment labels

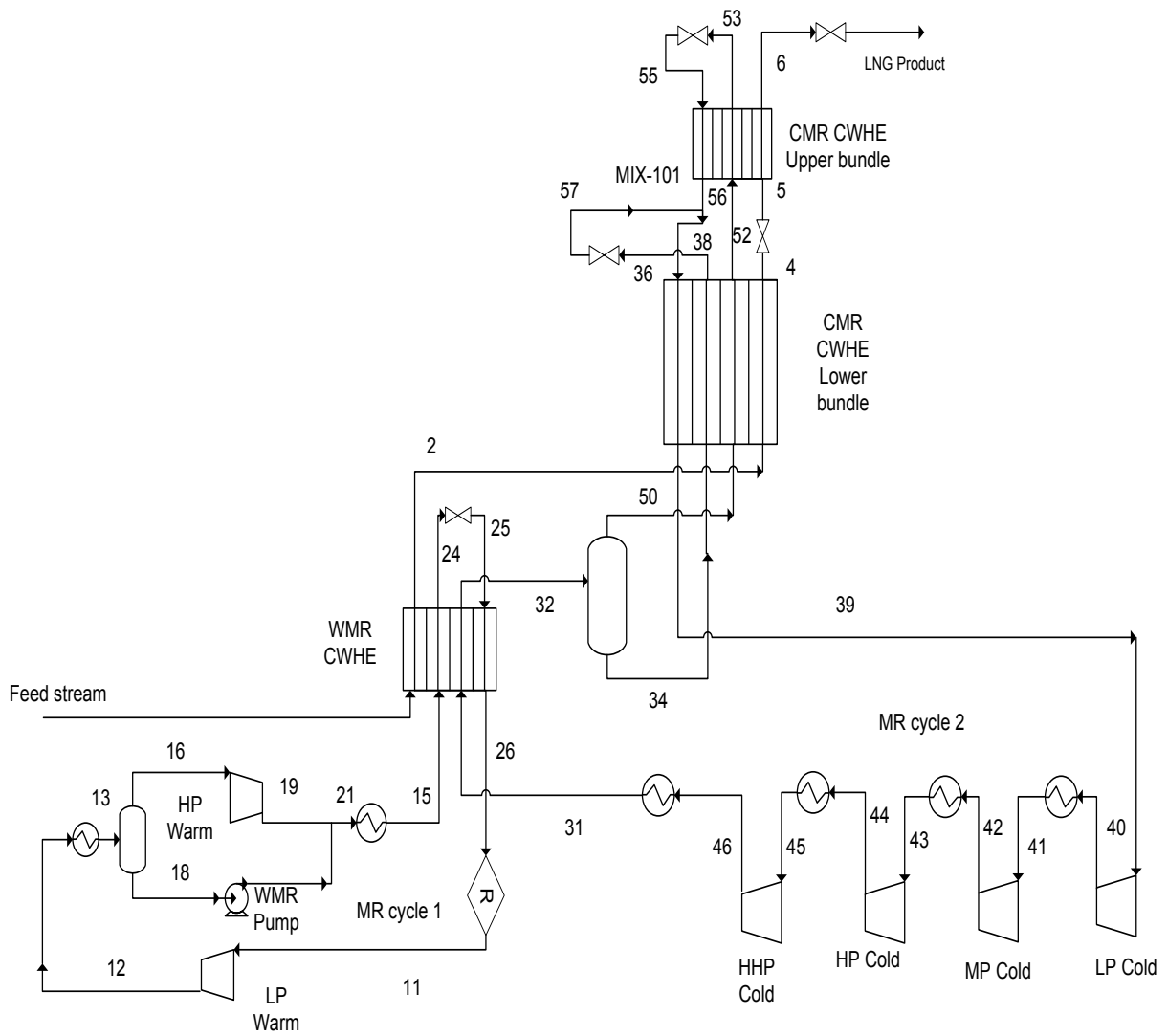


Figure 2: Model of APCIs DMR process with equipment labels

3. Assumptions & basis for comparison

3.1 Assumptions

Assumptions were established for undetermined data in the processes. The assumptions used in this Master thesis are the same as in the project thesis and a summary of the assumptions are given in Table 3.

Table 3: Assumptions for the simulations of liquefaction processes

Assumptions for simulations	
Both processes	
Temperature of refrigerant stream after water cooling (°C)	22
Min. Approach in heat exchangers, plate-fin and coil-wound (°C)	3
Adiabatic efficiency for expanders, compressors and pumps (%)	80
Pressure drop in water cooler heat exchangers (bar)	0
TOTAL turbo-expander	
High pressure nitrogen (bar)	70
Low pressure nitrogen (bar)	9-15
<i>Pressure drop heat exchangers</i>	
Low pressure side (bar)	0.3
High pressure side (bar)	0.5
CO2 system	
High pressure (bar)*	62
APCI DMR	
<i>Pressure drop in cryogenic heat exchangers (coil wound heat-exchangers)</i>	
Warm side (bar)	5
Cold side (bar)	0.3

**this pressure is slightly higher than the saturation pressure for CO2 at 22°C*

LM 6000 gas turbines are used as drivers for the compressors in all liquefaction circuits. The LM 6000 has an effective power output of 32 MW at a site condition with air temperature of 27°C. (Pettersen, 2013) The output of the gas turbine is increasing with decreasing air temperature. A study of possible weather condition of the FLNG site is not included and a power output of 32 MW is used throughout the study.

3.2 Natural gas composition entering liquefaction

The composition of the natural gas used in this Master thesis is the same as used in the project thesis. This is a lean gas composition consisting of almost 93% methane. The amount of C4+ is close to zero. A lean gas composition like this may be assumed to come from extraction unit prior to liquefaction for removal of

the heavy hydrocarbons (primarily C5+) in the stream. The extraction unit will not be considered in this report. The gas composition from is listed in Table 4.

Table 4 Gas composition entering liquefaction unit

Gas composition	
Component	Mole fraction
Methane	0.92960
Ethane	0.05000
Propane	0.00800
i-Butane	0.00300
n-Butane	0.00020
i-Pentane	0.00020
n-Pentane	0.00000
Nitrogen	0.00900
CO2	0.00000
Sum	1.00000

Some nitrogen is present in the gas composition as seen in Table 4. Nitrogen is an inert gas and will not contribute to the heating value of the gas. If the nitrogen content is too high, a flash gas system might be needed at the product outlet of liquefaction. A lean gas composition will require more energy in the liquefaction process because of the lower condensing temperature of the lighter hydrocarbons.

3.3 Conditions of natural gas entering liquefaction

The composition into the liquefaction unit is discussed in section 3.2. The gas exiting NGL extraction will require compression and cooling of the gas. The extraction system is not considered in this report as discussed earlier and the work of compression of the upstream gas to liquefaction is therefore not considered. Gas conditions after extraction of heavy hydrocarbons are showed in Table 5.

Table 5: Feed gas conditions entering the liquefaction unit

Feed gas conditions	
Temperature (°C)	22
Pressure (bar)	60
Mass flow (ton/hr)	440

The mass flow rate of the feed gas equals a LNG production of 3.5 Mtpa. This number is only valid if there is no end flash system in the liquefaction models and if sufficient power is available. The outlet LNG product will have a temperature of about -160°C and a pressure of around 1 bar.

4. Alternative configurations of the turbo-expander process

Two turbo-expander processes are looked at in this Chapter. These expander processes are slightly different than the turbo-expander process modeled in the project thesis when it comes to the nitrogen loop and the precooling section. These expander models are simulated to compare the turbo-expander processes and compare numbers of power consumption, refrigerant flow rate, volume flow and other parameters of interests to the existing simulations of the turbo-expander and DMR process. This section describes the two processes and the simulation procedure. The comparison between the processes is looked at in Chapter 8.

A turbo-expander process from APCI (Bukowski, 2011) and a turbo-expander process from US patent 5,768,912 (Dubar, 1998) are described in this Chapter. The simulations of these processes in Aspen HYSYS and results of the simulations are given in Chapter 5.

4.1 Turbo-expander process from APCI

The turbo-expander process from APCI (Bukowski, 2011) has a precooling unit and a nitrogen refrigerant loop for liquefaction and subcooling of the natural gas as can be seen in Figure 3. A main compressor compresses the warm refrigerant gas returning from a nitrogen-to-nitrogen heat exchanger. The compressed nitrogen gas is then divided into two separate streams routed to two different expanders for expansion and cooling of the nitrogen gas. The work released from the turbo-expanders are used to power two additional compressors to unload some of the work from the main compressor. Power needed to run the main compressor is supplied by LM 6000 gas turbines.

This liquefaction process is a relatively simple turbo-expander cycle where the nitrogen gas is used as an internal refrigerant in addition to cooling and liquefaction of the natural gas. There are several stream splits in the refrigerant circuit so the nitrogen gas can both cool the refrigerant stream returning from compression and the natural gas. The nitrogen stream will have about the same pressure reduction when going through the expanders seen in Figure 3. The temperature of the refrigerant will however be lower coming out of the 2nd expander because of cooling of this stream with a portion of nitrogen exiting from the 1st turbo-expander.

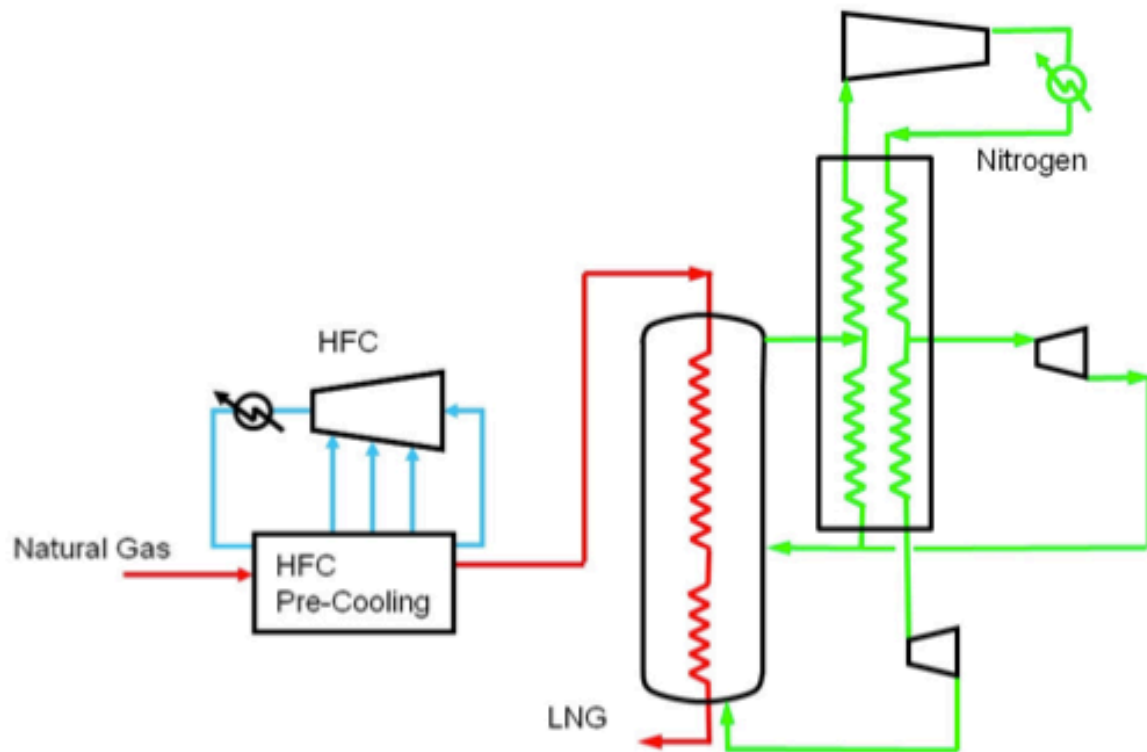


Figure 3: APCI turbo-expander (Bukowski, 2011)

Figure 3 illustrates the process with a precooling section placed upstream of the nitrogen loop to assist in the cooling of the natural gas. Hydrofluorocarbon (HFC) is suggested as the precooling refrigerant in this illustration as it is less flammable than the more conventional hydrocarbons used for precooling (Bukowski, 2011) Other suitable refrigerants such as propane or CO₂ can however be used and hydrofluorocarbon is substituted with CO₂ in the current simulation. CO₂ is used as the precooling refrigerant in the two other turbo-expander processes that are studied, and this gives a better basis of comparison between the three models. Hydrofluorocarbons must be imported at a high cost and the refrigerant will require a storage unit on the FLNG. HFC also have a much higher global warming potential than CO₂ and the use of hydrofluorocarbons should be avoided (ThinkGlobalGreen, 2008)

4.2 Turbo-expander process from U.S. patent

U.S patent number 5,768,912 (Dubar, 1998) describes a turbo-expander process for liquefaction of natural gas with nitrogen as the refrigerant. There are three versions of the liquefaction process described in the patent. The simpler version of the process, A, has two nitrogen expanders in parallel and no precooling of the feed gas or the refrigerant gas. The other versions, B and C, have three nitrogen expanders in parallel and a precooling unit for cooling of both the natural gas and the nitrogen refrigerant. The three versions are shown in Figure 4.

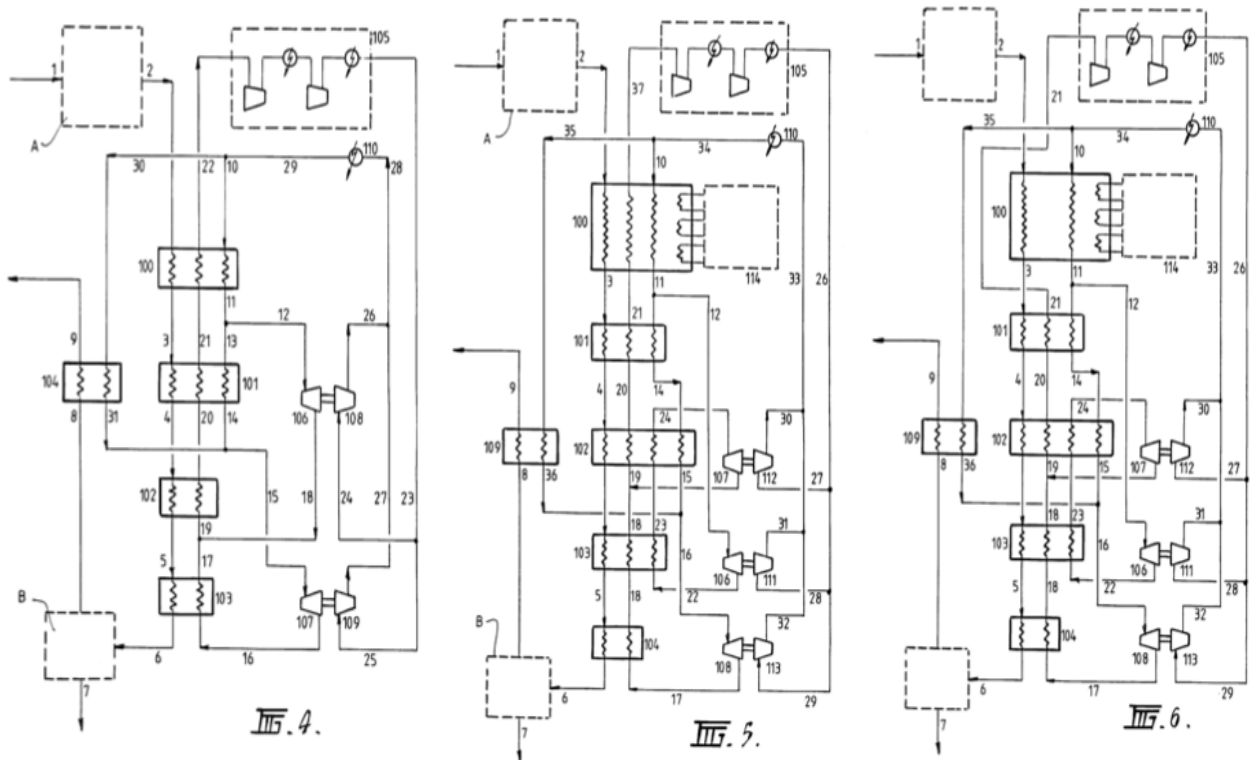


Figure 4: Three versions of the liquefaction process from U.S patent 5,768,912 showing versions A, B and C (Dubar,1998)

From Figure 4 it can be seen that the high-pressure nitrogen stream exiting from the main compressor in all three versions of the turbo-expander are split into separate streams for further compression. The compressors following the main nitrogen compressor are driven by power released from the expanders in a compander system. A third compander system is added in Versions B and C of Figure 4. This complicates the process with several split temperatures and pressure stages but will increase the efficiency of the process since there are more temperature levels to better match the cooling curve of the natural gas as it goes through the liquefaction unit. Versions B and C are improvements of Version A, where one portion of the nitrogen stream is expanded in two expanders with reheating of the stream before entering the second expander.

The nitrogen streams are mixed after compression and cooled down to ambient temperature. The compressed nitrogen is then split in two where a small portion of the nitrogen is cooled down by the end flash gas seen to the far left in Figure 4. This is simply a “cold recovery” feature. The larger portion of the stream goes through the first heat exchanger before it is split in two where one part goes through the warm expander while the rest of the nitrogen stream is cooled by cold nitrogen gas in a second heat exchanger. The nitrogen stream is then sent through the cold expander before it is routed through the heat exchangers as a cold nitrogen stream. This stream is mixed with the cold exiting stream from the warm nitrogen expander before it continues to the main compressor.

A precooling unit is added on processes B and C in Figure 4. The patent describes the precooling unit as a conventional refrigeration cycle. Refrigerants such as propane, “freon” or ammonia are suggested as the precooling media for the cycle (Dubar, 1998). Other refrigerants can be used and CO₂ is chosen as the precooling refrigerant to have a better basis of comparison with the other turbo-expander processes. CO₂ is also considered safer to use than the other refrigerants and it is easy to provide. CO₂ precools the warm stream of feed gas and nitrogen in the upper heat exchanger segment of this process.

Version C of the turbo-expander process is similar to Version B with precooling of the refrigerant and feed gas and with three compressor systems. The cold refrigerant stream in Version C is routed straight to compression instead of entering the upper heat exchanger segment with precooling of the natural gas and warm refrigerant. The advantage of this method is a lower temperature of the gas to compression than in Version B. The power consumption in the CO₂ system is expected to increase since the cooling power for the two warm streams in the upper heat exchanger will solely come from the precooling unit for Version C of the turbo-expander.

The end flash system is a semi-integrated part of this process and can unload some of the duty in the heat exchangers and reduce the amount of refrigerant needed. The end flash is considered to have a small flow rate and will only cool a small portion of the nitrogen stream in a heat exchanger. The two other turbo-expander processes described are simulated without end flash system and this will also be the basis for this process. Simulation of the processes with end flash is included as a separate study in Section 5.4.1 to see the effects of this system.

Larger models of the three versions of the turbo-expander from Figure 4 are included as attachments in Appendix A.

5. Simulations and results of the turbo-expanders from APCI and US Patent 5,768,912

5.1. Simulation of APCI turbo-expander process

A model with of APCIs turbo-expander process with equipment labels is included in Figure 5. The equipment labels are the same as in the HYSYS representation of the model from Figure 6 at the end of this Section.

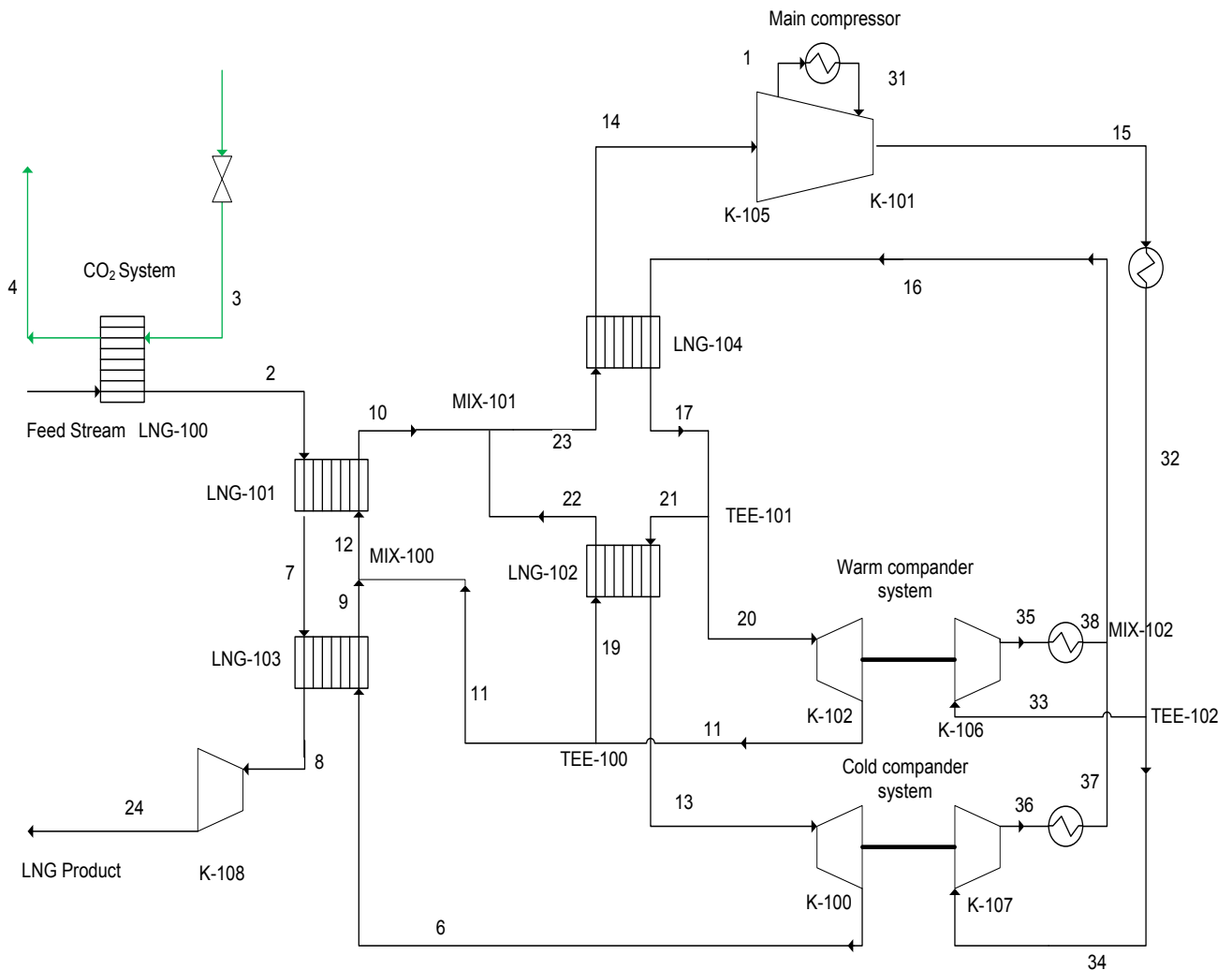


Figure 5: Model of APCI turbo-expander process with equipment labels

The Feed stream of natural gas enters LNG-100 for precooling of the feed. A simple two-stage CO₂-system with one evaporator temperature level was chosen as the preliminary precooling system to simplify the model and focus on optimization in the other parts of the process. Alternative configurations of the CO₂ system are considered in Chapter 7. The temperature out of the precooling is depended on the split temperature of the natural gas in Stream 7 and the mixing temperature of refrigerant in Stream 12. The temperature of the natural gas out of precooling should not be below -40°C due to the limit given by the

triple point of CO₂. The triple point of CO₂ occurs at -56°C and a pressure of approximately 5.2 bar. The natural gas was precooled down to -40°C in the simulation.

The split temperature of the natural gas in the cryogenic heat exchanger LNG-101 was set to -100°C at the starting point of the simulation. The exiting temperature of the liquefied gas was set to -160°C out of heat exchanger LNG-103. The split temperature was changed during the simulation of the process and a temperature of -96°C was the final split temperature for the modeling of the process. The temperature splits of the turbo-expander processes are also further investigated in Section 6.6.

The high pressure of the nitrogen was set to 70 bar according to the assumptions in Section 3.1. The compressor work was performed by a main compressor and side compressors powered by work from the two expanders. The main compressor was modeled in two stages with intercooling in between in order to reduce compressor power. Additional compressor stages with intercooling for the main compressor are looked at in Section 6.4. The added compressor power to compress the gas after the main compressor was linked to the two expanders K-100 and K-102 with the use of adjustment controllers in HYSYS. One adjuster was placed between compressor K-106 and stream 32 to regulate the pressure after main compressor K-101. Expander K-102 had the highest energy release and was linked to compressor K-106. The second adjuster was placed between compressor K-107 and TEE-103. The adjuster controlled the split ratio so the compressor power matched the energy released from expander K-100.

Many stream splitters and stream mixers made the modeling of the process more difficult with several degrees of freedom. Mixers MIX-100 and MIX-101 were set to "Equalize all" to simplify the simulation with the same pressure of the stream entering the mixer. The flow ratio in splitters TEE-100 and TEE-101 were variables and were adjusted in the process to achieve low LMTD temperatures in the heat exchangers.

All free variables in the simulation of the turbo-expander process are listed below:

- Temperature of natural gas in stream 7 after 1st heat exchanger LNG-101
- Exiting temperature of liquefied natural gas in stream 8 after 2nd heat exchanger LNG-103
- Pressure of nitrogen stream 1 after 1st pressure stage in main compressor K-105 before intercooling
- Temperature of warm nitrogen stream 17 going out of heat exchanger LNG-104
- Flow ratio of nitrogen in splitter TEE-101 after heat exchanger LNG-104
- Flow ratio of nitrogen in splitter TEE-100 after expander K-102
- Temperature of cold nitrogen stream 6 after 2nd expander K-100
- High pressure of CO₂ after 2nd high-pressure compressor in the CO₂ system
- Pressure of stream 4 in the CO₂ system after heat exchanger LNG-100

The low side pressure after the second expander, K-100, will be around 11-16 bar as stated in the assumptions in Section 3.1. If the pressure is too high for stream 6 when exiting expander K-100, liquid can form during the expansion of the gas. Nitrogen in liquid form should be avoided throughout the turbo-expander process and the pressure of stream 6 is therefore a limiting factor for this simulation. The extra compressor work will however be extensive if the pressure of stream 6 is too low. The low-pressure out of expander K-100 was 14.75 bar in the final model of the process.

The LNG pressure needs to be reduced to atmospheric conditions by a valve or a liquid expander after liquefaction. Temperature increase of the liquid LNG product is avoided with a liquid expander. A liquid expander was assumed and can also provide work to the main compressor. The energy release from liquid expander K-108 was subtracted from the total compressor work in the process.

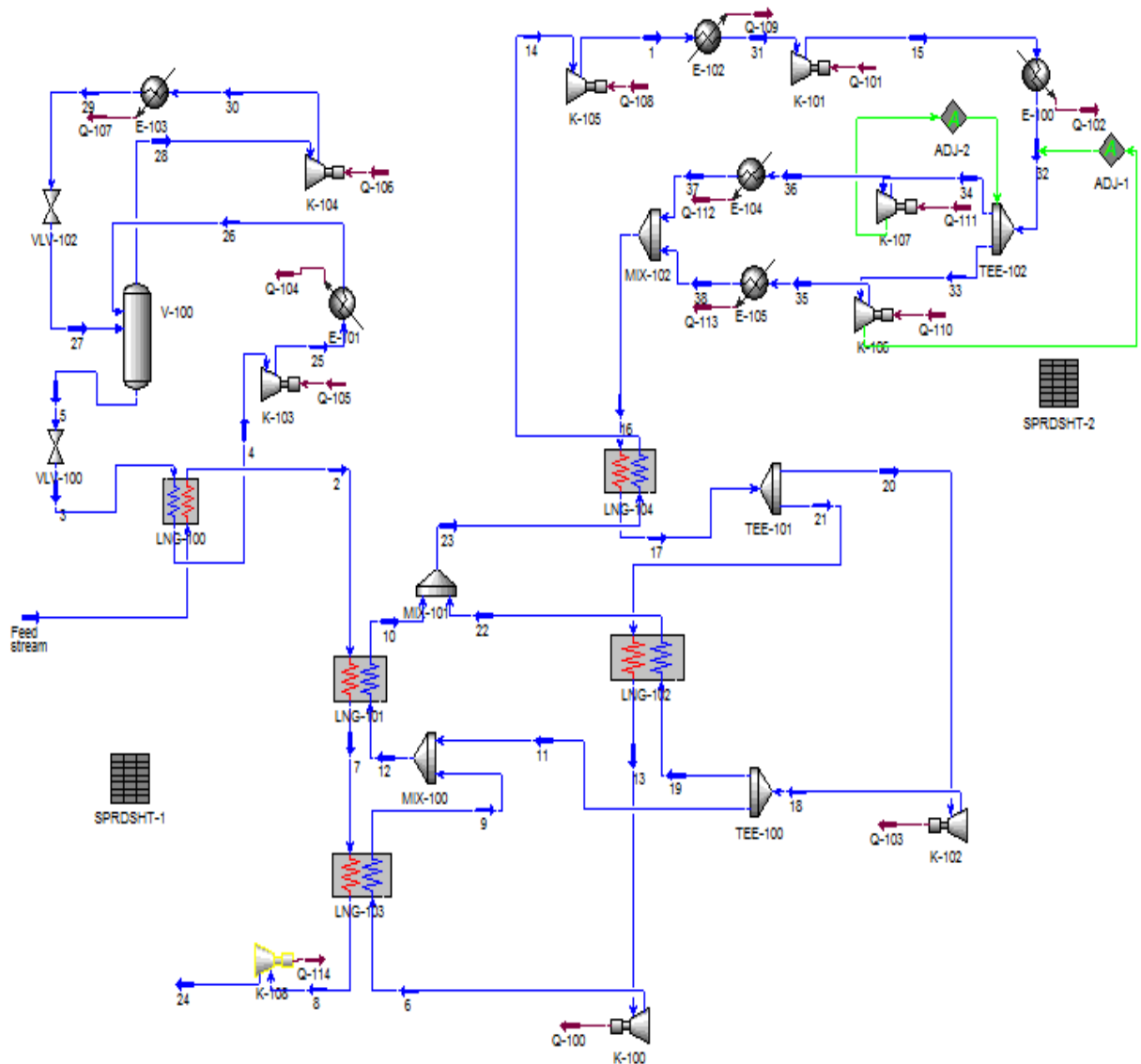


Figure 6: Simulation of APCIs turbo-expander process in HYSYS

5.2 Results from the simulation of APCIs turbo-expander

Results from the simulation of the process in Aspen HYSYS are listed in Tables 6-10. Parameters such as specific power consumption, work of the CO₂ system and refrigerant flow rate are included in the study in addition to volume flow rates and UA values for the heat exchangers. Driver configurations and number of trains are also evaluated.

Table 6 Results APCI turbo-expander with an LNG production of 3.5 Mtpa

Results APCI turbo-expander	
<i>Specific power consumption (kWh/ton LNG)</i>	
Total power consumption	405.7
CO ₂ system (kWh/ton LNG)	27.0
CO ₂ system of total power consumption	6.7%
<i>Refrigerant flow rate</i>	
Nitrogen (ton/hr)	4319.0
CO ₂ (ton/hr)	1109.4
Total refrigerant (ton/hr)	5428.4

The power consumption of the process is about 406 kWh/ton LNG. This is a relatively high number for a turbo-expander process. A turbo-expander process would normally have a specific power consumption of 350-400 kWh/ton LNG (Pettersen, 2013). The energy requirement for the CO₂ precooling of the natural gas is only about 7% of the total power need for the liquefaction process. This is not a critical number, but the power consumption of CO₂ system is still evaluated in Chapter 6. The flow rate of nitrogen and CO₂ in the process is high.

The volume flow rate of the refrigerant is important in determining the size of the compressors, which are dependent on the suction volume going in to the device. The pipe sizes necessary in the liquefaction process are also determined based on the volumetric flow rate. Volume flow rates for compressors and expanders are included in Tables 8 and 9. Heat exchanger properties are given in Table 7. The volume flow rates and UA values for the different processes are further discussed in Section 8.

Table 7: Heat exchanger values for APCIs turbo-expander

Heat exchanger	Minimum approach temperature (°C)	LMTD (°C)	UA (MJ/C-h)
Feed - CO ₂ LNG-100	3.0	19.0	4,160
Feed - N ₂ LNG-101	3.2	7.1	24,350
Feed - N ₂ LNG-103	3.0	5.9	17,750
N ₂ - N ₂ LNG-104	3.1	5.6	52,560
N ₂ - N ₂ LNG-102	4.6	5.5	22,960

Heat exchanger LNG-100 between the feed gas and CO₂ is the least efficient from Table 7 according to the LMTD values. A LMTD value of 19°C in the heat exchanger indicates that the CO₂ system should be evaluated. The UA value for this exchanger is small. The LMTD value in the upper Feed-N₂ heat exchanger LNG-101 is high with a value of 7.1°C as seen in Table 7.

Table 8: Volume flow rates of expanders in APCIs turbo-expander process

	Cold expander outlet K-100	Warm expander outlet K-102	LNG product expander K-108
Volume flow (m ³ /h)	20,740	93,570	1,228

Table 9: Suction volume of compressors in APCIs turbo-expander process

	Main compressor inlet K-105	Main compressor inlet K-101	Comander compressor K-107	Comander compressor K-106
Volume flow (m ³ /h)	278,000	154,300	16,230	70,740

The warm expander outlet K-102 has a volume flow rate of 93,570 m³/hr as seen in Table 8. This is a much higher volume flow rate than the outlet from cold expander K-100 with a volume flow of 20,740 m³/hr. The need for refrigerant in the “warm” part of the process is high and refrigerant from warm expander K-101 provides refrigerant to the internal nitrogen heat exchanger LNG-102 and to the feed-nitrogen heat exchanger LNG-101. The inlet to the main compressor has the highest volume flow rate of refrigerant throughout the process with 278,000 m³/hr. Volume flows of expander outlets and suction volumes of the compressors are further investigated in Chapter 8. The volume flows in Tables 8 and 9 are based on the simulation of the process with a production capacity of 3.5 Mtpa and will be the total value for all liquefaction trains in the process.

Table 10: Compressor and expander work for APCIs turbo-expander

Compressor & expander work in liquefaction process	
Compressor work	
<i>Nitrogen cycle</i>	
1 st stage of main compression in K-105 (MW)	85.3
2 nd stage of main compressor in K-101 (MW)	82.6
Total compressor work nitrogen cycle (MW)	167.9
<i>CO2 cycle</i>	
Low pressure compressor (MW)	7.8
High pressure compressor (MW)	4.1
Compressor work CO2 cycle (MW)	11.9
Total compressor work (MW)	179.8
CO2 % of total compressor work	6.7%
Expander power released	
Warm nitrogen expander K-102	55.0
Cold nitrogen expander K-100	12.6
Work from liquid LNG-expander K-108 (MW)	1.3
Total expander work (MW)	68.9

Table 10 shows the distribution of energy consumption and power generation in the process. The main compressor has two compressor stages with intercooling between. The pressure between the compressor stages is selected to have the same temperature increase of refrigerant in each stage to minimize thermodynamic losses in the process. This results in power consumptions of 85.3 MW and 82.6 MW for the two stages of main compression shown in Table 10. The power release from liquid expander K-108 is subtracted from the total compressor power in the system. Work from expanders K-102 and K-100 are used to power the compressors in the compander system.

The number of trains required for the process is determined by the power generated by the expanders in the compander systems. A compander system has a maximum proven capacity of ca. 15 MW (Pettersen, 2013) The power from each of the expanders is listed in Table 10. The power release from expanders K-102 and K-100 is respectively 55 MW and 13 MW. A total of 4 trains are hence required for an expansion power of 55 MW. A number of 4 trains will increase the equipment and pipes needed for the liquefaction process. Smaller production capacities per train can have smaller equipment at lower costs.

LM 6000 gas turbines are chosen as the drivers to run the compressors in the liquefaction system. The number of gas turbines required for the process is determined by the total power consumption of the compressors. The total power requirement for the process is 180 MW as seen in Table 10. An LM 6000 gas turbine has an effective power output of about 32 MW at the assumed site conditions specified in Section 3.1. A total number of 6 LM 6000 gas turbines are

required to run the liquefaction process. A number of four liquefaction trains and six drivers creates unbalanced load for the gas turbines with mechanical drive of the compressors and six LM 6000 gas turbines will not be sufficient to power the process. The process is suggested with electric drive to maintain a production capacity of 3.5 Mtpa split in four trains. Mechanical vs. electric drive for the processes are discussed in Section 8.11.

5.3 Simulation of turbo-expander process from US patent 5,768,912

The three versions of the turbo-expander process from US patent 5,768,912 in Figure 4 in Section 4.2 were simulated to see the effects in power consumption with and without precooling of the natural gas and nitrogen and the effects of using three compressor systems instead of two. The simulation steps described in this Section are for Version C of the process, but the simulations of the two other processes were similar. Figure 7 shows a model of Version C with the same equipment labels as used in the simulation of the process. The HYSYS model of the process is included at the end of this Section in Figure 8.

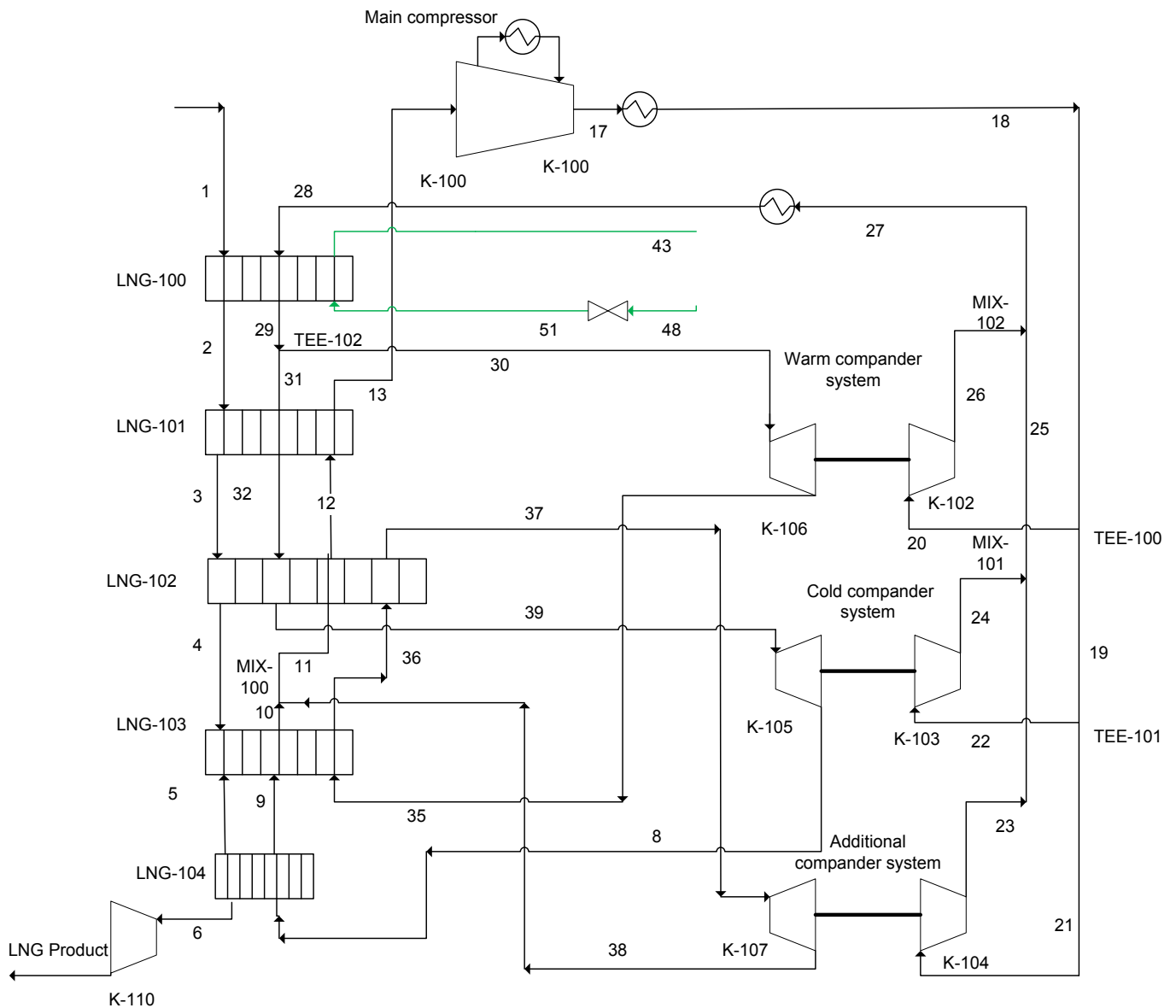


Figure 7: Model of expander process from US patent 5,768,912

The patent describes the liquefaction process with suggestions to pressure levels and split temperatures in the heat exchangers (Dubar, 1998). The patent suggest a temperature of -30°C of the feed gas after precooling in heat exchanger LNG-100. A temperature of -82°C after the 3rd heat exchanger LNG-102 and an exiting temperature -152°C for the feed gas is also suggested in the patent (Dubar, 1998). The temperature of the precooling was set to -30°C in the simulation while the temperature out from heat exchanger LNG-102 was changed to -84°C . The two other turbo-expander processes had exiting temperatures of -160°C and this temperature should be the same for all the studied liquefaction processes. Set controllers and heat exchanger specifications between the streams were used in the simulation of the process to ensure that the warm streams exiting from the heat exchanger segments had the same temperature. The split temperatures of feed gas after heat exchanger LNG-101 and LNG-103 were not

free variables and had split temperatures of respectively -51°C and -100°C for the described model.

A pressure after main compressor of 30 bar and a high pressure of 50 bar is suggested in the patent (Dubar, 1998) The high pressure of nitrogen was changed to 70 bar as stated in Section 3.1. The pressure after the main nitrogen compressor K-101 was determined based on the compressor power in the compander system. The main compressor was modeled in two steps with intercooling in between. The low-pressure in the process after temperature and pressure reduction in cold expander K-105 was 9.2 bar.

Adjusters were used in the simulations to meet the power requirements between the expanders and the compressors in the compander systems. Three adjusters were used for the modeling of the process. The first adjuster was placed between stream 18 and compressor K-102 to regulate the pressure after the main compressor. Expander K-106 with the highest energy release was paired up with compressor K-102 so the pressure after main compression was set as low as possible. A second adjuster was placed between compressor K-103 and TEE-100. The adjuster controlled the flow ratio in the splitter so the power consumption of the compressor would match the energy release from cold expander K-105. Adjuster number three was placed between compressor K-104 and splitter TEE-101. Compressor K-104 was powered by additional expander K-107.

All free variables in the simulation of the turbo-expander process are listed below:

- Temperature of feed stream 2 and warm nitrogen stream 29 after precooling in 1st heat exchanger LNG-100
- Split ratio of nitrogen streams 30 and 31 in TEE-102
- Temperature of feed stream 4 and warm nitrogen stream 39 after 3rd heat exchanger LNG-102
- Exiting temperature of liquefied natural gas in stream 6 after 5th heat exchanger LNG-104
- Temperature of cold nitrogen stream 8 going in to heat exchanger LNG-104 after cold expander K-105
- Temperature of cold nitrogen stream 9 exiting heat exchanger LNG-103
- Pressure in stream 35 after warm expander K-106
- Temperature of cold nitrogen streams 12 and 37 after heat exchanger LNG-102
- Pressure of nitrogen stream 38 after additional expander K-107
- Pressure of nitrogen stream 15 after the 1st compressor stage of main compressor K-100
- Pressure after high-pressure compressor in the CO₂ system
- Pressure of stream 43 in the CO₂ system after heat exchanger LNG-100

The precooling system for the turbo-expander process described in this Section precools both the feed gas and the warm nitrogen refrigerant in heat exchanger LNG-100. The CO₂ system chosen for this process was the same as for the two other turbo-expander processes with two pressure stages, an open intercooler

and one evaporation stage of the CO₂. This model is shown in Figure 12 in Section 7.1. Models of Versions B and C in the patent suggest a precooling system with three evaporation stages of CO₂. Precooling system with two and three evaporation stages are investigated for the turbo-expander processes in Chapter 7.

The results given in Section 5.4 are based on simulations of the three Versions without end flash. A liquid expander is used for pressure reduction of the LNG product. The end flash system is described in Section 5.4.1 for Versions of the turbo-expander process.

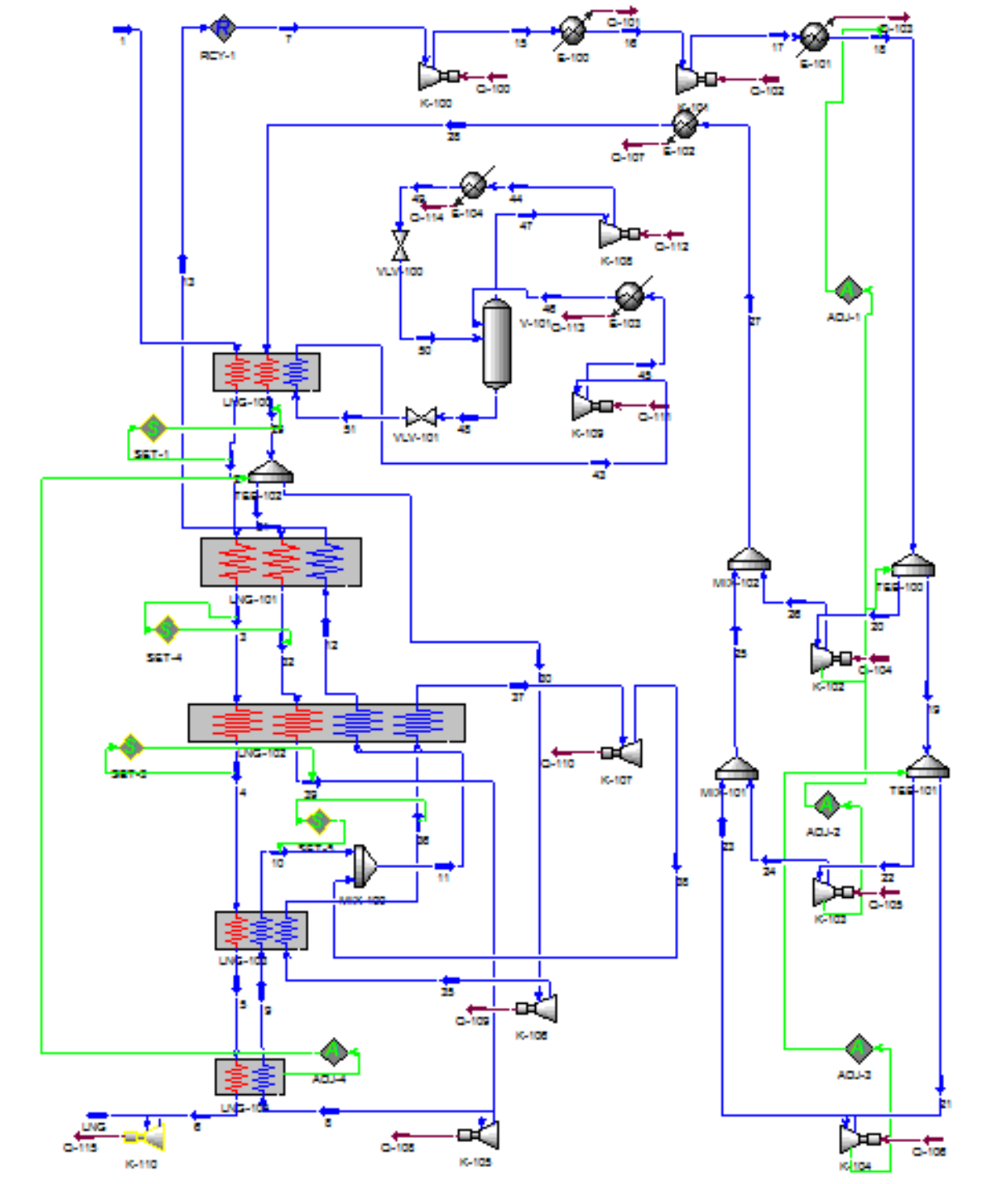


Figure 8: HYSYS model of US patent 5,768,912

5.4 Results from the simulations of turbo-expander from US patent 5,768,912

Values of specific power consumption, power consumption of CO₂ system and expander power for all three Versions of the turbo-expander process are included in Table 11.

Table 11: Results from simulations of Versions A, B and C

	Turbo-expander Version A	Turbo-expander Version B	Turbo-expander Version C
Specific power consumption (kWh/ton LNG)	459.5	448.0	422.5
Power consumption CO ₂ system (kWh/ton LNG)	-	10.4	30.7
CO ₂ system of total power consumption	-	5.3%	16.5%
Mass flow rate nitrogen (ton/hr)	4689.0	3147.0	3147.0
Power outlet warm expander (MW)	73.4	28.7	28.7
Power outlet cold expander (MW)	15.5	21.5	21.5
Power outlet additional expander (MW)	-	16.0	16.0

Version B of the turbo-expander process has a specific power consumption of 2.6% less than Version A from Table 11. This is due to an added CO₂ precooling system in the process and an additional expander in this Version. The power outlet of the warm expander is 73 MW for Version A. This is a large compander capacity and Version A would require 5 production trains in the process. The duty of the warm expander decreases with an additional expander and with a lower refrigerant flow rate due to the added precooling system. The specific power consumption of Version 3 is 8.8% lower than for Version A and 6% lower than for Version B because of a lower temperature of nitrogen to compression. The refrigerant flow rate for Versions B and C are the same with the same expander power. Version C of the expander process has a CO₂ a higher load of the CO₂ system and accounts for 16.5% of the total power consumption for the process as seen in Table 11. The graphs in Figure 9 shows the temperatures vs. heat flow curves for the 1st heat exchanger segment for all three versions of the turbo-expander process.

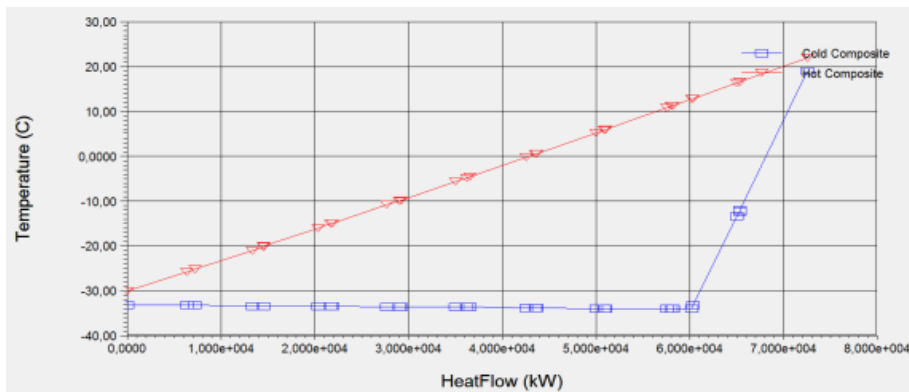
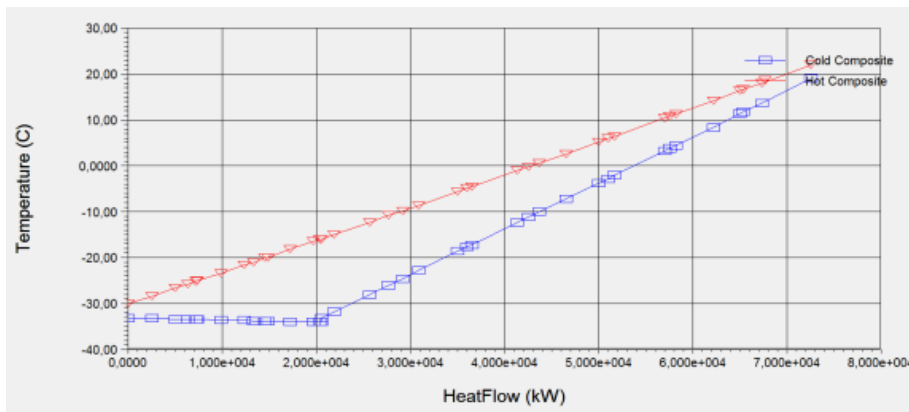
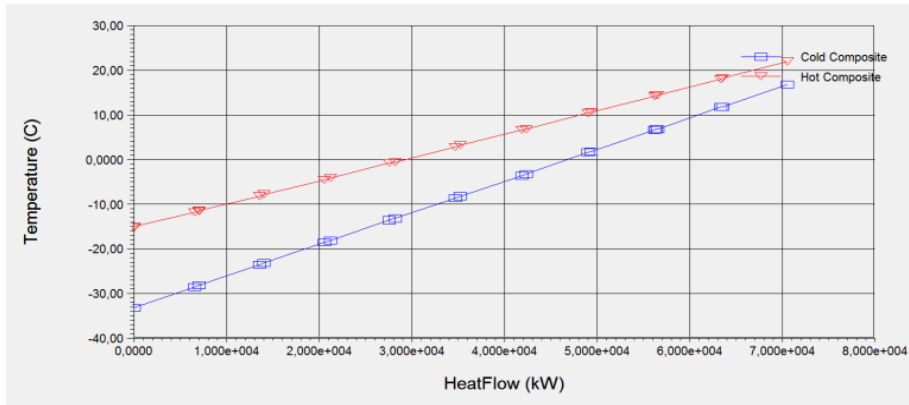


Figure 9: Heat flow curves for Versions A, B and C

The 1st graph in Figure 9 shows the temperature curve of the upper heat exchanger segment of Version A. The heating curve in the graph is the heating curve of nitrogen refrigerant only. The gap in the cold end of the 1st heat exchanger is higher for this process. The 2nd graph shows the temperature curves for Version B and the heating curve of refrigerant is the combined curve for nitrogen and CO₂. The gradient of the curve changes when CO₂ is introduced and creates a smaller gap between the curves in the cold end. The 3rd graph shows the temperature curves for Version C of the turbo-expander process. The temperature curve of refrigerant is constant before the CO₂ is superheated at the warm end of the heat exchanger.

Version C has the numbers in terms of energy consumption and is chosen for the further study of this turbo-expander process. Heat exchanger properties and volume flow rates are listed in the Tables 12-14.

Table 12: Heat exchanger values for Version C

Heat exchanger	Minimum approach temperature (°C)	LMTD (°C)	UA (MJ/C-h)
Feed-N2-CO2 LNG-100	3.0	15.7	16,630
Feed - N2 LNG-101	3.0	3.2	22,660
Feed - N2 LNG-102	3.0	5.0	38,630
Feed - N2 LNG-103	3.2	4.9	6,947
Feed - N2 LNG-104	3.0	5.2	18,560

The minimum approach temperature in all heat exchangers segments are close to the minimum approach temperature of 3°C as seen in Table 12. The LMTD values for the heat exchangers are relatively low except for CO2 heat exchanger LNG-100 with a LMTD value of 15.7°C. The CO2 system is evaluated in Chapter 7.

Table 13: Volume flows of the expander outlets of Version C

	Cold expander outlet K-105	Warm expander outlet K-106	Additional expander K-107	LNG product expander K-110
Volume flow (m3/h)	43,250	46,500	111,500	1,234

Table 14: Volume flows of the compressor suction of Version C

	Main compressor inlet K-100	Main compressor inlet K-101	Companion compressor K-102	Companion compressor K-103	Companion compressor K-104
Volume flow (m3/h)	305,200	124,600	31,890	23,750	17,820

The additional expander K-107 has over twice the volume flow from expansion of the gas compared with the two other nitrogen expanders with a value of 111,500 m3/hr seen in Table 13. The cold stream from warm expander K-106 is heated in heat exchangers LNG-103 and LNG-102 before entering the additional expander K-107. The refrigerant flow rate is equal through these expanders, but the volume flow from the additional expander is larger because of higher temperature and lower pressure of the nitrogen. The volume flow of the liquid LNG product is minor and only a small liquid expander will be needed for expansion of the liquid.

The volume flow to main nitrogen compressor K-100 is high due to the low refrigerant pressure of 7.3 bar entering compression. The inlet temperature to compression is low with a temperature of -33°C for the nitrogen refrigerant. The volume flow to companion K-102 is the highest of the compressor companions with a volume flow of 31,900 m3/hr as seen in Table 14. This was expected since

this compressor is powered by the expander with highest energy production, K-106, in the compander system.

Table 15: Compressor and expander work for Version C

Compressor & expander work in liquefaction process	
Compressor work	
<i>Nitrogen cycle</i>	
Main compressor K-100 before intercooling (MW)	101.5
Main compressor K-101 after intercooling (MW)	55.0
Total compressor work nitrogen cycle (MW)	156.5
<i>CO2 cycle</i>	
Low pressure (MW)	16.9
High pressure (MW)	13.8
Compressor work CO2 cycle (MW)	30.7
Total compressor work (MW)	187.2
CO2 % of total compressor work	16.5%
Expander power released	
Warm expander K-106 (MW)	28.7
Cold expander K-100 (MW)	21.5
Additional expander K-107 (MW)	16.0
Liquid LNG-expander K-110 (MW)	1.2
Total expander work (MW)	67.4

Table 15 lists power consumption for compressors in the process and released power from the expanders. Numbers in the table shows that the CO2 system accounts for as much as 16.5% of the total energy consumption for the process. Several trains are necessary for a liquefaction processes with a capacity of 3.5 Mtpa with limiting compander capacities. The expander process with the highest release of energy is warm expander K-106 with a value of 29 MW. Two trains with compander capacities of 15 MW are the minimum number of liquefaction trains required in the process. Three trains should possible be considered with an expansion power close to the maximum compander capacity, but two liquefaction trains are assumed for this turbo-expander in the discussion of the processes in Chapter 8.

LM 6000 gas turbines are previously introduced as drivers for the compressors in the liquefaction processes. The total power consumption of the process determines the number of gas turbines required when assuming a power output of 32 MW for the turbines. Total compressor work from Table 15 is about 187 MW and a number of six LM 6000 gas turbines are needed to power the liquefaction trains. Electric motor drive is considered for this process.

5.4.1 Evaluation of the integrated end flash system of U.S patent 5,768,912

An end flash system is necessary if there is high nitrogen content in the end product of LNG. A high nitrogen content in the LNG decreases the heating value of the natural gas. The composition of the feed gas used in the simulations of the processes has low nitrogen content and a flash system is not required in the turbo-expander processes. This Section evaluates the use of a “cold recovery” feature from an integrated end flash of the expander process as seen in Figure 4 in Section 4.2. All three Versions of the turbo-expander are studied with an integrated end flash in this Section.

The liquid LNG expander is replaced by a Joule-Thompson valve in the simulations to produce flash gas in the process. Cold end flash from a separator downstream of the valve is routed through a heat exchanger and cools a small portion of nitrogen stream at ambient temperature exiting from compression. A refrigerant fraction of about 0.01-0.03 is sent to cooling by the end flash while the rest of the nitrogen stream is sent through the 1st nitrogen-feed heat exchanger as a warm stream. The fraction of the nitrogen stream is cooled to -120°C by the flash gas at a temperature of approximately -160°C. The small fraction of cold nitrogen stream is mixed together with the warm nitrogen stream after cooling of the larger portion in several heat exchangers. The mixed stream is then routed to the cold expander in the process for further temperature reduction. The results from the simulations are given in Table 16.

Table 16: Results from simulations with integrated flash gas

	Turbo-expander version 1	Turbo-expander version 2	Turbo-expander version 3
Specific power consumption (kWh/ton LNG)	462.8	450.3	424.4
Power consumption CO2 system	-	10.3	30.5
Mass flow rate nitrogen (ton/hr)	4657.0	3136.0	3136.0
<i>Cold expander</i>			
Entering temperature (°C)	-95.41	-84.4	-84.4
Power cold expander (MW)	15.5	21.3	21.3
Volume flow cold expander (m3/hr)	27,140	42,700	42,700
<i>Flash gas heat exchanger</i>			
LMTD (°C)	6.1	6.1	6.1
UA (MJ/C-hr)	461.6	459.7	459.7

The specific power consumption for all processes is approximately 2 kWh/ton LNG higher in Table 16 than for the processes without end flash in Table 11. This indicates that a liquid expander for the product LNG is more energy efficient than an integrated flash system for these simulations. The specific power consumption in Table 16 is divided by the LNG production excluding the flash gas.

The temperature to the cold expander in Versions B and C of the turbo-expander decreases by -0.4°C from a value of -84°C in the original models without end flash. The expansion power decreases from 21.5 MW to 21.3 MW for Version B and C as seen in Table 16. This is due to the small reductions in circulation rate of refrigerant in the process and the slightly lower temperature to expansion. The reduction in nitrogen flow rate is however most likely caused by small differences in LMTD values of the heat exchangers and not by the integrated end flash system. The LMTD and UA values for the flash gas heat exchanger is similar from Table 16.

6. Evaluation of different process parameters

The effects of changing different parameters in the liquefaction processes are studied in this Section. All four liquefaction processes are included in the evaluation of parameters; APCIs DMR process (Bukowski, 2011) and the turbo-expander processes from TOTAL (Chrétien, 2011), APCI (Bukowski, 2011) and US patent 5,768,912 (Dubar, 1998). The idea of this study is to see how changes in process parameters influences energy consumption and other qualities of the different processes. The efficiency of the liquefaction processes is influenced by several parameters:

- Composition of the feed gas
- Inlet pressure of the feed gas
- Temperature of cooling water used in the process
- Number of compressor stages for the main compressor
- High pressure of nitrogen after compression
- Split temperatures of the refrigerant and natural gas
- The use of polytropic vs. adiabatic efficiency for the rotating equipment

Effects of volume flows of refrigerant in rotating equipment, power production of expanders and properties of heat exchangers are also included in this study. The suction volume to compression and expansion will have a great dependence of equipment size and pipe diameters in the liquefaction process. The power production of the expanders will also determine the number of trains required for the process. A study like this can be of importance if the FLNG is to be placed in a colder environment or operate with different feed conditions of the gas. This study will also show if the turbo-expander processes are more sensible to changes in the parameters described above than the DMR process.

Models with equipment labels for the study is found in Figures 1 and 2 in Chapter 2 for TOTALs turbo-expander process and APCIs DMR process. Models of APCIs turbo-expander and the turbo-expander from US patent 5,768,912 are found in Figures 5 and 7 in Chapter 5. This Chapter compares the results in the study with the original results from the simulations of the processes previously found in the project thesis and in Chapter 5. The total values of power consumption, volume flows and flow rates of refrigerant for all trains in the different processes are used in the study.

6.1 Richer feed gas composition

The gas composition used in the simulation of the processes was a relatively lean gas composition consisting of 93% methane. The gas composition can be seen in Table 4 in Section 3.2. A richer composition of the gas is studied in this Section for the DMR process and the turbo-expander processes. Higher fractions of heavier hydrocarbons will give a higher condensing temperature with increased boiling point of the gas and thus increase process efficiency. The richer gas composition studied in this Section is found in TOTALs article and is used in their simulation of the turbo-expander process (Chrétien, 2011). The gas composition is seen in Table 17.

Table 17 Gas composition from TOTALs article (Chrétien, 2011)

TOTALs gas composition	
Component	Mole fraction
Methane	0.91625
Ethane	0.06040
Propane	0.01690
i-Butane	0.00278
n-Butane	0.00300
i-Pentane	0.00019
n-Pentane	0.00007
Nitrogen	0.00036
CO ₂	0.00005
Sum	1.00000

The fraction of methane in Table 17 is lower than for the original gas composition while the fraction of ethane, propane and C₄+ is slightly higher. The gas composition in Table 17 has less nitrogen present in the feed gas than the original composition and a small trace of CO₂.

A richer feed gas gave a reduction in approach temperature from 3°C to 0.7°C in heat exchanger LNG-100 in TOTALs process seen in Figure 1 of Chapter 2. The volume flow of nitrogen was adjusted so a larger portion of the warm nitrogen stream was sent to precooling. This resulted in a larger stream of cold nitrogen through the second heat exchanger LNG-101 and hence a colder entering stream to the upper heat exchanger. The influence of a richer gas in terms of power consumption and volume flows for TOTALs process is found in Table 18.

A richer gas composition decreased the temperature of the feed gas in APCIs expander process from -40°C to -42°C when exiting precooling heat exchanger LNG-100 seen in Figure 5 of Chapter 5. This is a too low temperature out from precooling when considering the triple point of CO₂. Splitter TEE-101 was adjusted to send more refrigerant to expansion and through the upper heat exchanger LNG-101 to increase the temperature from precooling back to -40°C. The LMTD value for the feed – nitrogen heat exchanger LNG-101 increased from 7.1°C to 8.9°C with a richer feed gas. The influence of a richer gas in terms of power consumption and volume flows for APCIs expander process is found in Table 18.

The LMTD values in the heat exchangers of the expander process from US patent increased with a richer feed composition of the gas. The pressures after warm expander K-106 and additional expander K-107, seen in Figure 7 of Chapter 5, was increased in the study to decrease LMTD values in the heat exchangers. The influence of a richer gas in terms of power consumption and volume flows for the US patent process is found in Table 18.

Table 18: Comparison of the turbo-expander processes with a richer feed gas

	TOTAL turbo-expander (4 trains)		APCI turbo – expander (4 trains)		US Patent turbo-expander (2 trains)	
	Original	Study	Original	Study	Original	Study
Specific power consumption (kWh/ton LNG)	395.8	391.8 (-1.0%)	405.7	400.6 (-1.3%)	422.5	411.4 (-2.7%)
Nitrogen flow rate (ton/hr)	3973.0	3944.0	4319.0	4254.0	3147.0	3166.0
Volume flow to main compressor (m3/hr)	263,500	261,500	278,000	273,900	305,200	287,400
Power consumption CO2 process (MW)	15.7	15.7	11.9	12.3	30.7	31.0
Warm expander						
Power production (MW)	48.5	48.7	55.0	54.5	28.7	27.7
Volume flow outlet (m3/hr)	84,070	84,290	93,570	92,830	46,500	44,310
Cold expander						
Power production (MW)	12.6	12.9	12.6	12.2	21.5	21.6
Volume flow outlet (m3/hr)	20,930	20,330	20,740	20,090	43,250	43,510
Additional expander (US patent)						
Power production (MW)	-	-	-	-	16.0	16.4
Volume flow outlet (m3/hr)	-	-	-	-	111,500	105,000

The turbo-expander process from US patent has the highest decrease in specific power consumption of 2.7% from Table 18. The flow rate of refrigerant in this process is higher because of less efficient heat exchangers with higher LMTD values. The power production from the expanders in all processes remains about the same and the number of trains required in the liquefaction process is unchanged. The volume flows entering and exiting rotating equipment is about the same for TOTALs and APCIs processes. The volume flow to the main compressor in the US patent model is however reduced by 6% due to a higher incoming pressure of refrigerant to compression.

The DMR process is dependent on the boiling point of the mixed refrigerant in the process. A richer composition of the gas causes a small fraction of liquid to the 1st compressor LP COLD in the 2nd MR cycle. The equipment labels are found in Figure 2 of Chapter 2. The temperature from the first cryogenic heat exchanger WMR CWHE is increased to avoid liquid formation. The LMTD value in the lower bundle of heat exchanger CMR CWHE increases from 6.9°C to 7.8°C with the adjustment of inlet temperature of the heat exchanger. Lowering the pressure in the 2nd MR cycle can also prevent liquid in the compressor. The influence in compressor power and volume flows are seen in Table 19.

Table 19: Results for DMR process with a richer feed composition

	APCI DMR (1 train)	
	Original	Study
Specific power consumption (kWh/ton LNG)	284.0	283.8 (<0.1%)
Refrigerant flow rate (ton/hr)	2412.6	2412.6
<i>1st MR circuit</i>		
Power consumption of LP Warm (MR)	20.1	20.1
Volume flow to LP Warm (m3/hr)	105,900	105,800
<i>2nd MR circuit</i>		
Power consumption LP Cold (MW)	39.0	38.9
Volume flow to LP Cold (m3/hr)	159,200	159,100

A decrease in specific power consumption of less than 0.1% for the DMR process is seen in Table 19. The volume flow to compression is decreased with 100 m3/hr for each of the MR cycles.

A higher condensing temperature of the gas due to a richer feed composition has highest effect for the turbo-expander processes seen in Table 18. Small changes in volume flow for the equipment in the processes is not expected to influence the size of the equipment. A richer gas composition from upstream extraction can be evaluated for the liquefaction processes if the heating value of the product LNG is within the specifications of the market.

6.2 Increased feed gas pressure

An initial feed gas pressure of 60 bar was used in the simulations of all four liquefaction processes. The entering pressure of feed gas could be the pressure from an upstream compressor after extraction of heavy hydrocarbons from the gas. A pressure of 80 bar of the feed gas is tested in this section. This was the pressure introduced in TOTALs article when describing the turbo-expander process (Chrétien, 2011).

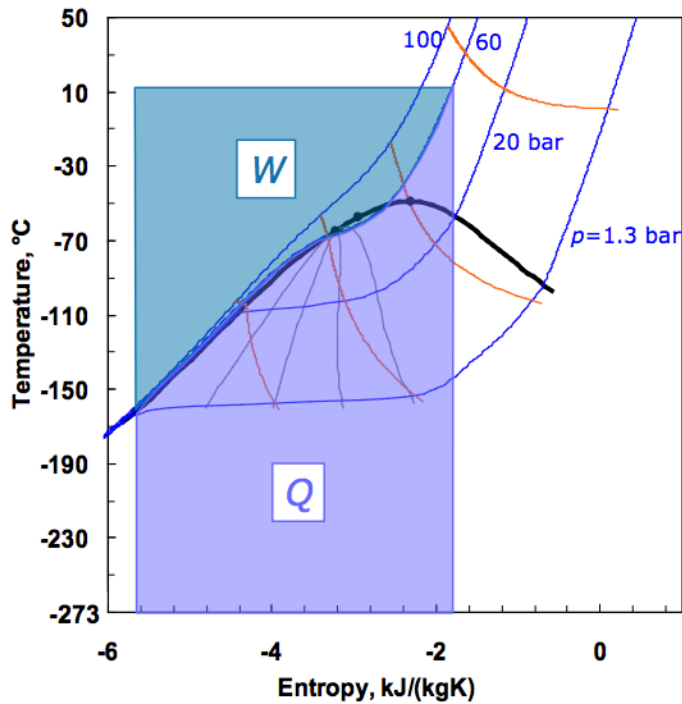


Figure 10: TS-diagram showing liquefaction of the gas at 60 bar (Pettersen, 2012)

Figure 10 shows the work and heat removed for an ideal liquefaction process in a temperature-entropy diagram. The natural gas will follow the lines of constant pressure during condensation of the gas. The Q in Figure 10 symbolizes the heat removed from the process in liquefaction of the gas while the W represents the ideal work done by the compressors in the process. The work area will decrease while the area of heat removed in the process increases with increasing pressure of the feed gas as seen in Figure 10. The natural gas will start to condensate at a higher temperature with a higher inlet pressure of the feed. The ambient temperature used in the simulations of the processes is 22°C and the ideal work area will be larger than the area seen in Figure 10, which has an ambient temperature of 10°C. The work will not be ideal in an actual liquefaction process due to pressure losses through heat exchangers and loss of energy due to heating of the refrigerant in the compressors.

Increasing the feed gas pressure to 80 bar in TOTALs expander process increases the minimum approach temperature to about 4°C in heat exchanger LNG-100 from Figure 1 in Chapter 2. A lower refrigerant flow to precooling and expansion will increase the amount of warm nitrogen going through the second heat exchanger segment LNG-101. This increases the temperature of the cold nitrogen stream and an approach temperature of 3°C is then obtained in heat exchanger LNG-100. The influence of a higher feed gas pressure in terms of power consumption and volume flows for TOTALs process is found in Table 20.

The temperature after precooling of the feed in APCIs expander process increases from -40°C to -30°C when introducing a higher pressure of the feed gas. The split ratio of TEE-101, from Figure 5 in Chapter 5, is changed to obtain a temperature of -40°C of the natural gas from precooling. The influence of a

higher feed gas pressure in terms of power consumption and volume flows for APCIs expander process is found in Table 20.

The minimum approach temperature of heat exchanger LNG-103 from Figure 7 in Chapter 5, decreases to 2.2°C when changing the feed gas pressure to 80 bar. Lowering the exiting pressure of warm expander K-107 decreases the temperature of cold refrigerant entering heat exchanger LNG-103 and increases the approach temperature. The influence of a higher feed gas pressure in terms of power consumption and volume flows for the US patent process is listed in Table 20.

Table 20: Increased pressure of the feed gas for the expander processes

	TOTAL turbo-expander (4 trains)		APCI turbo-expander (4-trains)		US Patent turbo-expander (2 trains)	
	Original	Study	Original	Study	Original	Study
Specific power consumption (kWh/ton LNG)	395.8	383.3 (-3.3%)	405.7	378.0 (-7.3%)	422.5	396.5 (-6.6%)
Nitrogen flow rate (ton/hr)	3973.0	3854.0	4319.0	3937.0	3147.0	2927.0
Volume flow to main compressor (m3/hr)	263,500	255,600	278,000	253,400	305,200	284,200
Power consumption CO2 process (MW)	15.7	15.2	11.9	14.2	30.7	30.2
Warm expander						
Power production (MW)	48.5	46.9	55.0	48.6	28.7	27.3
Volume flow outlet (m3/hr)	84,070	81,170	93,570	82,740	46,500	45,280
Cold expander						
Power production (MW)	12.6	12.4	12.6	12.3	21.5	21.1
Volume flow outlet (m3/hr)	20,930	20,500	20,740	20,220	43,250	43,120
Additional expander (US patent)						
Power production (MW)	-	-	-	-	16.0	12.8
Volume flow outlet (m3/hr)	-	-	-	-	111,500	104,300

The increased feed gas pressure gives reduction in specific power consumption for all turbo-expander processes. APCIs turbo-expander process has the highest reduction in power consumption with 7.3% from Table 20. This makes APCIs expander process the most efficient of the turbo-expander processes with an energy consumption of 378 kWh/ton LNG. The substantial decrease in power consumption comes from the increased load of the CO2 system with a higher condensing temperature of the gas. The compressor power for the CO2 system in APCIs model increases from 11.9 MW to 14.2 MW in Table 20. The circulating refrigerant in the cycles is reduced and decreases the volume flow to the main nitrogen compressor in all processes. The process from US patent has a decrease in volume flow of 7.4% to compression. The warm expander in the turbo-expander process from TOTAL has a reduction in power output from 48.5 MW to 46.9 MW.

APCIs DMR process was also modeled with a feed gas pressure of 80 bar. The increased pressure of the feed gas caused a liquid fraction in the streams entering compression in both MR cycles. A reduction in flow rate of refrigerant in the MR loops will reduce the volume flow through the heat exchangers and fully vaporize the refrigerant streams upstream of compression. The reduction in refrigerant mass flow was 3.6% for the first circuit and 14.3% for the second circuit. Compressor power and volume flows from the study are listed in Table 21.

Table 21: Results for APCIs DMR processes with a higher feed pressure

	APCI DMR (1 train)	
	Original	Study
Specific power consumption (kWh/ton LNG)	284.0	265.3 (-7.0%)
Refrigerant flow rate (ton/hr)	2412.6	2237.2
<i>1st MR circuit</i>		
Power consumption of LP Warm (MR)	20.1	19.6
Volume flow to LP Warm (m3/hr)	105,900	102,400
<i>2nd MR circuit</i>		
Power consumption LP Cold (MW)	39.0	36.8
Volume flow to LP Cold (m3/hr)	159,200	153,700

The DMR process has a reduction in power consumption of 7% with increased feed pressure of the gas as seen in Table 21. The volume flow to compression is reduced by 3.4% in the warm MR loop and 3.6% for the cold MR loop.

APCIs turbo-expander process has the highest reduction in power consumption of 7.3% with APCIs DMR process following close behind with a reduction of 7% for a higher inlet pressure of the gas. The savings in compressor power for the processes with a higher feed pressure must be weighted against the extra compression power required after the extraction unit upstream of liquefaction. From theory it is stated that the extra work of compressing the natural gas before entering liquefaction is compensated for by savings in the liquefaction unit if the pressure level of the natural gas is 80-100 bar (Pettersen, 2012)

6.3 Decrease in cooling temperature

The ambient temperature in the liquefaction process will vary with sea temperature and intake depth at the FLNG site. An FLNG operating in warm climates can reduce the cooling temperature by increasing the depth of the water intake. Figure 10 in Section 6.2 shows how the work area of the graph decreases with a lower ambient temperature in the process.

The sea temperature used in the original model was 13°C. This gave a temperature of 17°C for the fresh water loop assuming a ΔT of 4°C in the heat exchangers. The cooling temperature for the process could be lower is direct sea

water was used, but this can cause corrosion of the pipes and equipment in the long run and are costly to repair. Heat exchange between the refrigerant and fresh water leaves the gas at a temperature of 22°C, assuming a ΔT of 5°C in the heat exchangers for water cooling. The effects of using a sea water temperature of 6°C are studied in this Section. This sea water temperature can be found in a colder climate or at a higher water depth. This leaves a temperature of 10°C for the fresh water loop and a temperature of 15°C for the cooled gas and refrigerant assuming the same ΔT in the heat exchangers. The possibility of condensation of refrigerant must be checked with a lower cooling temperature in the process.

The three turbo-expander processes from TOTAL, APCI and US patent 5,768,912 were simulated with a sea water temperature of 6°C. There were no other changes in free variables in the processes for obtaining a minimum approach temperatures of 3°C in the heat exchangers. Power consumptions and volume flows for the processes with decreased cooling temperature are given in Table 22.

Table 22: Comparison of the expander processes with lower cooling temperature

	TOTAL turbo-expander (4 trains)		APCI turbo-expander (4 trains)		US Patent turbo-expander (2 trains)	
	Original	Study	Original	Study	Original	Study
Specific power consumption (kWh/ton LNG)	395.8	378.8 (-4.5%)	405.7	387.4 (-4.7%)	422.5	401.2 (-5.3%)
Nitrogen flow rate (ton/hr)	3973.0	3973.0	4319.0	4319.0	3147.0	3147.0
Power consumption in 1 st stage of main compressor (MW)	83.3	81.6	85.3	83.0	101.5	101.4
Power consumption in 2 nd stage of main compressor (MW)	76.4	71.8	82.6	78.8	55.0	51.8
Volume flow to 1 st stage of main compressor (m3/hr)	263,500	254,400	278,000	270,400	305,200	305,200
Volume flow to 2 nd stage of main compressor (m3/hr)	141,400	136,700	154,300	150,400	124,600	121,500
Power consumption in CO2 system (MW)	15.7	14.5	11.9	11.0	30.7	25.3
Warm expander						
Power production (MW)	48.5	48.5	55.0	55.0	28.7	28.7
Volume flow outlet (m3/hr)	84,070	84,070	93,570	93,570	46,500	46,500
Cold expander						
Power production (MW)	12.6	12.6	12.6	12.6	21.5	21.5
Volume flow outlet (m3/hr)	20,930	20,930	20,740	20,740	43,250	43,250
Additional expander (US patent only)						
Power production (MW)	-	-	-	-	16.0	16.0
Volume flow outlet (m3/hr)	-	-	-	-	111,500	111,500

The process from US patent has the highest reduction in power with 5.3% from Table 22. The second stage of the main compressor has highest reduction in power for all processes because of a lower temperature of intercooling between the stages. The power consumption reduces from 76.4 MW to 71.8 MW in the second stage for TOTALs main compressor and has a reduction in suction volume of 3.4%. The power release and volume flows for the expanders are the same in Table 22 because of unchanged split temperatures in the processes.

The DMR process had a fraction of 0.06 liquid entering the 1st MR circuit with a water cooling temperature of 10°C. The circulation rate of refrigerant in the circuit was reduced by 12% for full vaporization of the refrigerant in heat exchanger WMR CWHE from Figure 2 in Chapter 2. Compressor power and volume flows from the study are listed in Table 23.

Table 23: Results for the DMR processes with lower cooler temperature

	APCI DMR (1 train)	
	Original	Study
Specific power consumption (kWh/ton LNG)	284.0	261.1 (-8.8%)
Refrigerant flow rate (ton/hr)	2412.6	2258.6
<i>1st MR circuit</i>		
Total compressor power (MW)	50.3	41.8
Volume flow to LP Warm (m3/hr)	105,900	92,240
Volume flow to HP Warm (m3/hr)	49,090	38,210
<i>2nd MR circuit</i>		
Total compressor power (MW)	74.4	73.1
Volume flow to LP Cold (m3/hr)	159,200	159,200
Volume flow to MP Cold (m3/hr)	50,070	48,530
Volume flow to HP Cold (m3/hr)	21,340	20,440
Volume flow to HHP Cold (m3/hr)	17,080	16,260

The DMR process has a power reduction of 8.8% with a lower cooling temperature in the process as seen in Table 23. The first MR circuit has a power reduction of 20% and a reduction in suction volume of 14.5% for the low-pressure compressor in the circuit.

6.4 Additional stages for the main compressor in the turbo-expander process

The main compressor in the turbo-expander processes has intercooling of the refrigerant after the 1st compressor stage. Intercooling of the refrigerant will reduce the temperature to the next compressor stage and increase the density of the gas. One intercooler was used between the two compressor stages in the modeling of the main nitrogen compressor for the turbo-expander processes. Several compressor stages with intercooling are looked at in this section and the results for the turbo-expanders are given in Table 24.

Table 24: Several compressor stages of the main compressor for expander processes

	Specific power consumption (kWh/ton LNG)	Main compressor power (MW)	Temperature exiting compression (°C)	Suction volume to last compressor stage (m3/hr)
TOTAL (4 trains)				
2-stage (original)	395.8	159.7	88.0	141,400
3-stage (study)	385.3 (-2.7%)	155.1	66.1	117,90 (-19.9%)
4-stage (study)	380.2 (-4.1%)	152.9	53.5	105,80 (-33.6%)
APCI (4 trains)				
2-stage (original)	405.7	167.9	87.6	154,300
3-stage (study)	395.0 (-2.7%)	163.2	63.3	126,000 (-22.4%)
4-stage (study)	389.8 (-4.1%)	160.9	53.4	115,700 (-33.4%)
US Patent (2 trains)				
2-stage (original)	422.5	156.5	82.0	124,600
3-stage (study)	417.4 (-1.2%)	154.2	59.6	103,200 (-20.7%)
4-stage (study)	415.0 (-1.8%)	153.2	50.2	95,000 (-31.2%)

Table 24 lists the reduction in power, temperatures and volume flows for several stages of the main compressor. TOTALs and APCIs model has the highest reduction in power with 2.7% for the first compressor stage and 4.1% in the second as seen in Table 24. The turbo-expander from US patent has power reductions of less than 2% with additional compressor stages. The processes from TOTAL and APCI have temperatures of respectively 88°C and 87.6°C exiting compression from the initial two-stage model. The main compressor for all processes was modeled to have similar temperatures after the 1st and 2nd stage of compression. This was also the case for several stages of compressor with intercooling. The process from US patent has a temperature of 82°C after compression and between compressor stages for the original model. The lower temperature between compressor stages explains the lower reduction in power for the US patent process. The suction volume in the final compressor stage is reduced with about 20% for 3-stages and over 30% for 4-stages of compression for all processes as seen in Table 24. The negative effect of pressure drops in the intercoolers is not accounted for in this study.

The DMR process has two mixed refrigerant cycles with compression of the gas. The process has two compressors and a liquid pump in the first MR circuit and four stages of compression in the MR second circuit with cooling of the refrigerant between stages. The refrigerant to compression has less than 5°C superheat when entering compression in both MR cycles and losses in efficiency will be less than for the turbo-expander processes. Additional compressor stages with intercooling for the DMR process are not considered in this study.

6.5 High pressure of nitrogen

The high pressure of nitrogen after compression was set to 70 bar for the simulations of the turbo-expander processes. Compression of nitrogen from a low side pressure of 9-15 bar to 70 bar requires a large compression power. A

selected high-pressure of 65 bar for the nitrogen is tested in this section to see how a lower pressure in the process influences the compressor and expander power and volume flow rates throughout the process. The results for the three turbo-expanders are given in Table 25.

Table 25: High-pressure of nitrogen for the expander processes

	TOTAL turbo-expander (4 trains)		APCI turbo-expander (4-trains)		US Patent turbo-expander (2 trains)	
	Original	Study	Original	Study	Original	Study
Specific power consumption (kWh/ton LNG)	395.8	402.1 (+1.6%)	405.7	410.3 (+1.1%)	422.5	425.1 (+0.6%)
Nitrogen flow rate (ton/hr)	3973.0	3996.0	4319.0	4381.0	3147.0	3221.0
Volume flow to main compressor (m3/hr)	263,500	289,900	278,000	303,000	305,200	327,400
Power consumption CO2 process (MW)	15.7	15.5	11.9	12.0	30.7	31.0
Warm expander						
Power production (MW)	48.5	48.9	55.0	55.5	28.7	28.0
Volume flow outlet (m3/hr)	84,070	91,720	93,570	101,800	46,500	48,350
Cold expander						
Power production (MW)	12.6	13.4	12.6	13.2	21.5	22.6
Volume flow outlet (m3/hr)	20,930	24,200	20,740	23,630	43,250	49,890
Additional expander (US patent)						
Power production (MW)	-	-	-	-	16.0	16.5
Volume flow outlet (m3/hr)	-	-	-	-	111,500	113,400

The reduced pressure of nitrogen increases the power consumption for all turbo-expander processes. TOTALs process has the largest increase in power consumption with 1.6% seen in Table 25. The expanders in TOTALs process have increased power outputs of 0.4 MW and 0.8 MW for the warm and cold expanders in the process. The volume flow through the main compressor for the same process is increased by 10%. APCIs process has an increase in volume flow of 9% through the main compressor while the turbo-expander from US patent has an increase of 7.3%. A higher expander power and larger volume flows through compression is the tendency for all the turbo-expander processes in Table 25 with reduced high-pressure of nitrogen. The exception is the warm expander from US patent with a power reduction of 0.7 MW from Table 25.

The pressure of the mixed refrigerant in the DMR process is dependent on the boiling and condensing temperatures and is difficult to change without changing the composition of the mixed refrigerant. A change in high-pressure of the DMR process is therefore not included in this Section.

6.6 Split temperatures in heat exchangers

The turbo-expander processes have several split temperatures between the heat exchanger segments in the liquefaction cycle. Split temperatures of the gas are introduced when a stream enters the heat exchanger from expansion or mixing of refrigerant streams. The volume flow and power consumption in the processes are influenced by minimum approach temperatures and LMTD values in the heat exchangers. The split temperatures are chosen based on requirements of single-phase flow for streams entering a heat exchanger.

The split temperatures were adjusted during the simulations of the processes and the initial split temperature were found using trial and error methods for energy optimization in the processes. Split temperatures around this initial temperature should be studied for further reductions in power consumption and LMTD values. Several values were studied and the two split temperatures of most relevance for each split were included in Tables 26-28.

6.6.1 TOTALs turbo-expander

TOTALs turbo-expander has two refrigerant splits of the natural gas and nitrogen in the process. The first split is introduced when a portion of warm nitrogen is sent to precooling after heat exchanger LNG-100, from Figure 1 in Chapter 2. The second split is from mixing of two cold streams of refrigerant between heat exchangers LNG-101 and LNG-102.

Table 26: Split temperatures in TOTALs process

TOTALs turbo-expander process (4 trains)			
	Original	Study	Study
<i>Split 1</i>	-8.5 (°C)	-9 (°C)	- 7(°C)
Specific power consumption (kWh/ton LNG)	395.8	396.4	401.7
Power warm expander (MW)	48.5	48.8	47.5
Power cold expander (MW)	12.6	12.6	13.4
LMTD LNG-100 (°C)	7.4	7.4	7.2
LMTD LNG-101 (°C)	6.8	7.1	7.0
UA LNG-100 (MJ/C-hr)	24,250	24,870	23,490
UA LNG-101 (MJ/C-hr)	57,000	54,880	56,470
<i>Split 2</i>	-101.4 (°C)	-100 (°C)	-103(°C)
Specific power consumption (kWh/ton LNG)	395.8	401.2	393.8
Power warm expander (MW)	48.5	47.6	50.0
Power cold expander (MW)	12.6	13.4	11.9
LMTD LNG-101 (°C)	6.8	6.9	7.0
LMTD LNG-102 (°C)	5.5	5.5	5.4
UA LNG-101 (MJ/C-hr)	57,000	56,220	55,620
UA LNG-102 (MJ/C-hr)	17,380	17,830	17,960

The two studies split temperatures to precooling of -7°C and -9°C gave increases in specific power consumption of the process compared to the initial value of -8.5°C as seen in Table 26. The LMTD values for the heat exchangers were about the same for the three temperatures. The second split in the process was studied for temperatures of -100°C and -103°C. The temperature of -103°C gave a reduction in energy consumption of 0.5%. The power outlet of the cold expander was reduced from 12.6 MW to 11.9 MW due to the lower ingoing temperature to the expansion. The LMTD values for the studied temperatures were close to the initial values.

6.6.2 APCIs turbo-expander

The turbo-expander process from APCI has two split temperatures of the natural gas. The split temperature of natural gas after precooling is however not a variable and the split temperature of natural gas between heat exchangers LNG-101 and LNG-103 is the only temperature that can be studied for optimization. Figure 5 of Chapter 5 shows the heat exchangers in the process.

Table 27: Split temperatures in APCIs expander process

	APCI turbo-expander (4 trains)		
	Original	Study	Study
<i>Split 1</i>	-96 (°C)	-90 (°C)	-100 (°C)
Specific power consumption (kWh/ton LNG)	405.7	407.8	403.2
Power warm expander (MW)	55.0	54.9	55.8
Power cold expander (MW)	12.6	13.0	12.2
LMTD LNG-101 (°C)	7.1	7.8	6.9
LMTD LNG-103 (°C)	5.9	6.5	5.6
UA LNG-101 (MJ/C-hr)	24,350	20,970	26,590
UA LNG-103 (MJ/C-hr)	17,750	18,120	17,270

Split temperatures of -90°C and -100°C were studied for APCIs expander process and Figure 27 shows some of these results. The temperature of -100°C gave a reduction in power consumption of 0.6%. The split temperature of -90°C increased the specific power in the process and the LMTD values of the heat exchangers. The power outlet from the cold expander increased from 12.6 MW to 13.0 MW due to the increased cooling requirements in heat exchanger LNG-103.

6.6.3 Turbo-expander from US patent

The turbo-expander process from US patent has four split temperatures of the natural gas and nitrogen refrigerant. Only two of the split temperatures are free variables and can be changed for optimization of the process. The warm streams between heat exchangers LNG-102 and LNG-103 is a free variable and determines the temperature of the refrigerant to cold expander K-105, from Figure 7 in Chapter 5. The split temperature after precooling in heat exchanger LNG-104 is also a free variable.

Table 28: Split temperature in the US patent process

US Patent turbo-expander (2 trains)			
	Original	Study	Study
<i>Split 1</i>	-30 (°C)	-25 (°C)	-35 (°C)
Specific power consumption (kWh/ton LNG)	422.5	423.7	425.4
Power warm expander (MW)	28.7	30.3	27.0
Power cold expander (MW)	21.5	22.1	21.0
Power additional expander (MW)	16.0	16.5	15.5
LMTD LNG-100 (°C)	15.7	15.7	17.0
LMTD LNG-101 (°C)	3.2	3.2	3.4
UA LNG-100 (MJ/C-hr)	16,630	15,290	16,700
UA LNG-101 (MJ/C-hr)	22,660	28,410	16,580
<i>Split 2</i>	-84 (°C)	-82 (°C)	-86(°C)
Specific power consumption (kWh/ton LNG)	422.5	418.9	424.5
Power warm expander (MW)	28.7	28.7	29.2
Power cold expander (MW)	21.5	21.9	21.0
Power additional expander (MW)	16.0	15.6	15.8
LMTD LNG-102 (°C)	5.0	4.9	4.8
LMTD LNG-103 (°C)	4.9	4.9	5.7
UA LNG-102 (MJ/C-hr)	38,630	38,330	42,170
UA LNG-103 (MJ/C-hr)	6,947	7,509	4,537

Split temperatures of -25°C and -35°C from precooling are studied and some results from the simulations are included in Table 28. The process has an increase in power consumption for the studied temperatures. The warm nitrogen stream from the first split is sent to the warm expander for cooling. The higher temperature from precooling with -25°C increases the duty of the warm expander, as seen in Table 28, while the lower temperature decreases the expander duty. The second split temperature determines the temperature to the cold expander in the process. A temperature of -82°C decreases the specific power consumption by 0.9%. The power outlet in the cold expander is increased by 0.4 MW due to the higher temperature of nitrogen. A split temperature of -86°C gave an increase in power consumption for the process. The power from the warm expander is 29.2 MW and even closer to the maximum compander capacity of 30 MW for two liquefaction trains.

6.7 Isentropic to polytropic efficiency in rotating equipment

The rotating equipment in the processes was simulated with adiabatic efficiencies of 80% in HYSYS. Polytropic efficiencies of 80% will however give a more correct and realistic model of a centrifugal compressor with several compression stages. Rise in temperature of the gas and loss of energy is included in the polytropic efficiency.

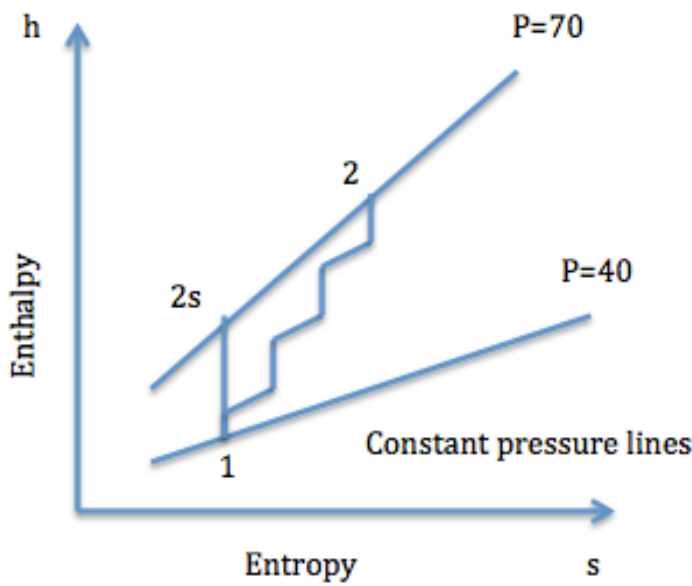


Figure 11: Mollier diagram with isentropic and polytropic compression

Figure 11 shows the difference between isentropic and polytropic compression. Isentropic compression has an exit state at point 2s in the figure. The polytropic work accounts for the divergent pressure lines in the Mollier diagram and the sum of the small pressure steps from point 1 to point 2 in Figure 11 gives the enthalpy change, H_p , for the polytropic process. The work for the compressors in the process will follow the equation,

$$\left(-\frac{\dot{W}_{cv}}{\dot{m}} \right) = h_2 - h_1 \quad (1)$$

State 1 is fixed before entering compression so the work input is dependent on the state in point 2. The polytropic compression will have a higher enthalpy in point 2 than in the isentropic compression to point 2s. The work in (1) is therefore higher for the polytropic work of the compressor. The effect for the turbine is opposite and the turbine will have a higher adiabatic efficiency for a given polytropic efficiency. An expander turbine in LNG production usually has one stage of expansion and the polytropic efficiency will be close to the isentropic efficiency of the expander (Bakken, 2013).

Table 29: Adiabatic to polytropic efficiency for the expander processes

	TOTAL turbo-expander (4 trains)		APCI turbo-expander (4 trains)		US Patent turbo-expander (2 trains)	
	Original	Study	Original	Study	Original	Study
Specific power consumption (kWh/ton LNG)	395.8	392.8 (-0.8%)	405.7	398.9 (-1.7%)	422.5	424.5 (+0.5)
Nitrogen flow rate (ton/hr)	3973.0	3950.0	4319.0	4179.0	3147.0	3067.0
Power consumption of 1 st stage of main compressor (MW)	83.3	82.9	85.3	84.4	101.5	103.1
Power consumption of 2 nd stage of main compressor (MW)	76.4	75.1	82.6	80.2	55.0	54.1
Volume flow to 1 st stage of main compressor (m3/hr)	263,500	256,100	278,000	269,100	305,200	297,500
Volume flow 2 nd stage of main compressor (m3/hr)	141,400	139,400	154,300	149,300	124,600	121,500
Power consumption in CO2 system (MW)	15.7	16.1	11.9	12.2	30.7	30.9
Warm expander						
Power production (MW)	48.5	50.1	55.0	54.7	28.7	29.1
Volume flow outlet (m3/hr)	84,070	80,710	93,570	87,410	46,500	44,620
Cold expander						
Power production (MW)	12.6	12.8	12.6	13.1	21.5	21.5
Volume flow outlet (m3/hr)	20,930	20,290	20,740	20,740	43,250	38,300
Additional expander (US patent only)						
Power production (MW)	-	-	-	-	16.0	16.0
Volume flow outlet (m3/hr)	-	-	-	-	111,500	108,200

The turbo-expander processes from TOTAL and APCI has a decrease in power consumption of 0.8% and 1.7% respectively from Table 29. The increased efficiency of the expanders decreases the circulation rate of refrigerant in the process. The turbo-expander process from US patent has an increase in power consumption of 0.5%. The original model had a power consumption of 101.5 MW in the first stage of the main nitrogen compressor. The adiabatic efficiency of this compressor drops to 76.7% when a polytropic efficiency is used due to the large compression power and heating of the refrigerant. The power consumption in the CO2 systems had an increase in power ranging from 0.2-0.4 MW for all the processes seen in Table 29. The volume flow throughout the process decreases with a reduced circulation rate of refrigerant.

The polytropic efficiency was the only free variable changed in the process for the study of APCIs DMR process.

Table 30: DMR process with adiabatic vs polytropic efficiency

	APCI DMR (1 train)	
	Original	Study
Specific power consumption (kWh/ton LNG)	284.0	291.3 (+2.5%)
Refrigerant flow rate (ton/hr)	2412.6	2412.6
<i>1st MR circuit</i>		
Power consumption LP Warm (MW)	20.1	20.4
Power consumption HP Warm (MW)	30.1	30.9
Total compressor power (MW)	50.2	51.3
Volume flow to HP Warm (m3/hr)	49,090	49,090
<i>2nd MR circuit</i>		
Power consumption LP Cold (MW)	38.9	40.6
Power consumption MP Cold (MW)	25.0	25.5
Power consumption HP Cold (MW)	5.2	5.2
Power consumption HHP Cold (MW)	5.2	5.2
Total compressor power (MW)	74.3	76.5
Volume flow to HHP Cold (m3/hr)	17,080	17,080

The specific power consumption in the process increases by 2.5% from Table 30 when introducing a polytropic efficiency of the compressors. There are no turbo-expanders in the DMR process to offset the increased power consumption of the compressors with a polytropic efficiency. The increase in compressor power is 2.1% for the first MR circuit and 2.9% for the second MR circuit. LP Cold in the second MR loop has the highest increase with 1.7 MW due to the larger compressor power of this compressor.

7. Evaluation of CO₂ precooling system for turbo-expander processes

7.1 General

A two-stage CO₂ system with one evaporating temperature for precooling was used in the simulation for all three turbo-expander processes. Two compressors compress the gas to around 62 bar before the CO₂ is cooled to ambient temperature and condenses in the system. The open intercooler works as a de-superheater after the 1st compressor and places the refrigerant gas on the saturation line. The liquid in the bottom of the intercooler is saturated and evaporates through heat exchange with a warm counter-current stream after pressure reduction in a JT-valve. The warm streams to precooling can be the feed gas, the nitrogen refrigerant or both these streams as for the turbo-expander from US patent. The initial CO₂ system can be seen in Figure 12.

The power consumption of the CO₂-system was about 9% of the specific power requirement for the expander process from TOTAL stated in the project thesis (Hasle, 2012). The turbo-expander processes from APCI and the turbo-expander from US patent number 5,768,912 were modeled with the same CO₂ system and had power consumptions of respectively 6.7% and 16.5% of the total energy requirement. The CO₂ system is studied in this Section to look at improvements for the precooling unit.

CO₂ Precooling cycle

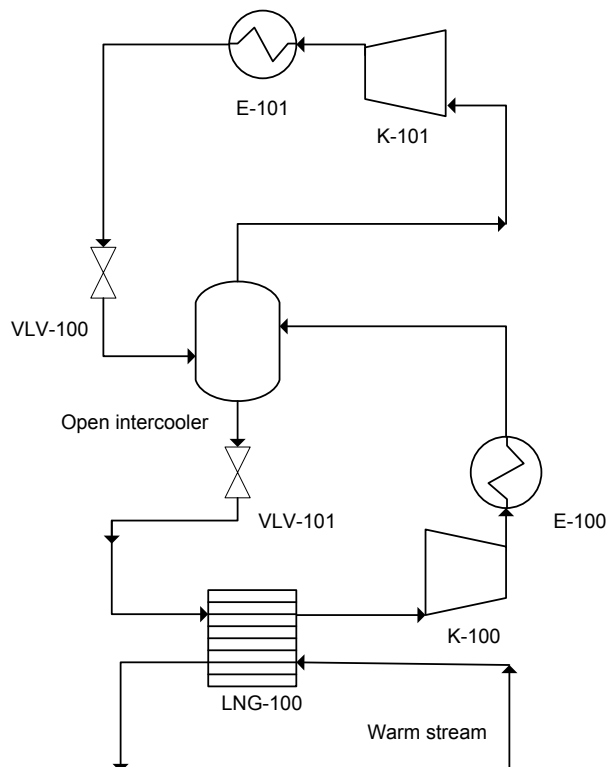


Figure 12: CO₂ Precooling system used in the initial modeling of the turbo-expander processes

Precooling of the refrigerant has the objective of minimizing the gap between the heating and cooling curves in the heat exchangers. A smaller space between the combined heat curves will reduce power consumption and thermodynamic inefficiencies in the process (Dubar, 1998) Precooling changes the gradients in the heating curves when introducing a different refrigerant in addition to nitrogen. This was seen in Figure 9 in Chapter 5. The CO₂ uses latent heat transfer and will be more efficient than nitrogen in the warmer parts of the process.

The CO₂ system from Figure 12 has only one heat exchanger for evaporation of CO₂. Heat transfer with only one evaporating temperature of CO₂ will be inefficient because of large differences in the temperature curves. Several heat exchanger steps with different evaporating temperatures of the CO₂ will increase the efficiency of the precooling unit. Figure 13 shows theoretical heat transfer curves for increasing evaporating stages for the precooling system.

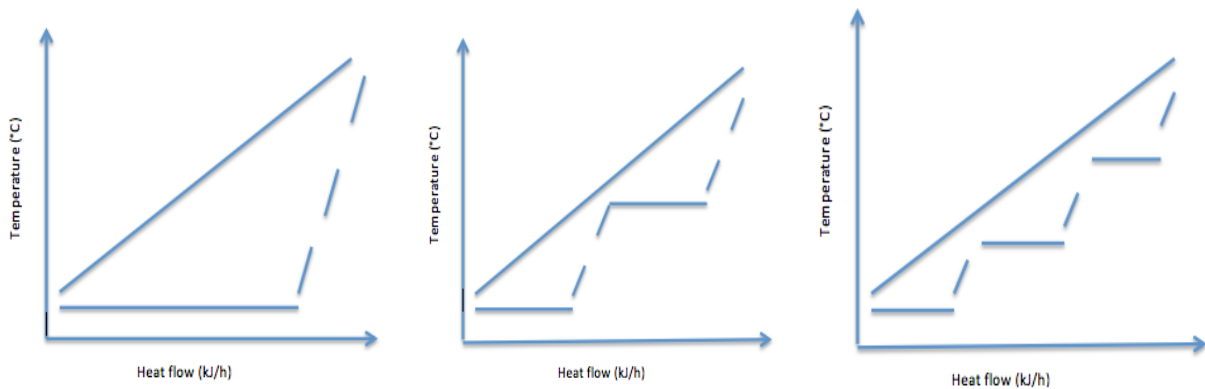


Figure 13: Heat flow curves for CO₂ system several evaporation stages

The temperature curves in Figure 13 illustrate the improvements in heat transfer with one, two and three evaporation stages of CO₂. The horizontal lines show the ideal temperature lines while the stippled lines illustrates superheating of the CO₂ in the heat exchangers. Several evaporation stages of the CO₂ will decrease the LMTD values in the heat exchangers for the precooling unit. The LMTD values were listed in the results of the simulations of the two expander processes from APCI and US patent in Chapter 5. The LMTD value for the CO₂ system was substantially higher than for the other heat exchangers and had values of 19°C and 15.7°C.

Two CO₂ precooling systems are looked at for minimizing inefficiencies in the turbo-expander process. One system is modeled with two evaporation stages and the other model has three evaporation stages of the CO₂. These systems have one compressor with respectively two and three side inlets unlike the system in Figure 12 with two separate compressors. Models of the two systems are found in Figures 14 and 15.

CO2 Precooling cycle

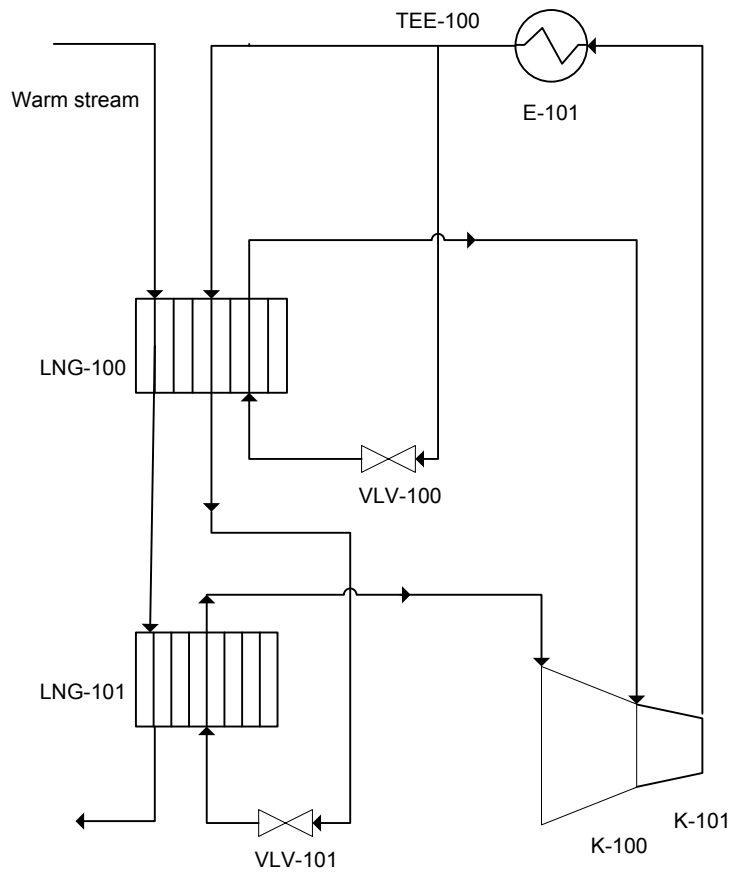


Figure 14: Alternative CO2 system with two evaporation stages of CO2

Figure 14 illustrates the precooling system with two evaporation stages of the CO2 refrigerant. The combined temperature curves from the heat exchangers should match the 2nd graph in Figure 13. The CO2 is compressed to a high pressure of 62 bar when exiting compressor K-101. The refrigerant is then split in two streams after cooling of the CO2 to ambient temperature. A portion of the stream is routed through heat exchanger LNG-100 for subcooling of the CO2 while most of the stream is sent through valve VLV-100 for temperature and pressure reduction. This stream enters side inlet K-101 of the compressor after vaporization of the CO2 in heat exchanger LNG-100.

The subcooled stream continues to heat exchanger LNG-101 as a warm refrigerant stream before it is cooled by pressure reduction through valve VLV-101. The liquid CO2 evaporates in heat exchanger LNG-101 upstream of compressor K-100. The stream is mixed with the cold stream returning from heat exchanger LNG-100 in the 2nd compressor stage K-101. The CO2 should not be superheated when exiting LNG-100 and LNG-101 after vaporization.

CO₂ Precooling cycle

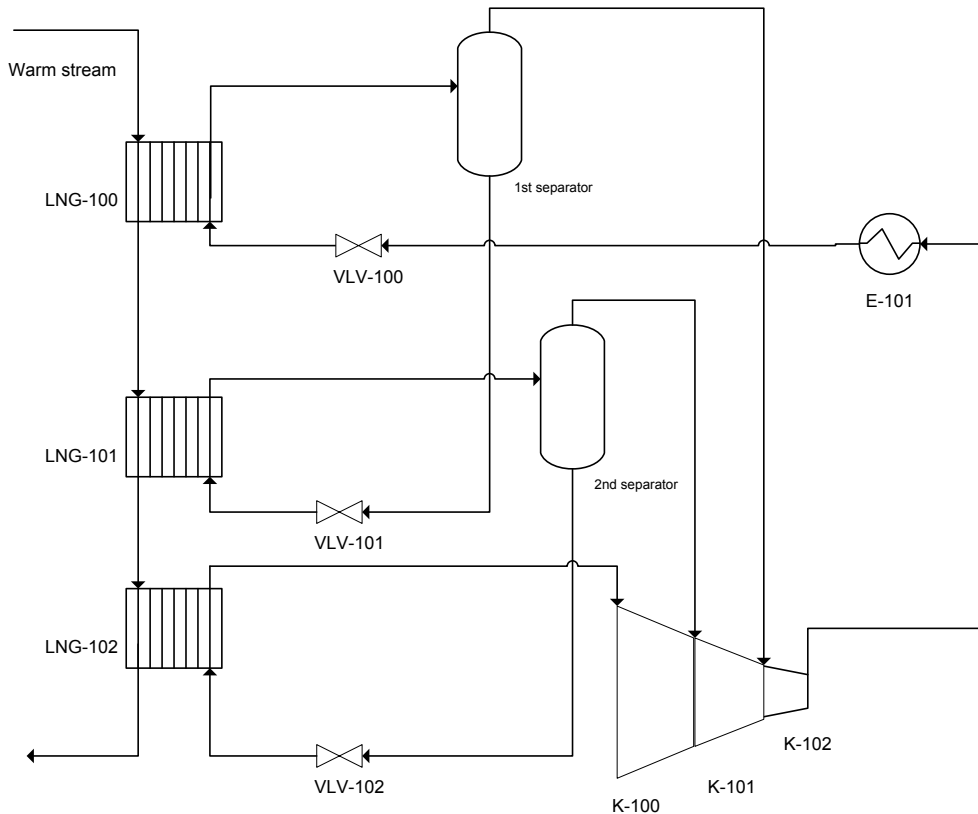


Figure 15: Alternative CO₂ system with kettle heat exchangers and three evaporation stages of the refrigerant

Figure 15 shows a CO₂ system with three evaporating stages of CO₂. The combined temperature curves from the heat exchangers should match the 3rd graph in Figure 13. Figure 15 is based on the representation of the model in HYSYS. The separators and heat exchangers combined are in reality kettle heat exchangers with one vapor outlet and one liquid outlet of CO₂ with the warm stream flowing inside tubes in the heat exchangers. The CO₂ compressor has two side inlets, K-101 and K-102, with inflowing streams of cold refrigerant from the vapor outlet of the two separators.

The critical part of the process is the inlet to compressor K-100 from LNG-102. The amount of CO₂ through heat exchanger LNG-102 must be small enough to completely vaporize in heat exchange with the warm stream so no liquid enters the compressor. This model is believed to be more efficient than the other precooling models because of three evaporating temperatures of CO₂ and no subcooling of CO₂ in the heat exchangers. Disadvantages with this precooling process are the increased amount of equipment and piping needed. Lower LMTD values in the heat exchangers will also increase the heat transfer area and requires larger heat exchangers.

7.2 Results from simulations of alternative CO2 system for the turbo-expander process

All three turbo-expander processes from TOTAL, APCI and US patent were simulated with the two alternative precooling systems described in Section 7.1.

TOTALs turbo-expander process had precooling of the nitrogen refrigerant to -40°C while the process from APCI had precooling of the feed gas to -40°C . The process from US patent number 5,768,912 had precooling of the warm nitrogen refrigerant and the feed gas down to -30°C . The reason for the higher temperature out from precooling for the expander process from US patent is several split temperatures of the refrigerant and one extra turbo-expander in the process. The load in this system is high because of precooling of two streams in the system. All systems have a high pressure of 62 bar for the CO2 refrigerant and are cooled to ambient temperature after compression. The precooling systems are further discussed in Chapter 8.7.

7.2.1 TOTALs turbo-expander process

TOTALs turbo-expander process has precooling of the warm nitrogen stream after the 1st heat exchanger in the process seen in Figure 1 of Chapter 2. The term precooling for this process can therefore be discussed and a more suitable term will be “cooling of refrigerant”. Nitrogen is cooled down to -40°C by CO2 in a system equal to the system seen in Figure 12. The nitrogen enters the precooling unit at -8.5°C found in the simulation of the process from the project thesis (Hasle, 2012). Tables 31-33 list numbers from the simulation of the initial CO2 system and numbers from the simulations of the alternative precooling systems from Figures 14 and 15. The precooling system with two evaporating temperatures has a split temperature of -20°C between the two heat exchanger segments. Split temperatures for the system with three evaporating stages of the CO2 are -15°C and -30°C .

Table 31: Compressor power for CO2 systems, TOTAL

	CO2 system with one evaporation stage	CO2 system with two evaporation stages	CO2 system with three evaporation stages
Refrigerant flow rate (ton/hr)	1039.8	688.0	635.0
Specific power consumption (kWh/ton_LNG)	35.7	36.9	33.3
% of total power consumption of the process	9.0%	9.3%	8.4%
Compressor power			
Compressor K-100 (MW)	9.7	2.5	0.6
Compressor K-101 (MW)	6.0	13.7	2.2
Compressor K-102 (MW)	-	-	11.9
Total compressor power (MW)	15.7	16.2	14.7

Table 31 gives numbers of power consumption and refrigerant flow rate for the three CO₂ processes described in Section 7.1. The system with three evaporating temperatures of the CO₂ has a decrease in power consumption of 7% compared with the initial model with one evaporating stage. The higher power consumption in the second model can be explained by the high pressure lift from 17 to 62 bar in compressor K-101. The decrease in refrigerant flow rate of 51% and 64% for the alternative precooling systems are due to the decreased LMTD values in the heat exchangers.

Table 32: Heat exchanger properties for CO₂ systems, TOTAL

Heat exchanger properties	CO ₂ system with one evaporation stage	CO ₂ system with two evaporation stages	CO ₂ system with three evaporation stages
<i>UA values</i>			
LNG-100 (MJ/C-hr)	8,570	6,643	3,563
LNG-101 (MJ/C-hr)	-	6,589	5,706
LNG-102 (MJ/C-hr)	-	-	4,614
<i>LMTD values</i>			
LNG-100 (°C)	12.3	10.1	5.9
LNG-101 (°C)	-	10.2	8.7
LNG-102 (°C)	-	-	7.3

UA and LMTD values for each precooling process can be seen in Table 32. The LMTD values for each heat exchanger are improved when using several evaporation stages of CO₂. The LMTD value for the initial system is 12.3°C and the highest LMTD value in the system with three evaporation stages of CO₂ is 8.7°C. The total UA value for the precooling system increases with smaller LMTD values in the heat exchangers as seen in Table 32.

Table 33: Volume flow rates of compression suction for CO₂ systems, TOTAL

Volume flow rates	CO ₂ system with one evaporation stage	CO ₂ system with two evaporation stages	CO ₂ system with three evaporation stages
<i>Compressor suction</i>			
K-100 (m ³ /hr)	21,410	10,910	4,952
K-101 (m ³ /hr)	7,566	15,490	9,705
K-102 (m ³ /hr)	-	-	13,260

Volume flow rates for the compressors and side inlets of the compressors are included in Table 33. Compressor K-100 in the 1st system has the highest volume flow of CO₂ with a value of 21,400 m³/hr. The volume flow to compressor suction decreases with increasing evaporation stages of the CO₂ due to a lower circulation rate of refrigerant and smaller equipment can be used.

7.2.2 APCIs turbo-expander process

APCIs turbo-expander process has precooling of the feed gas from ambient temperature to -40°C . This liquefaction process has the highest temperature reduction through precooling with a temperature reduction of 62°C of the natural gas. The CO_2 refrigerant must cover a large temperature range and a system with only one evaporating stage of CO_2 is considered inefficient. The split temperature for the precooling process with two evaporation stages is -20°C . Split temperatures for the process with three pressure stages of the CO_2 are 0°C and -20°C . Tables 34-36 include numbers for comparison between the different CO_2 systems described in Section 7.1

Table 34: Compressor power for CO_2 systems, APCI

	CO ₂ system with one evaporation stage	CO ₂ system with two evaporation stages	CO ₂ system with three evaporation stages
Refrigerant flow rate (ton/hr)	709.4	496.0	478.0
Specific power consumption (kWh/ton_LNG)	27.0	24.7	18.4
% of total power consumption of the process	6.7%	6.1%	4.6%
Compressor power			
Compressor K-100 (MW)	7.8	1.0	0.9
Compressor K-101 (MW)	4.1	9.9	2.0
Compressor K-102 (MW)	-	-	5.2
Total compressor power (MW)	11.9	10.9	8.1

Table 34 lists numbers of refrigerant flow rate and power consumption of the three models of the precooling system. The reduction in specific power consumption from the model with one evaporating stage of CO_2 to model with three stages is 8.6 kWh/ton LNG . The temperature decrease of natural gas in precooling is high and more efficient heat transfer of CO_2 has a high effect for this precooling process. The reduction in circulating refrigerant is 43% for the two-stage model and 48% for the three-stage model.

Table 35: Heat exchanger properties for CO_2 systems, APCI

Heat exchanger properties	CO ₂ system with one evaporation stage	CO ₂ system with two evaporation stages	CO ₂ system with three evaporation stages
UA values			
LNG-100 (MJ/C-hr)	4,160	4,024	2,482
LNG-101 (MJ/C-hr)	-	2,796	2,521
LNG-102 (MJ/C-hr)	-	-	2,774
LMTD values			
LNG-100 ($^{\circ}\text{C}$)	19.0	15.8	10.5
LNG-101 ($^{\circ}\text{C}$)	-	9.7	9.9
LNG-102 ($^{\circ}\text{C}$)	-	-	9.7

The initial system with one evaporation stage of CO₂ has a LMTD value of 19°C as seen in Table 35. The highest LMTD value decreases to 15.8°C with two evaporation stages and 10.5°C with three evaporation temperatures of CO₂. The combined UA values for the heat exchangers are higher for the more efficient precooling systems as seen in Table 35.

Table 36: Volume flow rates of compressors for CO₂ systems, APCI

Volume flow rates	CO ₂ system with one evaporation stage	CO ₂ system with two evaporation stages	CO ₂ system with three evaporation stage
<i>Compressor suction</i>			
K-100 (m ³ /hr)	17,300	4,240	4,096
K-101 (m ³ /hr)	10,160	11,170	5,162
K-102 (m ³ /hr)	-	-	6,483

The highest volume flow to compression in the initial CO₂ system is found in compressor K-100 with a volume flow of 17,300 m³/hr from Table 36. The highest suction volumes decreases with 55% for the two-stage model and 167% for the system with three evaporating temperatures of CO₂. This initial CO₂ system will larger compressors and pipe diameters than the two other processes.

7.2.3 Turbo-expander from patent number 5,768,912

The turbo-expander from US patent 5,768,912 has precooling of both the feed stream and the warm nitrogen stream from ambient temperature to -30°C. The temperature of the outgoing streams after precooling is higher than for the two other turbo-expander processes from TOTAL and APCI. This is explained further in Section 8.7. The modeling of the precooling system for this turbo-expander process will require an additional warm stream in the heat exchangers from Figures 12, 14 and 15. The split temperature for the CO₂ model with two evaporation temperatures of CO₂ was 0°C and the split temperature for the second model with three stages was 5°C and -15°C.

Table 37: Compressor power for CO₂ systems, US patent

	CO ₂ system with one evaporation stage	CO ₂ system with two evaporation stages	CO ₂ system with three evaporation stages
Refrigerant flow rate (ton/hr)	2380.9	1694.0	1601.0
Specific power consumption (kWh/ton_LNG)	69.7	57.4	49.9
% of total power consumption of the process	16.5%	13.6%	11.8%
Compressor power			
Compressor K-100 (MW)	16.9	9.1	2.0
Compressor K-101 (MW)	13.8	16.2	6.7
Compressor K-102 (MW)	-	-	13.3
Total compressor power (MW)	30.7	25.3	22.0

The power consumption for the CO₂ system with one evaporating temperature was 16.5% of the total power consumption for the expander process. This number is decreased to 13.6% and 11.8% with two and three evaporation stages of CO₂ as seen in Table 37. The precooling system has a reduction in refrigerant flow rate of 41% for the two-stage model and 49% for the three-stage model. The higher temperature of CO₂ to compression for this turbo-expander process increases the temperature between the compressor stages. The temperature exceeded 40°C after the first compressor step in the 2nd precooling system and an intercooler was installed in the process.

Table 38: Heat exchanger properties for CO₂ systems, US patent

Heat exchanger properties	CO ₂ system with one evaporation stage	CO ₂ system with two evaporation stages	CO ₂ system with three evaporation stages
<i>UA values</i>			
LNG-100 (MJ/C-hr)	16,630	14,470	9,083
LNG-101 (MJ/C-hr)	-	12,140	9,986
LNG-102 (MJ/C-hr)	-	-	8,952
<i>LMTD values</i>			
LNG-100 (°C)	15.7	10.9	9.1
LNG-101 (°C)	-	12.6	10.0
LNG-102 (°C)	-	-	8.7

The UA and LMTD values for the three precooling systems are listed in Table 38. The UA values for the heat exchangers in the CO₂ system for this expander process is high due to one extra warm stream to precooling. The UA value for the initial precooling system is 16,630 MJ/°C -hr as seen in Table 38. The heat exchangers in the two and three-stage models have smaller UA values but the combined values for these systems will be higher. The highest LMTD value is 10°C for the system with three evaporating temperatures compared with 15.7°C for the process with one evaporating temperature of CO₂.

Table 39: Volume flow rates of compressor for CO₂ systems, US patent

Volume flow rates	CO ₂ system with one evaporation stage	CO ₂ system with two evaporation stages	CO ₂ system with three evaporation stages
<i>Compressor suction</i>			
K-100 (m ³ /hr)	37,130	20,290	8,681
K-101 (m ³ /hr)	17,320	20,150	15,230
K-102 (m ³ /hr)	-	-	18,480

The suction volume for the initial precooling model is 37,130 m³/hr as seen in Table 39. The volume flow decreases with more efficient heat transfer between the CO₂ and the feed and nitrogen to precooling. The highest volume flow for the system with three pressure stages is 18,480 m³/hr. The reduced volume flows for the systems with several pressure stages allows for smaller pipes and equipment in these precooling systems.

8. Discussion and analysis of liquefaction processes for FLNG

Four liquefaction processes is studied in this Master thesis; a DMR process from APCI (Bukowski, 2011), a turbo-expander process from TOTAL (Chrétien, 2011), a turbo-expander from APCI (Bukowski, 2011) and a turbo-expander from US patent 5,768,912 (Dubar, 1998). This chapter discusses the results from the simulations of the liquefaction processes described in the sections above.

The specific power consumption gives an indication of the efficiency of the liquefaction processes. Table 40 includes the specific power consumption for the four liquefaction processes described in the previous chapters. The DMR has specific power consumption of 284 kWh/ton LNG as seen in Table 40. This number is substantially lower than for the turbo-expander processes with energy efficiencies of 396- 423 kWh/ton LNG. The difference in power consumption in between the two technologies is primarily based on thermodynamic features of the processes and is discussed in Section 8.3. The differences in power consumption of the turbo-expander processes are more complicated and several parameters are discussed in this chapter to explain the difference in specific power consumption of 7%.

Table 40: Specific power consumption for all four liquefaction processes

	APCI DMR	TOTAL turbo-expander	APCI turbo-expander	US Patent turbo-expander
Specific power consumption (kWh/ton LNG)	284.0	395.8	406.0	422.5

Specific power consumption for a turbo-expander process with precooling is expected to be around 300-400 kWh/ton LNG (Pettersen, 2013). The power consumption of the turbo-expanders will however vary with different process parameters for the processes. Parameters such as temperature of cooling water, composition and pressure of the natural gas entering liquefaction will influence the power consumption. Other thermodynamic reasons for lower expander process efficiency are temperature differences in cryogenic exchangers, heat rejection losses when the temperature of the refrigerant is much higher than the ambient temperature and losses in compressors and expanders. Larger compression power in the processes with efficiency losses represents more total power lost in the liquefaction process. Pressure drop in cryogenic heat exchangers and water-cooled heat exchangers will also reduce process efficiency. A higher ΔT in heat exchangers than necessary should be avoided from an efficiency point of view.

The specific power consumption listed in Table 40 is based on the numbers from HYSYS and is not a yearly average of energy required for the processes. The numbers does not consider break down or maintenance of equipment or other hold ups in production. The down time of the process is closely linked to the availability of rotating equipment in the process and is discussed in Section 8.7

8.1 Compression in liquefaction processes

The main nitrogen compressor represents most of the work in the turbo-expander processes. Power consumption and losses in the compressors in the three expander processes are therefore discussed in this section. The main nitrogen compressor has intercooling of the refrigerant between two pressure stages.

The high-pressure after compression in all turbo-expander processes were set to 70 bar as stated in Section 3.1. The main nitrogen compressor and compander compressors, powered by energy release from expanders in the process, compresses the refrigerant in the liquefaction processes. The load on the main compressor decreases if the expander power is high. Temperature of the entering nitrogen to compression is also an important parameter to consider. The pressure lift, temperature of refrigerant through compression and compression power are listed in Table 41. The numbers of volume flow rate and compression power for the compressors in Table 41 will be divided between several LNG production trains. The number of trains for each liquefaction process is discussed in Section 8.4.

Table 41: Main compressor for turbo-expander process

Turbo-expander model	TOTAL	APCI	US Patent
Pressure entering compression (bar)	13.0	13.5	7.3
Pressure after main compressor (bar)	43.9	43.5	37.5
Refrigerant temperature entering compression (°C)	18.9	18.9	-33.1
Temperature after 1 st stage of compression (°C)	91.0	87.0	78.8
Temperature out of compression (°C)	88.0	87.6	82.0
Volume flow of refrigerant to compression (m ³ /hr)	263,500	278,000	305,200
1 st compression stage (MW)	84.4	85.3	101.5
2 nd compression stage (MW)	75.3	82.6	55.0
Total compressor power (MW)	159.7	167.9	156.5

Table 41 shows that the turbo-expander process from US patent 5,768,912 has a pressure of 37.5 bar exiting the main compressor while the expander processes from TOTAL and APCI has outlet pressures of 43.9 and 43.5 respectively. These pressures are dependent on the compander compressors in the processes. The compander compressors for the US patent process will unload the main compressor with more power than in the two other turbo-expander processes. The refrigerant from the US patent process has however a lower incoming pressure to compression than the two other turbo-expander processes. The turbo-expander process from patent has a pressure of 7.3 bar while the processes from TOTAL and APCI have incoming pressures of 13-14 bar. This results in a similar pressure lift for the three turbo-expander processes with a compression of about 30 bar for the nitrogen refrigerant.

The process from US patent has the highest volume flow of refrigerant to compression with 305,200 m³/hr seen in Table 41. A larger suction volume to compression will require a larger and more costly compressor. The compression power for the US patent is 156.5 MW and the compression power for TOTALs and APCIs turbo-expander processes are respectively 159.7 MW and 167.9 MW from Table 41. The reason for the slightly lower compressor power from US patent despite the larger volume flow is the lower temperature of the refrigerant entering compression. Table 41 shows a difference in compressor inlet temperature of around 50°C between the three turbo-expander processes. The temperature of nitrogen is -33°C to compressor suction in the US patent model. A low incoming temperature decreases the work of compression. The temperature between compressor stages and after main compression is about 10°C lower for the process from US patent 5,768,912 and results in more efficient compression of the refrigerant. A disadvantage may be more costly materials and design solutions to cope with low temperature and the temperature variation from start-up conditions. Results from the simulations showed that the process was most efficient for similar heating of the refrigerant between compressor stages. This is the reason for the large difference in compressor power of 101.5 MW for the first stage of compression and 55 MW for the second stage in the US patent model.

Table 41 shows that TOTALs and APCIs process has equal temperatures of 18.9°C entering compression. The temperature increase of refrigerant through compression is also similar for the two turbo-expander processes. APCIs model has however a higher power consumption of the main nitrogen compressor than the turbo-expander process from TOTAL. The higher compression suction volume of 278,000 m³/hr for APCIs model can partly explain the higher compressor power than for TOTALs model which has a volume flow of 263,500 m³/hr. Higher compression power can also be explained by inefficiencies in the heat exchangers. Heat exchanger properties are discussed in Section 8.2.

Compressors in the DMR process will have low superheat of refrigerant because of latent heat transfer in the cryogenic heat exchangers. The efficient heat transfer of the mixed refrigerant minimizes losses in the compressors. The heat transfer properties of mixed refrigerant and nitrogen are discussed in Section 8.3.

8.1.1 Improvements of nitrogen compression

Additional compressor stages of the main nitrogen compressor were studied in Section 6.4. The additional intercooling stages have most effect for TOTALs and APCIs turbo-expander processes with reductions in specific power consumptions of 4% for both processes with four compression stages. The turbo-expander from US patent had a reduction in specific power consumption of less than 2%. This was due to a lower initial temperature of the nitrogen between compressor stages. All turbo-expander processes had a decrease in volume flow above 30% entering the final stage of the main compressor. A decrease in cooling temperature from 17°C to 10°C gave reductions in power consumptions of 4-5% for all expander-processes.

A richer feed gas was studied in Section 6.1. A richer feed gas increases the condensing temperature of the gas and decreases the power consumption in the process. The turbo-expander from US patent had a reduction of 2.7% with a richer feed gas. The increasing the feed gas pressure from 60 bar to 80 bar will have the same effect and increase the condensing temperature of the natural gas. APCIs turbo-expander process had the largest reduction in power consumption of 7.3%.

8.2 LMTD, UA values and minimum approach temperature in heat exchangers

Heat exchangers properties are discussed in this Section with main focus on minimum approach temperatures, LMTD values and the UA values of the heat exchangers. These numbers are listed in Table 42. The equipment numbers listed for the different processes can be found in Figures 1 and 2 in Chapter 2 for TOTALs turbo-expander process and APCIs DMR process. Figures 5 and 7 in Chapter 5 shows process models with equipment labels for APCIs turbo-expander process and the turbo-expander from US patent 5,768,912.

Table 42: Heat exchanger properties for the four liquefaction processes

Liquefaction process/exchanger	Min approach temperature (°C)	LMTD values (°C)	UA values (MJ/C-hr)
APCI DMR			
Feed-MR1-MR2 WMR CWHE	3.4	5.8	124,000
Feed- MR2 CMR CWHE (lower bundle)	3.0	6.9	71,810
Feed - MR2 CMR CWHE (upper bundle)	5.0	5.9	10,300
TOTAL turbo-expander			
Feed - N2 LNG-100	3.1	7.4	24,250
Feed - N2 LNG-101	3.0	6.8	57,000
Feed - N2 LNG-102	3.0	5.5	17,380
N2 - CO2 LNG-103	3.0	12.3	8,570
APCI turbo-expander			
Feed - CO2 LNG-100	3.0	19.0	4,160
Feed - N2 LNG-101	3.2	7.1	24,350
Feed - N2 LNG-103	3.0	5.9	17,750
N2 - N2 LNG-104	3.1	5.6	52,560
N2 - N2 LNG-102	4.6	5.5	22,960
US patent turbo-expander			
Feed - N2 - CO2 LNG-100	3.0	15.7	16,630
Feed - N2 LNG-101	3.0	3.2	22,660
Feed - N2 LNG-102	3.0	5.0	38,630
Feed - N2 LNG-103	3.2	4.9	6,947
Feed - N2 LNG-104	3.0	5.2	18,560

A large approach temperature in the heat exchangers will require more circulating refrigerant and increase the power consumption of the system. Heat exchanger areas will increase with smaller approach temperatures. The processes were optimized to achieve the lowest possible approach temperature. Column 2 in Table 42 lists the minimum approach temperatures for the four liquefaction processes. Most of the heat exchangers had approach temperatures of 3°C, which was the assumed minimum approach of cryogenic heat exchangers from Section 3.1. The minimum approach temperature of the upper bundle of heat exchanger CMR CWHE has an approach temperature of 5°C. The reason for the higher temperature is to meet requirements of full vaporization of refrigerant through the lower bundle of the heat exchanger. The penalty is higher for high temperature approaches in the cold end of the process. An approach temperature of 4.6°C for the internal nitrogen heat exchanger LNG-102 from APCIs model is found in Table 42. The higher temperature in this heat exchanger is necessary to offset a higher LMTD value for feed-nitrogen exchanger LNG-101.

The log mean temperature difference is a measure of driving force for a heat exchanger and is dependent on the circulation rate of refrigerant in the process. A low LMTD value is preferable due to the reduced power consumption of the compressors, but it will also require larger heat exchangers. Mixing of several streams with different pressures and temperatures induces losses and makes it more difficult to achieve low LMTD values for the heat exchangers. Column three in Table 42 lists the LMTD values for all heat exchangers in the liquefaction processes studied in this Master thesis. The heat exchangers for precooling have high LMTD values and the value for APCIs model with 19°C is the highest LMTD value in Table 42. These values can be reduced with several evaporation stages of CO₂ in the precooling systems, but temperature differences are of less concern in the near-ambient temperature of the process. The precooling systems are discussed in Section 8.7.

The process from US patent 5,768,912 has the lowest LMTD values of the processes with the most efficient heat transfer in the heat exchanger segments with values ranging from 3.2-5.2°C, excluding the inefficient heat exchanger for precooling. APCIs and TOTALs turbo-expander processes has similar LMTD values for the heat exchangers seen in column 3 of Table 42. The high LMTD value for the precooling system of 19°C makes the heat transfer less efficient than for TOTALs turbo-expander process. APCIs DMR model has three heat exchanger segments in the model while the turbo-expander processes has four or five. The LMTD values for the DMR process ranges from 5.8-6.9°C. These values are relatively high for a DMR process with evaporating heat transfer.

The UA values for the heat exchangers are listed in column four of Table 42. The U is the overall heat transfer coefficient for the heat exchanger while A is the area of the heat exchanger. The U -values for mixed refrigerant is higher than for nitrogen and this makes it difficult to compare the UA values for the two liquefaction technologies. An estimation of the gas side heat transfer and vaporization coefficient can be performed in order to compare the two process types, but this will not be evaluated here. The heat exchanger types are also

different for the two process technologies with Plate-fin heat exchangers (PFHE) for the turbo-expander processes and Coil-wound heat exchangers for the DMR process. The equipment in the processes will be discussed in Section 8.8.

The DMR process has a UA value of 124,000 MJ/°C-hr for heat exchanger WMR CWHE from Table 42. This heat exchanger has four large streams of feed gas and mixed refrigerants for and the combined U value for this heat exchanger segment is probably larger than for any of the other heat exchangers in the liquefaction processes. The UA values for the three heat exchangers of precooling is relatively small compared to the other UA values for the turbo-expander processes in Table 42. High LMTD values in these heat exchangers will decrease the UA values. The turbo-expander process has the largest UA value for a heat exchanger segment of 57,000 MJ/°C-hr. The model from APCI will have internal an internal heat exchange area of nitrogen and a heat exchange area of feed gas and nitrogen.

8.2.1 Improvements of LMTD, UA values and minimum approach temperature in heat exchangers

Reduction in approach temperatures and LMTD values in heat exchangers increases the efficiency of the processes. Approach temperatures in the process should be as close to the minimum allowable value of 3°C as possible. Heat exchangers with a smaller allowable temperature than 3°C can also be considered for the liquefaction processes. Aluminum brazed heat exchangers of the plate-fin type have minimum temperature approaches of 1-2°C (Thonon, 2012).

Split temperatures of natural gas and refrigerant between the heat exchanger segments have impacts on the heat exchanger properties. Matching of the split temperatures of the warm streams to the cold refrigerant streams can decrease the approach temperatures and the LMTD values for the heat exchangers. The influence of split temperatures for the fluids was tested in Section 6.6 and is discussed in Section 8.6.1.

8.3 Heat transfer properties

The efficiency of the liquefaction process will highly depend on the heat transfer properties of the refrigerants. A mixed refrigerant consisting of hydrocarbons will have boiling heat transfer between the fluids and increase the efficiency of the process as opposed to a single-phase gas. The DMR process is more efficient than the turbo-expander processes due to smaller LMTD values throughout the process with boiling heat transfer and less heat rejection losses. The DMR process would be the obvious choice when looking at the processes purely from an efficiency point of view. Other factors such as flammable refrigerants and liquid motions of the refrigerant must however also be considered and the selection of liquefaction processes becomes more complicated.

The refrigerant-side heat transfer between the mixed refrigerant and feed in the DMR process is primarily transferred by vaporization (latent heat). The

temperature increase of the MR through the heat exchangers is low due to the phase transition from liquid to gas of the refrigerant. Phase transition of the mixed refrigerant enables close matching of the temperature profiles, and decreases the superheating of the gas to compression. The mixed refrigerant should hold a temperature a couple degrees above the dew point to prevent liquid from entering the first stage of compression. A separator will also be installed upstream of compression for the same purpose and to protect the compressor. The mixed refrigerant had superheating of 5°C when entering compression in the first MR circuit in the DMR process. The mixed refrigerant to compression in the second MR circuit had initially no superheating of the gas and the circulating rate of refrigerant in this circuit should be lowered for a small superheat of the gas to compression, or the composition or pressure need to be adjusted.

The turbo-expander processes have single-phase operation of the refrigerant with sensible heat transfer between the natural gas and nitrogen. This causes heating of the gas exiting from the heat exchangers and decreases the efficiency of the processes. The nitrogen will require more circulating refrigerant in the process to liquefy the gas than for the DMR process because of the poorer heat transfer qualities of nitrogen. The combined effect of higher refrigerant circulation rate and temperature increase through the heat exchangers, as well as more difficulty in matching the feed gas temperature profile, increases the workload for the compressors in the turbo-expander processes. The temperature to compression should therefore be as low as possible to minimize additional thermodynamic losses in the liquefaction processes. The temperatures to the main compressor in the turbo-expander cycles are given in Table 41 from Section 8.1.

The precooling systems in the turbo-expander processes use latent heat transfer between the CO₂ and the warm streams for precooling. Pressure drop and superheat may cause temperature change of the CO₂ from the heat exchanger. CO₂ has superior heat transfer properties over nitrogen in the higher temperature ranges of the liquefaction process and the temperatures of warm streams from precooling should therefore be as close to the maximum allowable temperature of -40°C. The different CO₂ precooling systems are discussed in Section 8.7.

8.3.1 Improvements of heat transfer properties

A richer gas composition was tested in Section 6.1. The higher condensation temperature of the natural gas will reduce the temperature lift in the process and increase efficiency. The turbo-expander processes had reductions in specific power consumption ranging from 1.0-2.7% for a richer feed gas. The effect in power consumption for DMR process was less than 0.1%. A higher pressure of the feed gas will also reduce the temperature lift in the process. The decrease in power consumption for the turbo-expander processes was from 3.3-7.3%. The DMR process had a decrease in power consumption of 7% for a higher feed gas pressure.

The composition of refrigerant can also be changed to increase the efficiency in a DMR process. The effect of increasing the fraction of heavier hydrocarbons in the mixed refrigerant was studied in the project thesis from fall 2012 (Hasle, 2012). The mole fraction of n-Butane in the first MR circuit was increased by 5% from a fraction of 0.085 to a value of 0.089. The lighter hydrocarbons were reduced with an equal mole fraction. The increase in n-Butane was an arbitrary number chosen for the purpose of studying a marginally richer composition of the mixed refrigerant. A reduction in specific power consumption from 284 to 282.2 kWh/ton LNG was found for the richer composition of mixed refrigerant.

8.4 Production capacities and liquefaction trains

The four liquefaction processes had a LNG production capacity of 3.5 Mtpa. The turbo-expander processes have lower capacities per train than the DMR processes and several trains are needed in production for the turbo-expander processes. The compressor systems in the processes have limiting capacities of 15 MW and determine the number of trains required for the turbo-expander processes. The equipment for one DMR train is assumed large enough to handle the production capacity of LNG.

Table 43 lists the power production of each expander for the three turbo-expander processes in this Master thesis. The equipment labels for the expanders can be found in Figure 1 in Chapter 2 for TOTALs turbo-expander process and Figures 5 and 7 for APCIs expander process and the turbo-expander from US patent 5,768,912.

Table 43: Power production of turbo-expanders

Released power from turbo-expanders (MW)	
TOTAL turbo-expander	
Warm expander K-106	48.5
Cold expander K-103	12.6
<i>Total expander power</i>	<i>61.1</i>
APCI turbo-expander	
Warm expander K-102	55.0
Cold expander K-10	12.6
<i>Total expander power</i>	<i>67.6</i>
US patent turbo-expander	
Warm expander K-106	28.7
Cold expander K-105	21.5
Additional expander K-107	16.0
<i>Total expander power</i>	<i>66.2</i>

The warm expanders in Table 43 have the highest energy release out of the expanders for all processes. TOTALs and APCIs processes have about four times higher power release from the expanders in the warmer parts of the process than for the cold expander. The reason for the higher energy release is more

need for cooling power in this part of the process. The cold nitrogen from the warm expanders liquefies the natural gas and provides cooling of the warm nitrogen refrigerant in the process. The expander in the cold part of the process only provides refrigerant for the subcooling of the natural gas. The warm expanders determine the number of liquefaction trains required for the turbo-expander processes from TOTAL and APCI. Four trains are required for these processes with a compander capacity of 15 MW.

The difference in energy release for the three expanders in the US patent model is not as substantial as for the two other turbo-expander processes. The energy release from the warm expander is split in two expanders with heating of the cold refrigerant between the expanders. The warm expander K-106 and the additional expander K-107 from US patent have a total power release of 44.7 MW and the refrigerant streams from these expanders liquefy the natural gas. The cold expander K-105 has the highest energy release of the cold expanders for the three processes with a power production of 21.5 MW from Table 43. The reason for the high energy release is the warmer inlet temperature of this expander. The cold expander in this process has an inlet temperature of -84°C while the inlet temperatures for the two other processes is around -100°C . An outlet temperature of -163°C requires a higher pressure drop or the expander from US patent and more power is produced in the expander. A split of the warm expanders in two stages reduces the load on the compander system. The expander with the highest energy release is also the warm expander for this process with a power production of 28.7 MW. This requires two parallel trains for the US patent expander process assuming maximum compander capacities of 15 MW. The power in the warm compander is close to the maximum value of 30 MW in the companders for two trains and a third liquefaction train is possibly required.

Several liquefaction trains increases the weight and size requirements of the liquefaction unit. The total equipment count is higher for TOTALs and APCIs liquefaction processes, but smaller equipment at lower cost can be installed for smaller circulation rates of refrigerant. Several trains increase the availability of the process and induce higher flexibility of the equipment placement on the FLNG. A common CO₂ system serves all trains for the turbo-expander processes and increased availability of the liquefaction processes with several trains is dependent on full functionality of the CO₂ system.

8.5 Volume flow of refrigerant

The volume flow of refrigerant in the processes gives an indication of the piping and equipment sizes needed in the different liquefaction processes. Volume flows entering and exiting rotating equipment such as compressors and expanders are especially of interest to indicate the size and cost of equipment. This section includes the suction volume of the compressors for all four liquefaction processes and the volume flow of refrigerants from expander outlets for the turbo-expander processes. The volume flows of refrigerant are given in Tables 44 and 45. The numbers in the tables are based on the simulation in

HYSYS with one liquefaction train for the processes. Models with equipment labels for the processes are found in Figures 1 and 2 in Chapter 2 for TOTALs turbo-expander process and APCIs DMR process. Models of APCIs turbo-expander process and expander from US patent are found in Figures 5 and 7 in Chapter 5.

Table 44: Suction volume of compressors

Suction volume of compressors (m3/hr)	
APCI DMR (1 train)	
<i>1st MR circuit</i>	
Low pressure compressor LP warm	105,900
High pressure compressor HP warm	49,090
High pressure pump WMR Pump	327
<i>2nd MR circuit</i>	
LP Cold	159,200
MP Cold	50,070
HP Cold	21,340
HHP Cold	17,080
TOTAL turbo-expander (1 train/4 trains)	
1 st stage of main compressor K-101	65,875 / 263,500
2 nd stage of main compressor K-102	35,350 / 141,400
Warm compander compressor K-104	15,760 / 63,040
Cold compander compressor K-105	4103 / 16,410
CO2 low pressure	21,410
CO2 high pressure	7,566
APCI turbo-expander (1 train/4 trains)	
1 st stage of main compressor K-105	69,500 / 278,000
2 nd stage of main compressor K-101	77,150 / 154,300
Warm compander compressor K-106	17,683 / 70,730
Cold compander compressor K-107	4,060 / 16,240
CO2 low pressure	17,300
CO2 high pressure	5,161
US patent turbo-expander (1train/2 trains)	
1 st stage of main compressor K-100	152,600 / 305,200
2 nd stage of main compressor K-101	62,300 / 124,600
Warm compander compressor K-102	15,920 / 31,840
Cold compander compressor K-103	11,940 / 23,880
Additional compander compressor K-104	8,885 / 17,770
CO2 low pressure	37,130
CO2 high pressure	17,320

Table 44 lists the total volume flows for the compressors and the suction volume for each train in the four processes. The low-pressure compressors are highlighted in the Table.

APCIs DMR process is assumed with one train in operation for liquefaction of the natural gas. The low pressure compressors in the two MR circuits have the highest volume flow rates in the process as seen in Table 44. The incoming pressures of the refrigerant to compression are low with entering pressures of 8.5 bar and 4.1 bar for the first and second MR circuit respectively. The volume flow to compression in the second MR circuit has a volume flow of 159,200 m³/hr from Table 44, and will require a large compressor for the process. The limitations in equipment are discussed in Section 8.8.

The volume flow of refrigerant is divided between trains for the turbo-expander processes. The highest volume flow in the processes is through the main nitrogen compressor. The expander process from US patent will have a high suction volume of 152,600 m³/hr for the main compressor in each train. The suction volume for the main compressors in TOTALs and APCIs expander processes are 65,900 m³/hr and 69,500 m³/hr respectively, from Table 44. The compressors for TOTALs and APCIs expander processes will be much smaller than for the US patent expander. The compressor power in the first stage of the main compressor is also high for this process as discussed in Section 8.1 and the compressor required for the US patent model is assumed large and costly.

The largest compander compressors for TOTALs and APCIs expander processes has volumetric flow rates of 15,760 m³/hr and 17,780 m³/hr for each liquefaction train. This is for the companders linked to the warm expanders with the highest energy release. The US patent process has a volume flow of 15,920 m³/hr in the largest compander. The volume flows of the CO₂ compressors for each system are listed in Table 44. The turbo-expander processes have a common CO₂ system for each liquefaction process. The highest volume flow of a CO₂ compressor is found in the US patent process with a volume flow of 37,130 m³/hr. The volume flows in the CO₂ system are not considered to be limiting factors in the liquefaction processes.

Table 45: Volume flow from expansion of the gas for all processes

Volume flow from expansion of refrigerant (m ³ /hr)	
APCI DMR	
<i>There are no expanders in the DMR process</i>	
TOTAL turbo-expander (4 trains)	
Warm expander K-106	21,018 / 84,070
Cold expander K-103	5,233 / 20,930
APCI turbo-expander (4 trains)	
Warm expander K-102	23,393 / 93,570
Cold expander K-100	5,185 / 20,740
US patent turbo-expander (2 trains)	
Warm expander K-106	23,250 / 46,500
Cold expander K-105	21,625 / 43,250
Additional expander K-107	55,750 / 111,500

The volume flow of refrigerant is highly dependent on the temperatures and pressures of the streams entering and exiting the rotating equipment. Table 45 lists the volume flows of refrigerant exiting expanders in the turbo-expander processes. The LNG liquid expanders are not included in this discussion.

The turbo-expander from US patent 5,768,912 has the highest volume flow of exiting refrigerant from an expander in the three processes. The volume flow from the third expander in this process is 55,750 m³/hr for a single train as seen in Table 45. The high volume flow from this expander is a result of the low outlet pressure of 8.1 bar and a “warm” exiting temperature of -90°C for the refrigerant stream. The volume flows for the warm and cold expander in the US patent process are about the same. TOTAL and APCIs processes have similar volume flows exiting the cold expanders in the processes. The volume flows are approximately 5,200 m³/hr for TOTAL and APCIs cold expanders seen in Table 45. The reason for the similar volume flows is the temperature and pressure reduction from about -100°C to -163°C and pressures between 14-15 bar in both processes. The process from US patent has a low-pressure of 9 bar from the cold expander because of the larger temperature reduction in this expander from -84°C to -163°C.

The positive effects of a higher low-pressure of refrigerant for the expander process is offset by a larger circulation rate of refrigerant than in the DMR process, due to sensible heat transfer of nitrogen.

8.5.1 Improvement in volume flows for the process

High pressure and low temperature will decrease volume flow rates of the refrigerant streams. The volume flow will also decrease for reduced amounts of refrigerant in the process. Several compressor stages of the main nitrogen compressor with intercooling in between stages with were studied in Section 6.4. The study of three compressor stages had a reduction in volume flow of 19.9%-22.4% for the turbo-expanders. The reduction in volume flow for the final compressor stage was 31.2%-33.6% when a fourth stage of compression was used. The pressure drop in the intercoolers was not accounted for and the actual volume flow will be slightly higher. A lower cooling temperature in the process will also reduce the volume flow in the processes. The DMR process had a reduction in volume flow to the low-pressure compressor of 14.5% for the first circuit with a sea water temperature of 6°C.

A higher pressure of the feed gas was studied in Section 6.2. The volume flow to compression for the same pressure and temperature of was decreased for the turbo-expander processes because of a smaller circulation rate of refrigerant. The turbo-expander process from US patent had the highest decrease in suction volume to the main compressor with 7.4% for a higher feed gas pressure. The warm expander in APCIs system had a reduction in volume flow outlet of 13% for a higher feed gas pressure. A richer feed gas composition was studied in Section 6.1. The refrigerant flow rate was also reduced for this process, but the effects in volume flows were not as substantial.

8.6 Split temperatures of feed gas and refrigerant

All four liquefaction processes described have several heat exchanger segments with temperature splits of the feed gas and refrigerant. The splits between the heat exchanger segments must be modeled as separate heat exchangers in HYSYS when refrigerant streams are mixed or separated in the process.

The temperature splits for the four liquefaction processes are listed in Table 46. Models with equipment labels for the processes are found in Figures 1 and 2 in Chapter 2 for APCIs DMR process and TOTALs turbo-expander process. Figures 5 and 7 in Chapter 5 shows models of APCIs turbo-expander process and the turbo-expander from US patent 5,768,912. The heat exchangers have often requirements of single-phase flow entering the heat exchangers (Pettersen, 2013). This is accounted for when split temperatures are chosen for the processes. All processes have an exiting temperature of -160°C from the last heat exchanger segment.

Table 46: Split temperatures of feed gas and refrigerant for all liquefaction processes

	Split temperatures of natural gas and refrigerant	
	Warm streams (°C)	Cold streams (°C)
APCI DMR		
Split 1 after 1 st MR circuit	-49.1	-55.3
Split 2 mixing of MR streams in 2 nd circuit	-135.0	-138.0
TOTAL turbo-expander		
Split 1 refrigerant sent to precooling	-8.5	-23.7
Split 2 mixing of cold refrigerant after warm expander K-106	-101.4	-112.8
APCI turbo-expander		
Split 1 natural gas from precooling	-40.0	-48.0
Split 2 mixing of cold refrigerant after warm expander K-102	-96.0	-105.6
US patent turbo-expander		
Split 1 streams from precooling	-30.0	-33.1
Split 2 to additional expander K-107	-51.0	-55.0
Split 3 mixing of cold refrigerant after additional expander K-107	-84.0	-92.0
Split 4 from warm expander K-106	-100.0	-104.0

The DMR process has two split temperatures of refrigerants and natural gas. The first split occurs naturally after the first mixed refrigerant circuit. The feed is in gas phase when exiting the first heat exchanger segment WMR CWHE at a temperature of -49.1°C seen in Table 46. The second split in the DMR process is after liquefaction of the gas in the lower bundle of heat exchanger CMR CWHE of the second mixed refrigerant circuit. The temperature is -135°C of the feed gas

for this temperature split. The liquefied natural gas is subcooled in the upper bundle of heat exchanger CMR CWHE after the second split temperature in the process.

Several split temperatures in the turbo-expander processes changes the gradients of the refrigerant to better match the cooling curve of natural gas. A smaller gap between the heating and cooling curves will be crucial for the turbo-expander process with less efficient heat transfer than the DMR process. Introduction of temperature splits increases the efficiency of the process by lowering the approach temperatures and LMTD values in the heat exchangers. The turbo-expander from US patent has the highest number of split temperatures of the processes seen in Table 46. One additional expander in this process requires a split temperature between two heat exchanger segments. The LMTD values are better for this process for each heat exchanger segment as discussed in Section 8.2. The natural gas enters heat exchanger LNG-102 in a pure gas phase in split 2 of the heat exchanger segments at a temperature of -51°C. The gas is fully liquefied when exiting heat exchanger LNG-102 in the third split with a temperature of -84°C.

The turbo-expander processes from TOTAL and APCI has two split temperatures of gas and refrigerants seen in Table 46. TOTALs turbo-expander had the first temperature splits of feed and nitrogen at -8.5°C from the simulation of the process in Chapter 5. A portion of the warm nitrogen stream is sent to precooling in the first temperature split after heat exchanger LNG-100. The reason for the high split temperature is to better exploit the latent heat transfer of CO₂. The other fraction of the nitrogen and the natural gas is sent through heat exchanger LNG-101. The feed is in gas phase when entering LNG-101. The second split temperature for this process is at -101.4°C. The natural gas is fully liquefied at this temperature. The liquid natural gas is subcooled in heat exchanger LNG-102.

APCI's turbo-expander model has the first split temperature after precooling of the natural gas to -40°C seen in Table 46. The feed is in all gas phase when entering the upper feed – nitrogen exchanger LNG-101. The feed is liquefied through heat exchanger LNG-101 with an exit temperature of the liquid at -96°C. The lower feed – nitrogen heat exchanger LNG-103 subcools the liquid. APCI's turbo-expander model have also two internal nitrogen heat exchangers. These have split temperatures of -34.9°C for the warm stream and -45°C for the cold stream in the upper nitrogen exchanger LNG-104. The second nitrogen exchanger has a warm temperature of -102.1°C and a cold stream of -111.5°C. The high number of nitrogen splitters and mixers in this process induces losses when streams at different temperatures are mixed. This is also the reason for the larger temperature approaches of the warm and cold streams and the high LMTD values in the heat exchangers.

8.6.1 Improvements in split temperatures of feed gas and refrigerant

The split temperatures in the processes were evaluated in Section 6.6. TOTALs expander process has a reduction in specific power consumption of 0.5% when

the temperature was changed from -101.4°C to -103°C in the second split of the process. The split temperature in APCIs turbo-expander process was changed from -96°C to -100°C. This gave a power reduction of 0.6%. The LMTD values for the heat exchangers on each side of the split were decreased. The LMTD value in the first feed-nitrogen heat exchanger was reduced from 7.1°C to 6.9°C and the LMTD value in the second heat exchanger was changed from 5.9°C to 5.6°C.

The US patent process had a reduction in power consumption of 0.9% when the split temperature to the cold expander in the process was increased from -84°C to -82°C. The LMTD values in the heat exchangers on each side of the split were unchanged. The turbo-expander processes from TOTAL and APCI had a reduction in power consumption for a lower split temperature than the initial temperature, while the expander process from US patent had a decrease in power consumption for a higher temperature than the initial temperature.

8.7 Precooling systems

The three turbo-expanders from TOTAL, APCI and US patent 5,768,912 were modeled with a precooling system with CO₂ as the refrigerant. CO₂ has more efficient heat transfer with latent heat as opposed to sensible heat for the nitrogen refrigerant. The liquefaction processes has precooling of different streams and at different temperatures. Table 47 summarizes the streams to precooling and the cooling range of CO₂ in the three turbo-expander cycles.

Table 47: Description of precooling systems for turbo-expander processes

Turbo-expander model	TOTAL	APCI	US Patent
Warm stream to precooling	Nitrogen	Feed	Feed and nitrogen
Temperature to precooling (°C)	-8.5	22.0	22.0
Temperature exiting precooling (°C)	-40.0	-40.0	-30.0

TOTALs turbo-expander process had precooling of the nitrogen refrigerant after the 1st heat exchanger LNG-100 with an incoming temperature of -8.5°C seen in Table 47. The stream continued to temperature reduction in warm expander K-106 after cooling of the nitrogen to -40°C. The precooling of nitrogen reduces the pressure reduction in the warm expander and saves compressor work. It also prevents losses in mixer MIX-100 with same mixing pressures of the stream from warm expander K-106 and the nitrogen stream from cold expander K-103.

The model from APCI had precooling of the feed gas from ambient temperature to -40°C seen in Table 47. The CO₂ cools the nitrogen over 60 degrees before entering the nitrogen loop in the liquefaction process and will theoretically decrease the circulation flow of nitrogen. This is however dependent on the efficiency in the other parts of the liquefaction process. The simulation of APCIs model shows inefficiencies in the heat exchangers with high LMTD values and high circulation rates of nitrogen in the process.

The model from US patent 5,768,912 had precooling of the feed stream and the warm nitrogen refrigerant from ambient temperature to -30°C seen in Table 47.

The lower temperature from precooling for this process is due to the increased number of refrigerant splits for this process. A precooling temperature of -30°C was also described in the US patent (Dubar, 1998). A precooling temperature of -35% was studied in Section 6.6 and gave an increase in power consumption of 0.7%.. Two warm streams to precooling will increase the load of the CO2 system compared with the two other expander processes.

The three turbo-expanders from TOTAL, APCI and US patent 5,768,912 were originally modeled with a single evaporation stage CO2 system for heat transfer between the refrigerant and the warm stream to precooling. Two alternative precooling systems were evaluated in Chapter 7 with two and three evaporation stages of heat transfer for the CO2. The simulations of the different precooling models showed that the systems with several pressure stages had superior heat exchanger properties and less power consumption of the CO2 compressors. The model with three evaporating temperatures had the best numbers of the three CO2 systems studied and is compared with the initial model of with one evaporation stage in Table 48. The models of the precooling units can be found in Figures 12,14 and 15 of Chapter 7.

Table 48: Results for CO2 systems with one and two evaporating stage of CO2

CO2 system evaluation	TOTAL		APCI turbo		US Patent	
	1-stage	3-stages	1-stage	3-stages	1-stage	3-stages
Total specific power consumption of liquefaction process (kWh/ton LNG)	395.8	393.5 (-0.6%)	405.7	397.1 (-2.1%)	422.5	402.8 (-4.7%)
Refrigerant flow rate of CO2 (ton/hr)	1039.8	635.0	709.4	478.0	2380.9	1601.0
Power consumption compressors (MW)	15.7	14.7	11.9	8.1	30.7	22.0
LMTD values (°C)						
1st heat exchanger	12.3	5.9	19.0	10.5	15.7	9.1
2nd heat exchanger	-	8.7	-	9.9	-	10.0
3rd heat exchanger	-	7.3	-	9.7	-	8.7
Total UA value (MJ/C-hr)	8,570	13,883 (+62.0%)	4,160	7,777 (+86.9%)	16,630	28,021 (+68.5%)
Highest suction volume to compression (m3/hr)	21,410	13,260	17,300	6,483	37,130	18,480

The “stages” in Table 48 represents numbers of evaporation stages of the CO2. The turbo-expander from US patent has the highest reduction in specific power consumption of 4.7% with a more efficient CO2 system from Table 48. This result was expected because of the higher load for this system with two warm streams to precooling. The circulating CO2 in the precooling systems are improved for all systems with three evaporation stages of CO2. The LMTD values for each heat exchanger are also improved for several heat transfer stages. The UA values will however increase with smaller LMTD values as seen in Table 48. APCIs turbo-expander process had the highest initial LMTD value of 19°C. The

maximum value of LMTD for the three evaporating stages for this process was 10°C. The total UA value for this process increased with 87% with smaller LMTD values in the three-stage system. The highest suction volume of CO₂ to compression is decreased for all turbo-expander processes with several evaporating stages and the size and cost of equipment and pipes can be reduced.

TOTALs process had a power reduction of 0.6% for the expander process with the improved CO₂ system. The lower inlet temperature of the warm stream to compression can explain the lower power reduction for TOTALs process. The initial CO₂ system for this process had a temperature of -11.5°C to compression in the low-pressure compressor of the CO₂ system. This was to maintain a minimum approach temperature of 3°C in the heat exchanger. Simulations showed that a high approach temperature in the heat exchanger gave a higher penalty in energy consumption for the process than superheating of the gas to compression. This was also the case for the other turbo-expander processes. The warm streams to compression were 22°C for these systems and resulted in a temperature of 19°C of the CO₂ to compression. The initial precooling model for TOTALs expander process was more efficient than for the other models and this resulted in a lower efficiency increase for TOTALs process with three evaporating stages of CO₂.

8.8 Equipment

The size and weight of the processes equipment are important when selecting a liquefaction technology for FLNG. The size of the equipment is dependent on the volume flow of refrigerant and the power in rotating equipment. The volume flow in the four processes was discussed in Section 8.5. A list of equipment for the four processes is found in Table 49.

Table 49: Equipment count for the liquefaction processes

Equipment count	APCI DMR 1 train	TOTAL turbo- expander / 4 trains	APCI turbo- expander /4 trains	US patent turbo- expander /2 trains
Cryogenic heat exchanger segments	3	4/13	5/17	5/10
Heat exchangers for water cooling	6	5/14	5/14	4/6
Compressors	6	3/6	3/6	3/4
Compander systems	-	2/8	2/8	3/6
Liquid expanders	-	1/4	1/4	1/2
Pumps	1	-	-	-
Separators	3	1/1	1/1	1/1
JT-valves	5	2/2	2/2	2/2
LM 6000 gas turbines	4	6/6	6/6	6/6
Total	28	24/54	25/58	25/37

Table shows the equipment count for a single train and the equipment count for the required number of trains in the liquefaction processes. The number of equipment for each train is similar in Table 49. The DMR process has the highest

amount of equipment for handling of two-phase flow. The added equipment for TOTALs and APCIs process is high with respectively 54 and 58 units required for a production capacity of 3.5 Mtpa. The turbo-expander from US patent 5,768,912 has the least amount of equipment of the turbo-expander processes with 37 units for two production trains.

The availability of the process is linked to the availability of the liquefaction unit. The DMR process has a rotating equipment number of 10 units from Table 49. TOTALs turbo-expander process has 24 units of rotating machinery in four trains. The number for each train is 8 units assuming a number of 2 LM 6000 gas turbines for each train. The amount of rotating equipment for APCIs turbo-expander process is exactly the same as for TOTALs process. The turbo-expander from US patent will have one extra compander system and higher power consumption for each train. The amount of rotating equipment for a single train is therefore 10 units. The total number of rotating machinery for the process is 18 units. The availability of the processes is discussed in Section 8.10.

A liquid expander in the turbo-expander processes increases the number of rotating equipment by one unit for each liquefaction train. The liquid expander for LNG product expansion replaces the conventional Joule-Thompson valve. The liquid expander produces work that can be used to unload the main compressor or the CO₂ compressors in the system. The total released work for the liquid expander is approximately 1.2 MW. The liquid expander will not create flash gas in the system unlike the Joule-Thomson valve with a negative JT-coefficient and heating of the liquid LNG through expansion. The liquefaction processes usually operates with a flash system if the nitrogen content in the gas is high. The work released from the liquid expander is considered low compared with the power requirements for the compressors in the system. A rotating device is also more exposed for failure and the necessity of a liquid expander should be evaluated.

The main costs for liquefaction units are the compressors and drivers in the system. Compressors represent the highest capital cost for a LNG plant and about 40% of the total operating costs (Castillo, 2011). Selection of compressor units is based on the suction volume of the compressor and the power consumption of the unit. The turbo-expander from US patent has a suction volume of 152,600 m³/hr to compression and a power consumption of 78.3 MW for the main nitrogen compressor in each liquefaction train. A single train in US patent process is high due to only two production trains. This compressor has an intercooling of the gas between two compressor stages. The largest suction volume to compression for the DMR process is 159,200 m³/hr for the low-pressure compressor in the second MR circuit. The power consumption for this compressor is 39 MW. The compressors described in this Master thesis are centrifugal compressors. The largest centrifugal compressors can handle discharge pressures of 60+ bar and volume flows up to 500,000 m³/hr (Pelagotti, 2013). The maximum discharge pressure for the main compressor is found for TOTALs turbo-expander process at a value of 44 bar. A capacity of 44 MW is described for a centrifugal compressor for LNG production (Pelagotti, 2013) and several compressors units for the main compressor might be needed for the turbo-expander from US patent.

The highest volume flow of CO₂ in the precooling system is 37,000 m³/hr for the turbo-expander from US patent with a power requirement of 16.9 MW. The discharge pressure in the CO₂ system is 32 bar for the low pressure compressor with the largest volume flow. The CO₂ compressors are therefore not assumed to be a limiting factor for the liquefaction processes.

Linde provides both coil-wound heat exchangers (CWHE) and plate-fin heat exchangers (PFHE) for use in cryogenic systems. Plate-fin heat exchangers are suggested for the turbo-expander processes while Coil-wounded heat exchangers are used in the DMR process. The plate-fin heat exchangers are compact and are well suited for LNG technology. The PFHEs are made of aluminum alloy, which is a light material suitable for cryogenic temperatures (Linde, 2009). The PFHE can treat several process streams in one unit and handles gas at high pressures as well as condensation on the plates. Plate-fin heat exchangers also allow small approach temperatures and low pressure drops over the plates for increased efficiency in the process.

The coil-wound heat exchangers are robust and can tolerate high thermal stress. The CWHE can handle large temperature ranges and high pressures. A possible leak in a CWHE will be fully contained and no refrigerant is leaked to the environment (Bukowski, 2011). Thermal stress from liquid motions of the FLNG can cause maldistribution of liquid in the heat exchangers. This will be an issue for the DMR process with liquid refrigerant. The CWHE units are expensive with only a few suppliers.

The coil-wounded heat exchangers have higher capacities than the plate-fin heat exchangers. The plate-fin heat exchangers will require parallel units to handle the fluid flow in the turbo-expander processes. The number of heat exchanger units is based on the UA values for the heat exchanger segments discussed in Section 8.2. TOTAL had the highest UA value of the turbo-expander processes for the feed-nitrogen heat exchangers of 98,630 MJ/°C-hr. This was 13.6% larger than for the UA value for the feed-nitrogen heat exchangers for the turbo-expander from US patent and 105% larger than for APCIs turbo-expander. APCIs model has however internal nitrogen heat exchangers with a UA value of 75,520 MJ/°C-hr. The heat exchanger area will be difficult to determine without knowing the *U* values for the processes.

The equipment on an FLNG is exposed for salt water and will therefore need to be built in a non-corrosion material. This can increase the weight of the liquefaction unit since the unprotected material should be switched from aluminum to stainless steel (Bukowski, 2011). A cold box for the liquefaction unit will prevent heat transfer with the surroundings and protect the equipment for corrosion.

8.9 Refrigerant flow rate & storage of refrigerant

The refrigerant flow rate needed to liquefy the natural gas measured in ton/hr is not a very important parameter when it comes to the evaluation of liquefaction

processes. Refrigerant properties are highly dependent on temperature, pressure and composition of the refrigerant and a measure of volume flow rate will therefore give a better indication of equipment and pipe dimensions required in the process. The volume flow and equipment are previously discussed in Sections 8.5 and 8.8.

Refrigerant mass flow rate is still included in the discussion to get an indication of make-up refrigerant required to cover losses throughout the process. Make-up refrigerant is assumed to be 0.05-0.1% of the refrigerant flow of the process (Pettersen, 2013). Table 50 lists the refrigerant flow rate for the four processes and the required make-up refrigerant.

Table 50: Refrigerant flow rate and make-up refrigerant for all four liquefaction processes

	APCI DMR	TOTAL turbo-expander	APCI turbo-expander	US Patent turbo-expander
Refrigerant flow rate (ton/hr)	2412.6	5012.8	5028.4	5527.9
Make-up refrigerant (ton/hr)	1.2 - 2.4	2.5-5.0	2.5-5.0	2.8-5.5

The numbers in Table 50 is the total refrigerant flow rate in the liquefaction processes. The turbo-expander from US patent has the highest circulation rate in of the processes and is about 2.3 higher than the total refrigerant flow rate of APCIs DMR process. The make-up refrigerant for the turbo-expander processes are also over two times higher than for the dual mixed refrigerant process. Efficient sealing of equipment will minimize refrigerant losses and hence make-up refrigerant for the processes.

Storage facilities for the refrigerants can be extensive and will require large areas on the FLNG. The hydrocarbons in the mixed refrigerant will need to be stored separately in order to get the right mix of refrigerant for liquefaction of the natural gas. The FLNG is most likely dependent on a fractionation system on board the vessel to extract heavy hydrocarbons from the natural gas upstream of the liquefaction unit. A fractionation unit is not required if the gas composition is lean and hydrocarbons will then need to be imported to the vessel. Nitrogen is produced with the use of air-separation equipment.

The storage area of mixed refrigerant is expected to be the largest out of the two options of refrigerants discussed in this Master thesis. The mixed refrigerant will require safety zones for storage of the refrigerant as it is considered flammable. The turbo-expander processes on the other side will require large amounts of refrigerant for such a high capacity of the liquefaction unit and large containers are needed. CO₂ will also need a separate storing unit. These refrigerants however are not considered flammable and safety zones will not be necessary in the same extent as for the mixed refrigerant. The placements of refrigerant storage are in both cases suggested in the hull of the FLNG to avoid occupation of important deck space on the vessel.

8.10 Availability of rotating equipment

Availability is closely linked to the rotating equipment in the processes. The availability of the liquefaction process increases with increasing numbers of trains in production. The DMR process will consist of 1 train while the turbo-expander processes have four trains for TOTALs and APCIs models and two trains for the liquefaction process from US patent 5,768,912. This was based on the capacity of the compander system and is discussed in Section 8.4.

The number of rotating equipment in one liquefaction train was highest for APCIs DMR process and the turbo-expander process from US patent with 10 units each. A summary of rotating equipment in all trains gave highest number for TOTALs and APCIs turbo-expander processes with 24 units. These liquefaction systems have however several trains in operation, which will increase the availability of the process. A break-down in equipment of one train are assumed to not affect the operability of the three other trains for these processes. This requires a full functionality of the common CO₂ system in the liquefaction process. An example of the availability of parallel versus equipment in series is given in Figure 16.

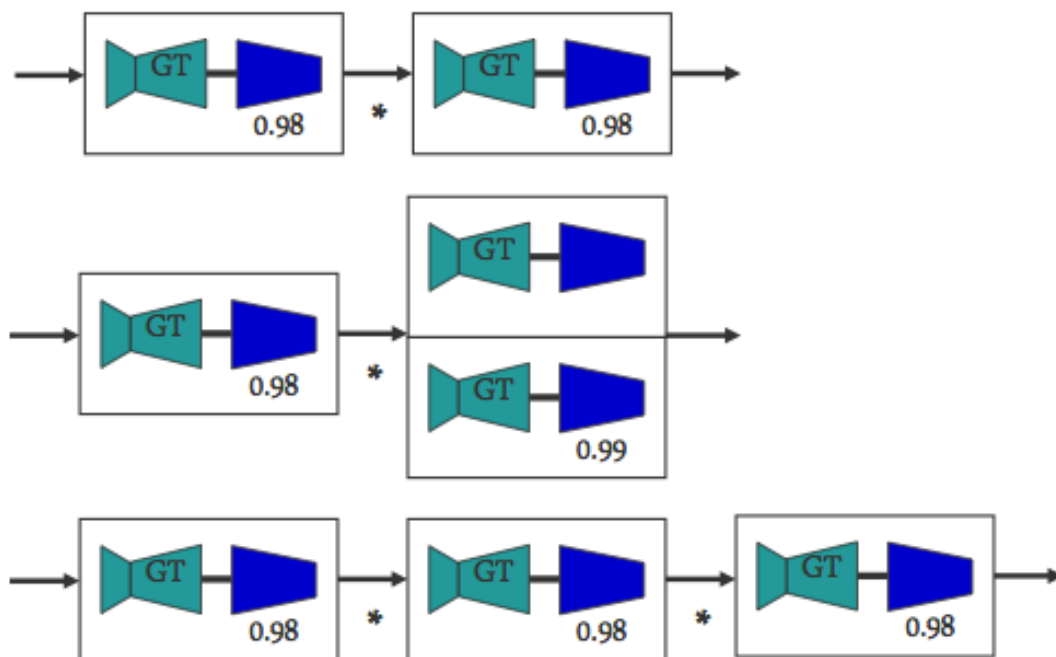


Figure 16: Availability of direct driver configurations (Pettersen, 2012)

Figure 16 shows a schematic of different configurations for drivers and compressors. The figure shows that two circuits with a parallel unit have a higher availability than two circuits with two units in series. The availability for the upper system is 0.96 while it is 0.97 for the second system in Figure 16. Several units in series will have decreased availability with 0.94 for the third system.

The availability of the system is also dependent on the drivers for the liquefaction unit. LM 6000 gas turbines are used as compressor drivers in the process. These types of gas turbines have a quick start-up time of about 10 minutes to maximum power. The LM 6000 has an expected repair interval of 3 years or 25,000 hours, but may require frequent water wash to maintain capacity (Hundseid, 2012). Site maintenance of aeroderivatives is more complex than for industrial gas turbines (Meher-Homji, 2007).

Stops in production can be improved with an analysis of failure of equipment and a best maintenance practice for the rotating machinery. The failure of one component should be analysed to the effect of the combined liquefaction unit. Historical data on the equipment behaviour can prevent down-time of the liquefaction unit.

8.11 Power generation & driver configurations

LM 6000 gas turbines are used as the drivers for the liquefaction processes. The power to weight ratio for LM 6000 aero derivative gas turbines is high, which is an advantage for FLNG technology. The LM 6000 is a multispool gas turbine with a large speed range and high speed flexibility. The number of gas turbines was determined based on the total power consumption of the compressors in the processes. Six LM 6000 gas turbines were required for all three turbo-expander process while four gas turbines were necessary to operate the DMR process. These are the driver turbines for the compressors in the processes. Two additional gas turbines are required for electric power generation covering, pumps, HVAC, thrusters, lighting etc. for the two liquefaction processes.

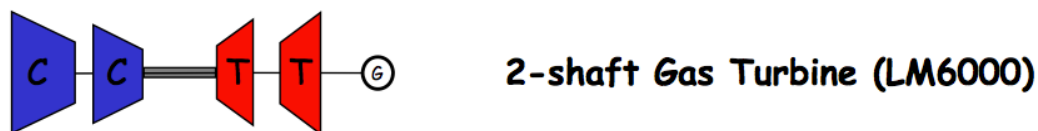


Figure 17: Schematic of a LM 6000 multispool gas turbine (Hundseid, 2012)

The LM 6000 gas turbine has a power output of 32 MW at site conditions and an outside air temperature of 27°C. The power output of the gas turbine must be estimated for a “worst case scenario” of decreased power output at higher ambient temperature at the FLNG site. The estimations must also consider a level of performance degradation for the gas turbine over time. The aeroderivative turbines are high-efficiency turbines with less CO₂ emissions than conventional industrial gas turbines.

Direct power drive of compressors is one possible configuration of the LM 6000. This is the most common solution of LNG refrigerant compressor drivers in today’s market. Direct power drive from the gas turbines is associated with low CAPEX and a small plot area. Decreased plot area is an advantage for FLNG. Direct power generation of the compressors will in a large degree limit the process configuration of the liquefaction unit. The capacity of the process will also depend on the available turbine capacity. A balanced load of the

compressors on the drivers can exploit more of the power from the gas turbines with direct power drive.

Another solution of the driver configuration is electric motor drive of the compressors. Electric motor generation will have higher availability than direct power drive of the compressors (Pettersen, 2012). Electric drive is more flexible when it comes to changes in production. This system also induces a higher flexibility of equipment placement in the liquefaction process, and may also have safety advantages by removing the gas turbine which is an ignition source from the process area. The power generation can be placed in a separate area on the FLNG with electric motor drive and increases the safety on the FLNG since the fuel gas for the gas turbines are located far from the liquefaction systems. The efficiency for electric drive is lower than for direct power drive of the compressors due to loss in electrical generation and transmission. The efficiency drops by 5 to 8% with electrical drive compared to direct power supply of the compressors and pumps (Wehrman, 2011). The liquefaction process at Snøhvit is currently the only production unit for LNG using electrical motor drive of the compressors (Pettersen, 2012).

Aeroderivative gas turbines have an efficiency of 41-42%. Motor drive with generation from an aeroderivative has efficiencies of 35-36% due to the extra losses of the electrical system (Wehrman, 2011) The efficiency is measured as the fraction of delivered shaft power versus the fuel consumed by the gas turbines. The efficiencies are based on ISO efficiencies for gas turbines (Wehrman, 2011) Electric drive of the compressors can even out unbalanced load of the gas turbines coupled to multiple compressors. This is more difficult with direct power generation of the compressors.

The number of LM 6000 gas turbines in this Master thesis was solely based on the limiting compander capacity of 15 MW. Direct power generation with LM 6000 gas turbines must consider the load for each gas turbine in addition to the compander capacity in the system. This complicates the configuration of the liquefaction units and can cause unbalanced load of the gas turbines.

9. Conclusions

Four liquefaction processes for production of LNG were studied in this Master thesis. Three turbo-expander processes from TOTAL, APCI and US patent 5,768,912 were simulated in Aspen HYSYS and compared with a dual mixed refrigerant process from APCI. The turbo-expander processes from TOTAL and APCI were dual expander processes while the turbo-expander from US patent 5,768,912 had three expanders for cooling of the nitrogen refrigerant. All three turbo-expander models were simulated with a CO₂ precooling system. The LNG production capacity for the four processes was 3.5 Mtpa.

APCI's DMR process was the most efficient of the four liquefaction processes with a specific power consumption of 284 kWh/ton LNG. The turbo-expander process with lowest power consumption was TOTAL's model with 396 kWh/ton LNG. The turbo-expander processes from APCI and US patent 5,768,912 had specific power consumptions of respectively 406 and 423 kWh/ton LNG. The increased efficiency for the DMR process is due to latent heat transfer of the mixed refrigerant as opposed to sensible heat transfer of the nitrogen in the expander processes. Sensible heat causes temperature increase through the heat exchangers to compression. The DMR process has lower heat rejection losses in the process and no expander losses.

The equipment in APCI's DMR process was assumed to be large enough to handle the production capacity of 3.5 Mtpa while the turbo-expander processes were divided in parallel liquefaction trains. A compressor capacity of 15 MW limited the train capacity for the expander processes. The expander processes from TOTAL and APCI required four liquefaction trains based on the power from the largest expanders in the "warm" end of the processes with power productions of 49 MW for TOTAL's process and 55 MW for APCI's process. The turbo-expander from US patent had an additional expander in the process, which reduced the load of the two other expanders in the process. The largest expander in this process had a power output of 29 MW. Two liquefaction trains were suggested for the US patent process. The power output is close to the maximum capacity of two compressors, and a third train may be required. A common CO₂ system was assumed to serve the turbo-expander trains in the liquefaction process.

The heat exchanger properties were studied for the two process technologies with focus on the LMTD and UA values in the processes. TOTAL's and APCI's process had LMTD values ranging from 5.5-7.4°C in the process, excluding the numbers of the inefficient heat exchangers for CO₂. The US patent had more efficient heat exchangers with LMTD values from 3.2-5.2°C. The process from DMR had relatively high LMTD values ranging from 5.8-7.0°C. The area of the heat exchangers increases with decreasing LMTD values. The UA values of the heat exchangers were also considered, but the areas of the heat exchangers was difficult to compare without knowing the *U* values of the exchanger. The heat exchanger segments with the largest UA values were DMR's process with a value of 124,000 MJ/°C-hr for the 1st MR circuit and TOTAL's process with 57,000 MJ/°C-hr for a feed-nitrogen heat exchanger segment. The DMR process is

expected to have a higher U value in the heat exchangers than the turbo-expander processes. A calculation of the U value for the heat exchangers can be evaluated in an extended version of this study.

The suction volume of the compressors in the processes and the volume flow of the expander outlets for the turbo-expander processes were studied. The turbo-expander process had the highest volume flow to compression with 152,600 m³/hr to the main nitrogen compressor in each liquefaction train. The turbo-expander processes from TOTAL and APCI had volume flow rates of respectively 65,900 and 69,500 m³/hr to the main compressor in each train. The reason for the higher suction volume in the US patent model is the lower pressure of refrigerant entering compression and only two production trains of LNG. The turbo-expander process from US patent will require a larger, and hence more costly, compressor than the two other expander processes. The largest compressor for the DMR process is found in the low-pressure compressor in the 2nd MR circuit with a volume flow of 159,200 m³/hr. The additional expander in the US patent model had the largest expander power with 55,800 m³/hr for each train.

The initial CO₂ system for the turbo-expander processes had one evaporation stage of the CO₂. More efficient CO₂ systems with two and three evaporation stages of CO₂ were studied. The expander process from US patent had highest power consumption of the CO₂ system because of two warm streams to precooling. The US process had accordingly the highest decrease in specific power consumption of the turbo-expander process with 4.7% for a precooling system of three evaporation stages. The LMTD value for the CO₂ heat exchanger decreased from a value of 16°C to a number of 10°C for the least efficient of the three heat exchangers. The total UA area increased by 69% for the precooling system with three evaporation stages of CO₂.

Process parameters such as feed gas composition and pressure, cooling temperature, high-pressure of nitrogen and split temperatures were among the parameters studied in a sensitivity analysis. A richer feed gas and a higher pressure of the natural gas to compression gave reductions in power consumption due to the increased condensing temperature of the natural gas. An increase in feed gas pressure from 60 to 80 bar gave a reduction in specific power consumption of 7.3% for APCI's turbo-expander process. A reduction in high-pressure of nitrogen from 70 to 65 bar increased the power consumption in the processes and the volume flows in rotating equipment were larger due to reduced pressures in the refrigerant streams. An extension of the sensitivity analysis for the processes with study of the mixed refrigerant composition and other relevant parameters can be of interest.

An equipment count was conducted for the four processes. The turbo-expander processes from TOTAL and APCI had the highest equipment count for four liquefaction trains with 54 units. The fraction of rotating equipment for a single train was however higher for APCI's DMR process and the process from US patent with 10 units. Rotating units are closely linked to the availability of the processes. The turbo-expander processes have several parallel production trains,

which increases the efficiency of the liquefaction process. A study of the size and weight of the liquefaction processes with exact equipment sizes from vendors is a suggestion for further study of the four processes. This will be an important factor when selecting a liquefaction process for FLNG. Availability calculations based on existing documentation of similar equipment will also be of interest.

Mechanical drive (direct drive) and electric drive of the compressors were also discussed. The turbo-expander processes required six LM 6000 gas turbines to power the compressors in the processes, while four LM 6000 were required to power the compressors in the DMR process. The calculations were based solely on the compressor power in the system and did not account for the load for each gas turbine. Electric drive of the compressors in both liquefaction technologies was therefore assumed. Electric drive has advantages with higher flexibility of equipment placement for the processes. The gas turbines can also be placed in another area of the FLNG to increase the safety on the vessel. The disadvantages with electric drive are the 5-8% efficiency loss compared with direct drive of the compressor due to transmission and electric generation losses. Electric drive of the compressors is a new technology for LNG and this should be taken in to consideration.

Literature list

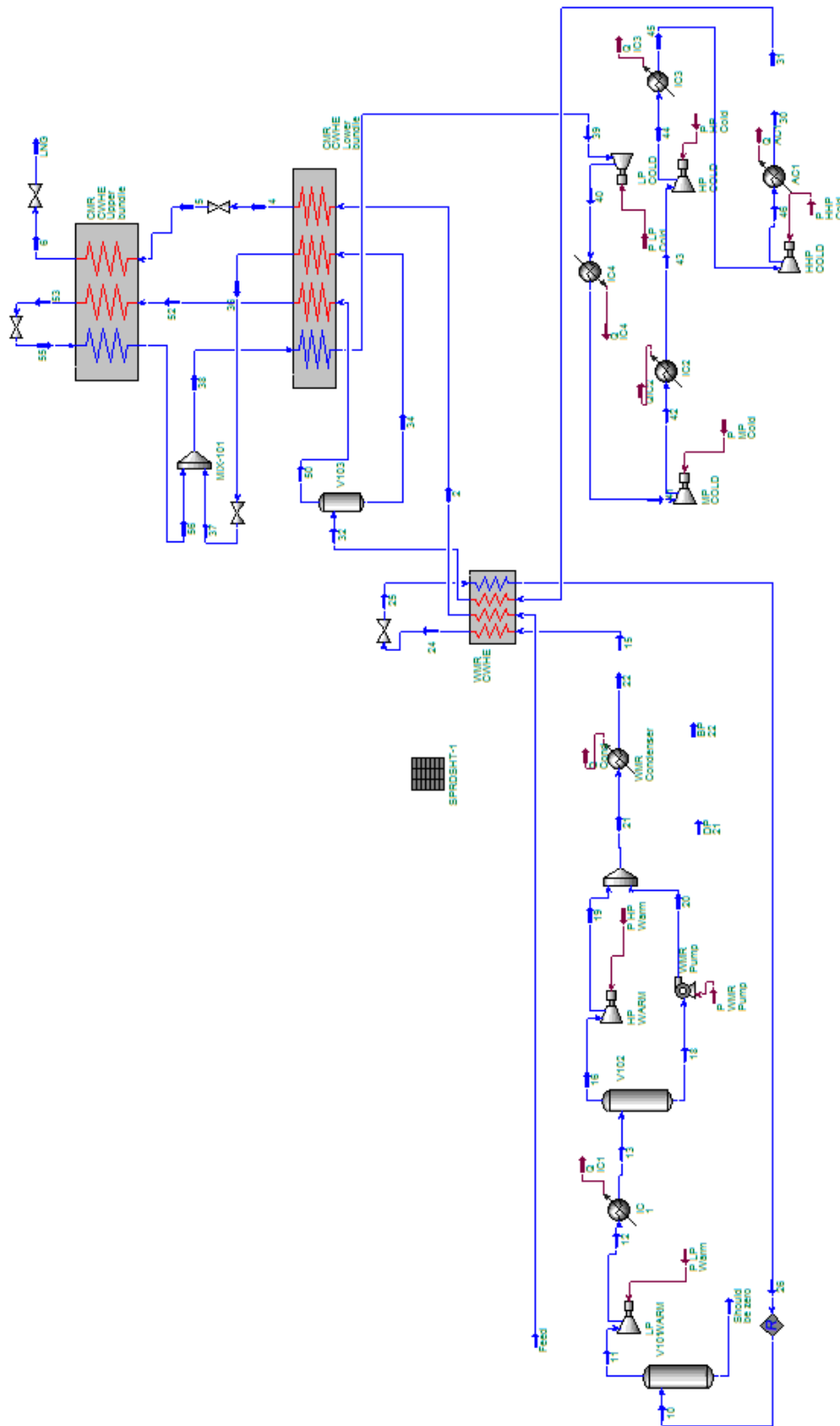
1. Bakken, Lars E. *Oral information at NTNU* (2013)
2. Bukowski, Justin et. Al. *Innovations in Natural Gas Liquefaction Technology for Future LNG Plants and Floating LNG facilities*. International Gas Union Research Conference (2011)
3. Castillo, L, Dorao, C.A. *On the conceptual design of pre-cooling stage of LNG plants using propane or an ethane/propane mixture*. Global Conference on Renewable energy and Energy Efficiency for Desert Regions (2011)
4. Chrétien, Denis, Morand, Elise. *TOTAL's approach to selecting the liquefaction process for F-LNG*. TOTAL (2011)
5. Dubar, C.A. US patent 5,768,912. United States Patent. (1998)
6. Hasle, Siv. *Evaluation of liquefaction systems for floating LNG*. NTNU (2012)
7. Hundseid, Ø. Gas Turbines. Lecture notes in TEP08 (2012)
8. Meher-Homji, Cyrus B. *Gas Turbines and Turbocompressors for LNG Service*. Proceedings of the Thirty-Sixth Turbomachinery Symposium (2007)
9. Pelagotti, A, Baldassarre, L. Latest advances in LNG Compressors. LNG 17 (2013)
10. Pettersen, Jostein. *Compendium LNG Technology*. Teaching material in TEP 4185 "Natural Gas Technology" (2012)
11. Pettersen, Jostein. *Oral information during supervising sessions* (2013)
12. Pettersen, Jostein. Natural Gas Liquefaction. Lecture notes in TEP08 (2012)
13. Product catalog Linde. *Aluminum Plate-Fin Heat Exchangers*. The Linde Group (2009)
14. Think GlobalGreen2008. *Hydrofluorocarbons (HFCs)* [Online] Accessible at: <http://www.thinkglobalgreen.org/hfc.html> [Accessed 14 March 2013]
15. Thonon B., Breuil E. *Compact heat exchangers technologies for HTRs recuperator application*. (2012)
16. Wehrman, J. et. Al. *Machinery/Process Configurations for an Evolving LNG Landscape*. Air Products (2011)

Appendix A

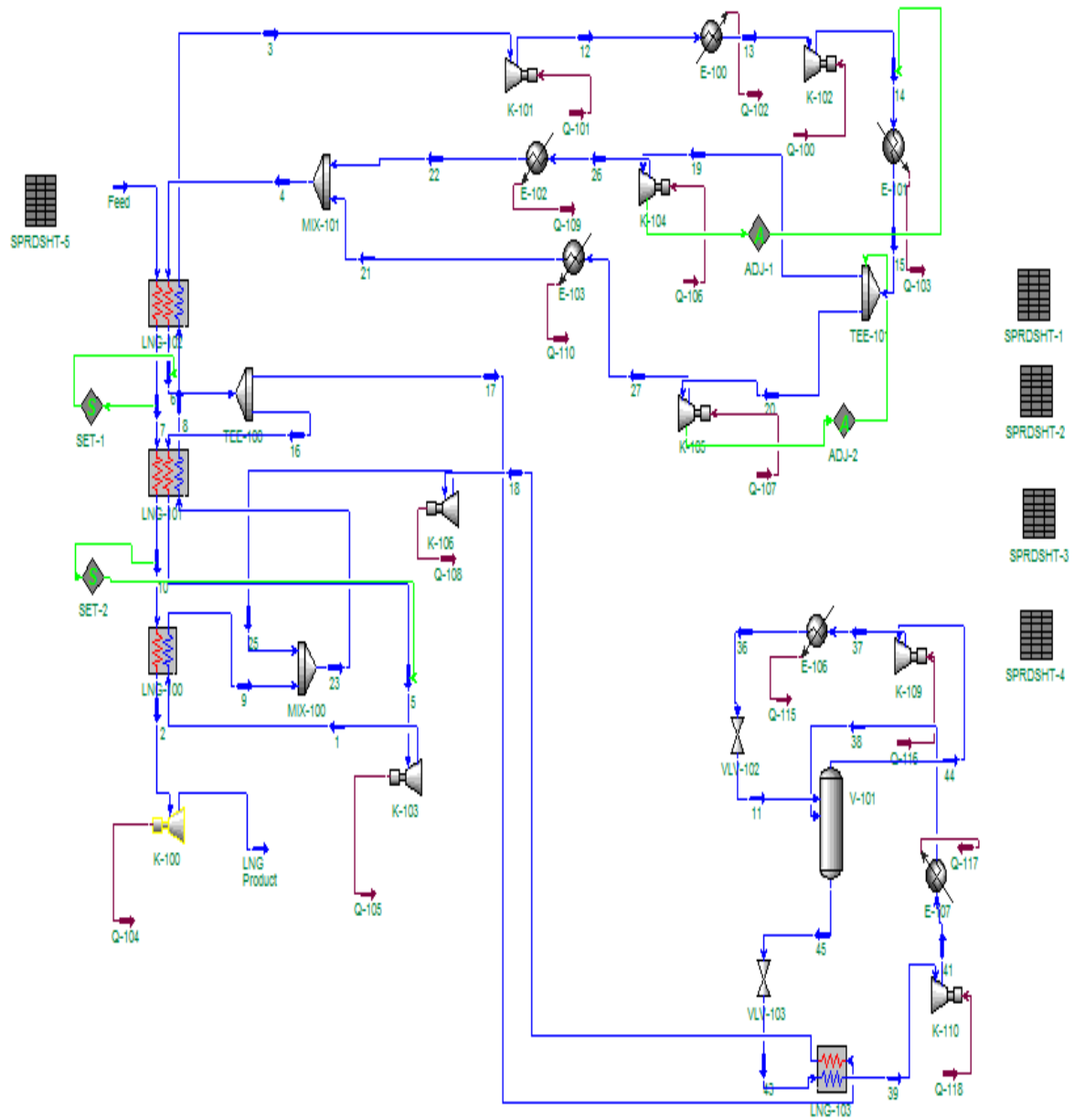
List of Content

- A.1 Model of the simulation of APCI DMR process from HYSYS*
- A.2 Model of TOTALs turbo-expander process from HYSYS*
- A.3 Temperature curves for the heat exchangers in APCI's DMR process*
- A.4 Temperature curves for the heat exchangers in TOTALs turbo-expander process*
- A.5 Temperature curves for the heat exchangers in APCI's turbo-expander process*
- A.6 Temperature curves for the heat exchangers in the turbo-expander process from US patent 5,768,912*
- A.7 Versions A, B and C of US patent 5,768,912 (Dubar, 1998)*

A.1 Simulation model of APCIs DMR process

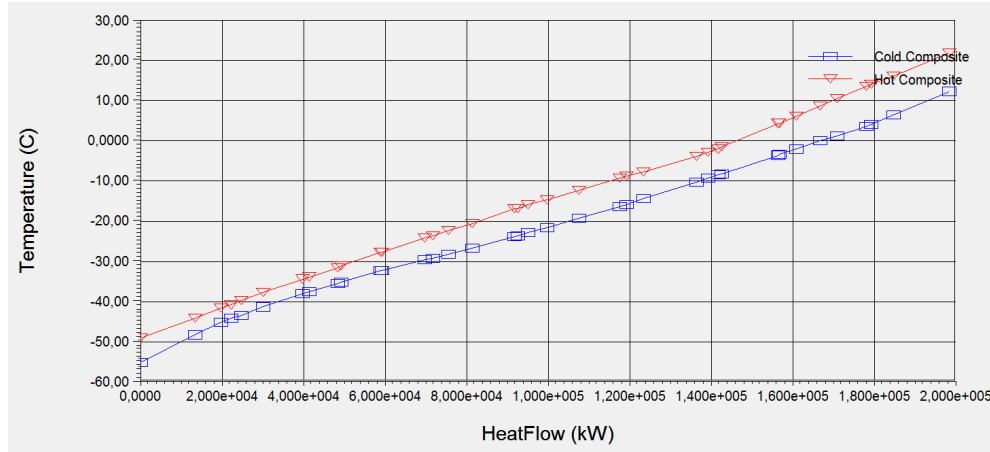


A.2 Simulation model of TOTALs turbo-expander process



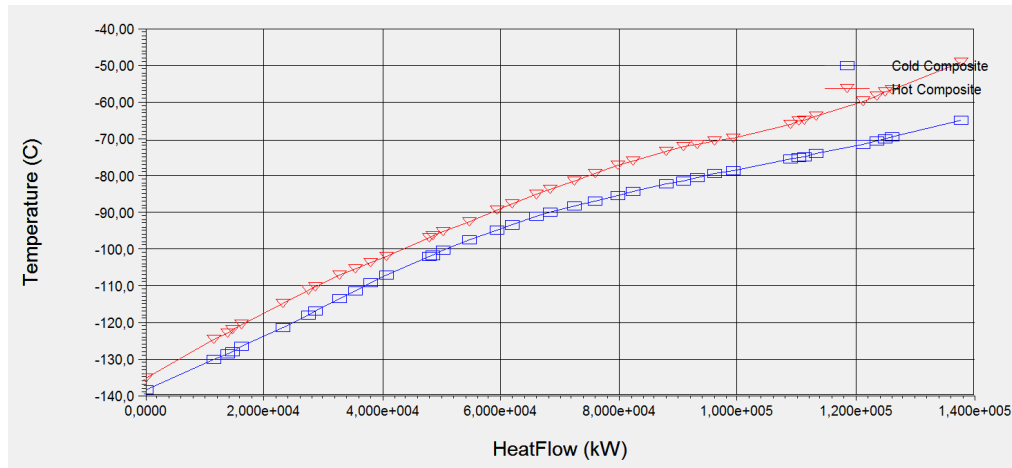
A.3 Temperature curves for heat exchangers in APCIs DMR process

WMR CWHE



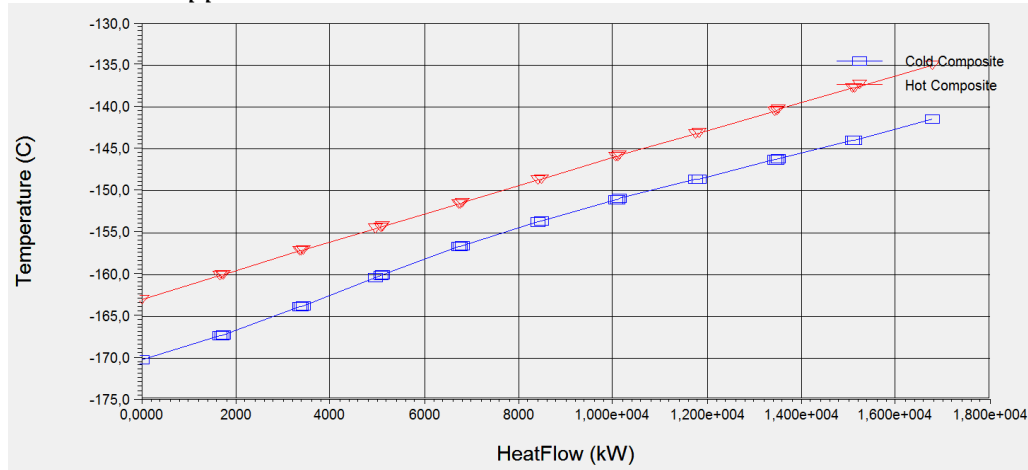
Min. approach: 3.4°C LMTD: 5.8°C

CMR CWHE Lower bundle



Min. approach: 3.0°C LMTD: 6.9°C

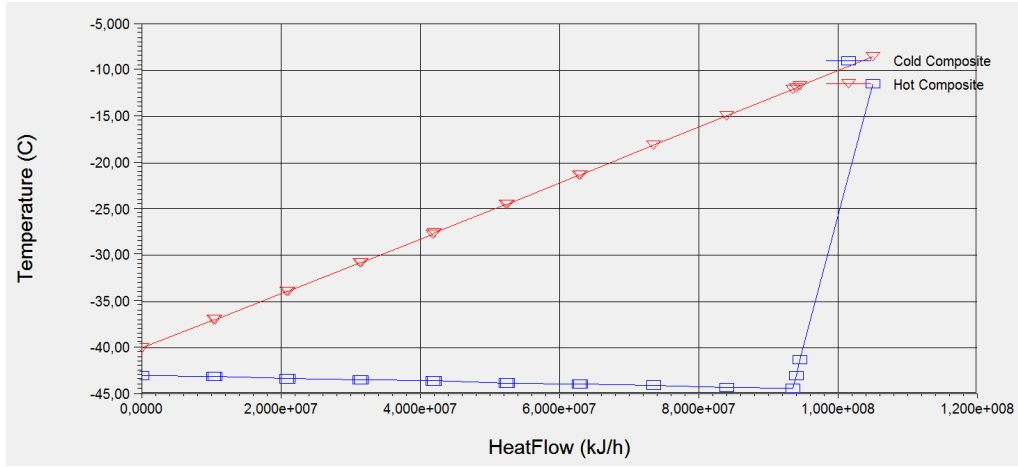
CMR CWHE Upper bundle



Min. approach: 5.0°C LMTD: 5.9°C

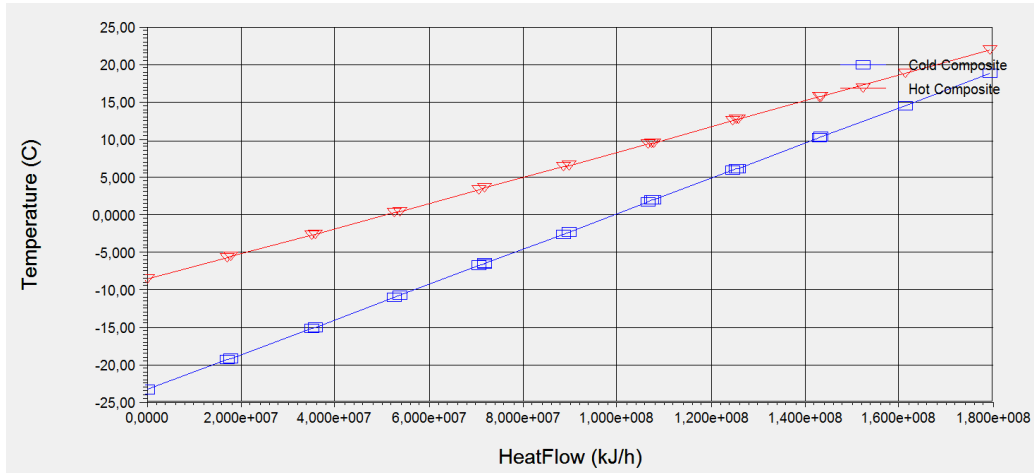
A.4 Temperature curves for the heat exchangers in TOTALs turbo-expander process

LNG-103 N2-CO2



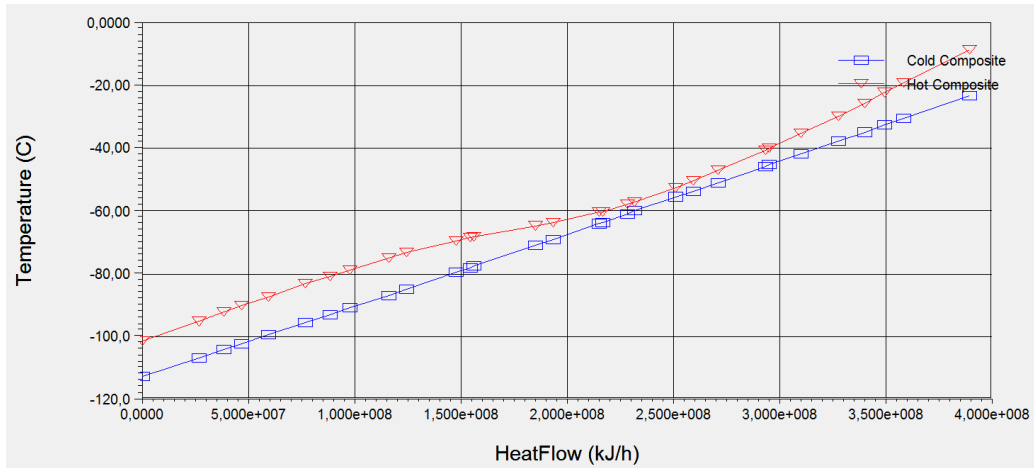
Min. approach: 3.0°C LMTD: 12.3°C

LNG-100 Feed-N2



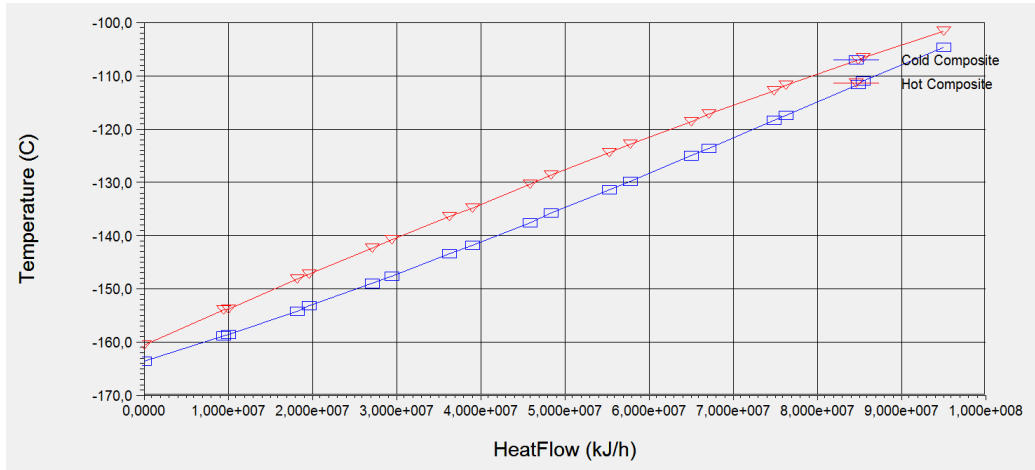
Min. approach: 3.1°C LMTD: 7.4°C

LNG-101 Feed-N2



Min. approach: 3.0°C LMTD: 6.8°C

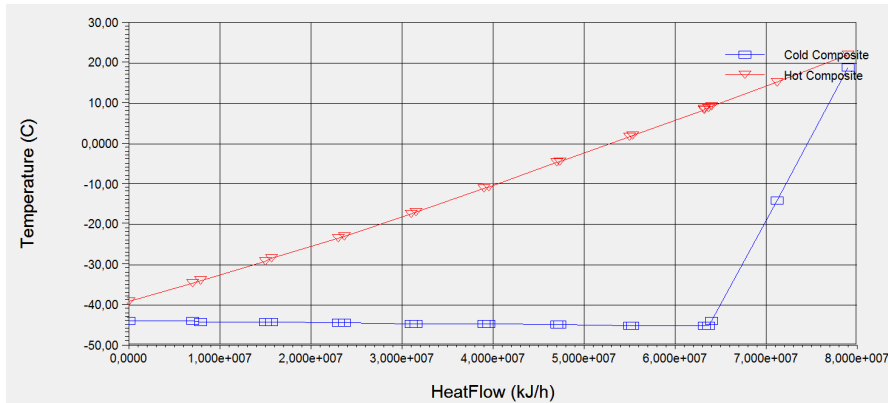
LNG-102 Feed-N2



Min. approach: 3.0°C LMTD: 5.5°C

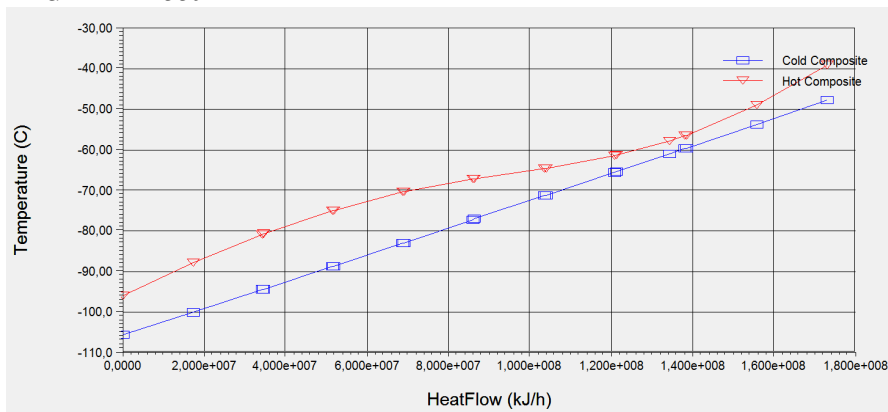
A.5 Temperature curves for the heat exchangers in APCIs turbo-expander process

LNG-100 Feed - CO2



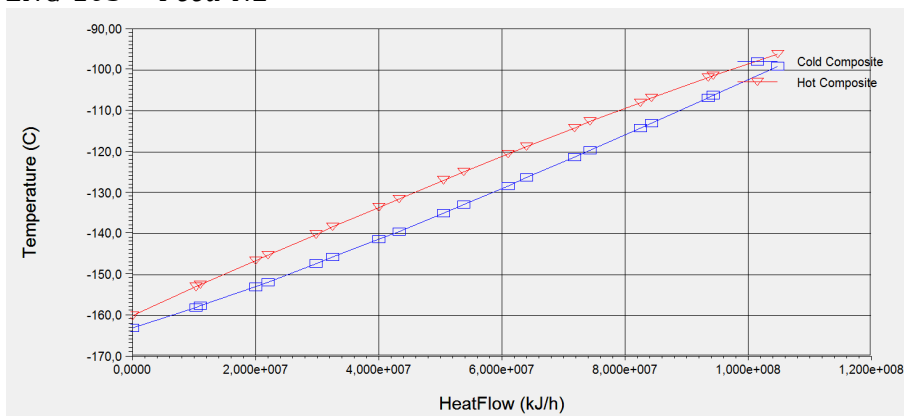
Min. approach: 3.0°C LMTD: 19.0°C

LNG-101 Feed-N2



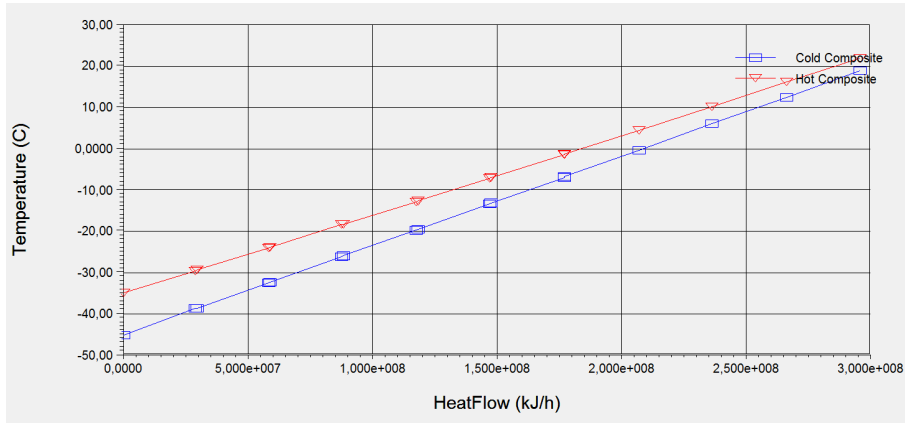
Min. approach: 3.2°C LMTD: 7.1°C

LNG-103 Feed-N2



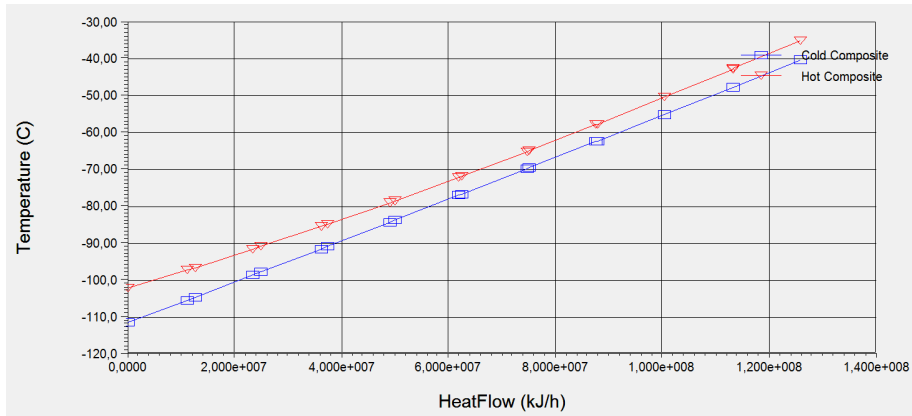
Min. approach: 3.0°C LMTD: 5.9°C

LNG-104 N2-N2



Min. approach: 3.1°C LMTD: 5.6°C

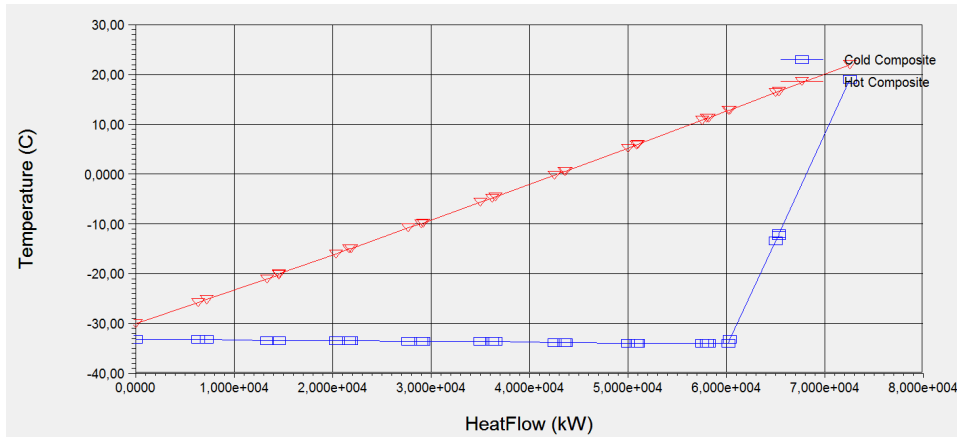
LNG-102 N2-N2



Min. approach: 4.6°C LMTD: 5.5°C

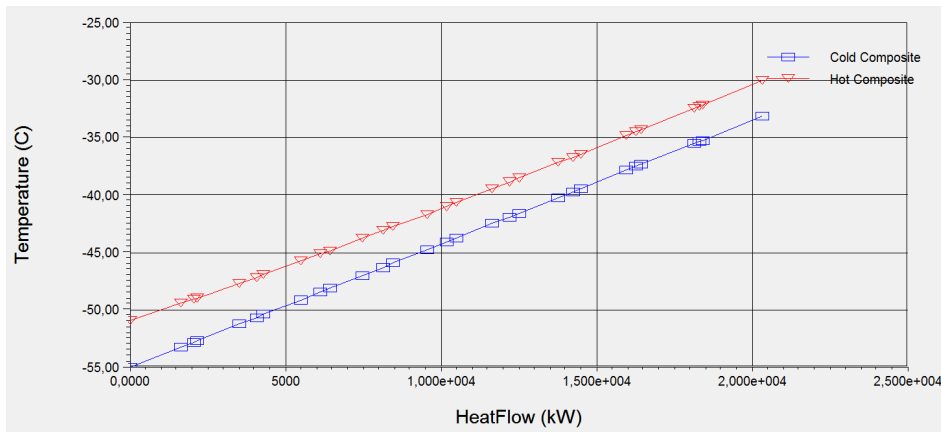
A.6 Temperature curves for the heat exchangers in the turbo-expander process from US patent 5,768,912

LNG-100 Feed- N2- CO2



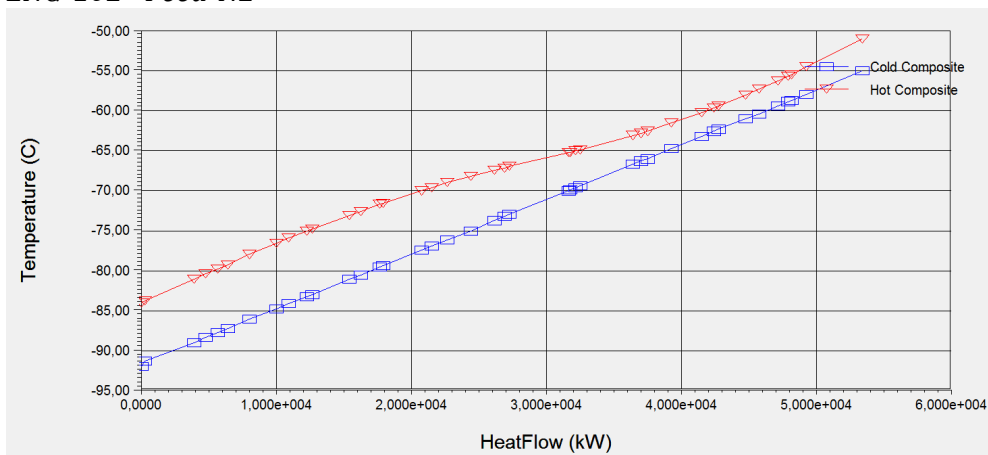
Min. approach: 3.0°C LMTD: 15.7°C

LNG-101 Feed- N2



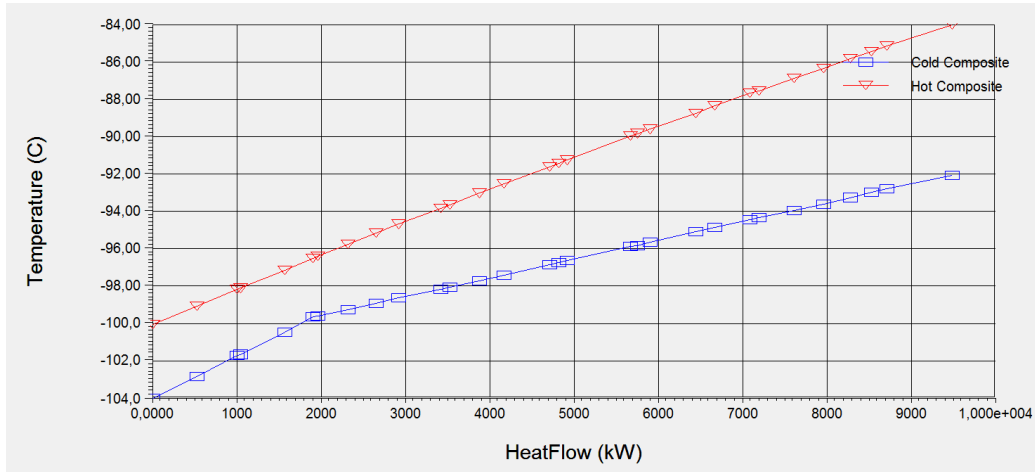
Min. approach: 3.0°C LMTD: 3.2°C

LNG-102 Feed-N2



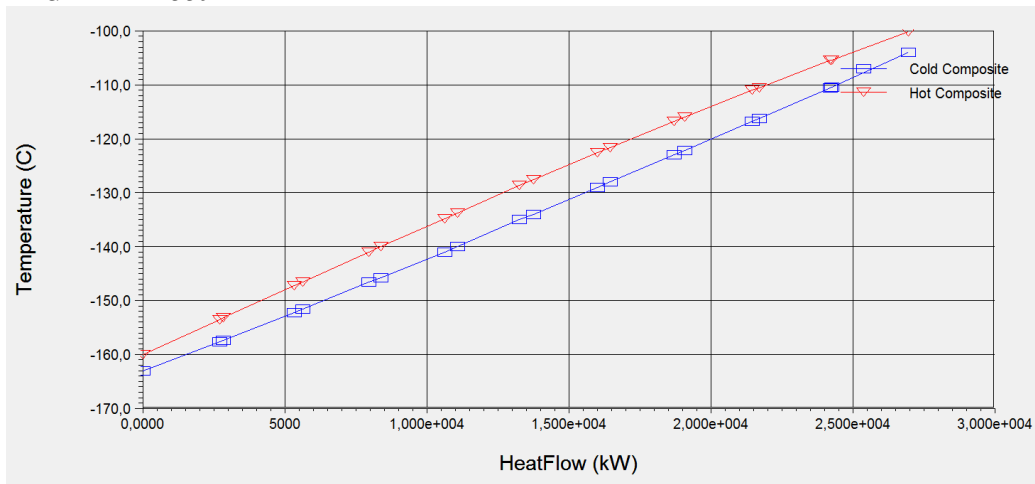
Min. approach: 3.0°C LMTD: 5.0°C

LNG-103 Feed-N2



Min. approach: 3.2°C LMTD: 4.9°C

LNG-104 Feed-N2



Min. approach: 3.0 °C LMTD: 5.2°C

